RICE UNIVERSITY

Fabrication of Petrochemical and Viral Resistant Membranes

by

Samuel J. Maguire-Boyle

A THESIS SUBMITTED
IN PARTIAL FULFILLMENT OF THE
REQUIRMENTS FOR THE DEGREE

Master of Science

APPROVED, THESIS COMMITTEE:

Andrew R. Barron
Charles W. Duncan, Jr. – Welch
Chair of Chemistry and Professor of
Materials Science

Lon J. Wilson,
Professor of Chemistry

Kenton H. Whitmire
Professor of Chemistry

Houston, Texas

January 2012

ABSTRACT

Fabrication of Petrochemical and Viral Resistant Membranes

By

Samuel J. Maguire-Boyle

Physical interaction between two bulk media occurs mainly at the surface interface. The surface properties of materials therefore dictate how a system will respond to different influences, while being just a fraction of the entire volume. Alteration of a surface can therefore have a significant effect on a system. In this thesis the functionalization of surfaces via covalent attachment of short chained molecules was undertaken to manipulate surface-surface interactions for different outcomes.

The separation and purification of bulk media of impurities has always been undertaken. Many different processes exist, however the removal of impurities from dynamic or open systems remains a problem. The use of filtration technologies remains the best option in this type of system. In filtration technology membranes are employed to selectively remove one or more elements from another generally under a driving force.

The selectivity of a membrane has either traditionally relied on either physical attributes such as pore size or chemical attributes such as charge, van der Waals etc. In this thesis we propose the use of organically functionalized ceramic nanoparticles alumoxanes to act as a coating of the side walls of the fibers of a base bulk fabric material Nomex©.

The side chain of cysteic acid has been found to be extremely hydrophilic due in part to its Zwitter ionic properties. The use of hydrophilic cysteic acid alumoxane was used as part of a composite membrane to screening hydrocarbons. Doping of this membrane with cysteic acid ferroxane the iron analogue of alumoxane was used as a membrane to screen MS2 bacteriophage.

Table of Contents

List of Figures

Introduction

Chapter 2

Chapter 3

List of Tables

Chapter 1

Appendix A.

Abbreviations and Glossary

AFM	atomic force microscopy
avg.	average
^{o}C	degrees centigrade
ca	approximately
CA	cysteic acid functionalized alumoxane
CA-Nomex	cysteic acid functionalized alumoxane deposited onto Nomex in a conformal layer
ccp	cubic close-packed
cm^{-1}	wavenumber the number of wavelengths given per unit distance
DLVO	Derjaguin, Landau, Verwey and Overbeek
d_s	solute diameter
Eq.	equation
EDX	energy dispersive X-ray spectroscopy
g	grams
GC	gas chromatography
hcp	hexagonal close-packing
HPLC	high pressure liquid chromatography

ICP-OES	inductively coupled plasmon optical emission spectroscopy
kDa	kilodalton, one hydrogen atomhas a mass of one dalton
L	liters
μm	micron, 10^{-6} m
mL	milliliters, 10^{-3} L
mm	millimeter, 10^{-3} m
min	minutes
mol	mole
M_w	molecular weight
MWCO	molecular weight cut-off
nm	nanometer, 10^{-9} m
NPOC	non-purgeable organic content
*n*ZVI	nanoscale zero-valent iron
pH	the measure of the acidity or basicity of an aqueous solution
pm	picometer, 10^{-12} m
ppm	parts per million
Q_p	flux rate, ms^{-1}
r	radius
rpm	revolution per minute

SEM	secondary electron microscopy
TEM	transmission electron microscopy
TGA	thermogravimetric analysis
TC	total carbon
TIC	total inorganic carbon
XPS	X-ray photoelectron spectroscopy
XRD	powder X-ray diffraction

agglomerate	Clustering of small particles through electrostatic attraction to form larger particles
alkali metals	comprise the group 1 elements including hydrogen on the periodic table
alkaline earth metals	comprise the group 2 elements on the periodic table

alumina	Al_2O_3 in any phase
alumoxane	An oligomeric or polymeric material consisting of an Al-O backbone and containing various pendant groups
amorphous	lacking in crystallinity
amide	an organic compound that contains the functional group consisting of a carbonyl group (R-C=O) linked to a nitrogen atom (N)

amine	organic componds and functional groups that contain a basic nitrogen atom with a lone pair
aspirated	fluid or solid turned into small particulates which can be easily inhaled
bacteriophage	a virus that parasitizes a bacterium by infecting it and reproducing inside it
boehmite	γ-alumina, AlO(OH), a naturally occurring mineral
cake layer	a filter cake layer is formed by the substances that are retained on a filter
capsid	the protein coat or shell of a virus particle, surrounding the nucleic acid or nucleoprotein core
ceramic	A class of inorganic, non-metallic material which is subjected to temperatures in excess of 500 ^{o}C for the purposes of manufacture of use
composite	engineered or naturally occurring materials made from two or more constituent materials with significantly different physical or chemical properties which remain separate and idstinct at the macroscopic or microscopic scale within the finished structure
conformal	a uniformaly thick layer on a on an object
contact angle	The interior angle formed between the edge of a solvent "bubble" and the surface on which it rests. Angles are measured either advancing or receding; low numbers indicate hydrophilic surfaces

	("wetting") while high numbers represent hydrophobic surfaces ("non-wetting")
crossflow filtration	filtration utilizing tangential flow of the permeate
dead-end filtration	filtration when the permeate is forced perpendicular through the filter
dehydration	loss of water
dextran	group of long-chain polymers of glucose of distinct hydrodynamic size
dip-coating	a coating applied to a physical form by immersion into a vessel containing that coating in liquid form
entropy	the amount of order, disorder, and/or chaos in a thermodynamic system
entropic barrier	a state where a large decrease in entropy is required to alter the interaction between two interfaces
ferroxane	an oligomeric or polymeric material consisting of an Fe-O backbone and containing various pendant groups
filtration	material, especially liquid, that has passed througha filter
flux	the flow rate across the membrane
fouling	the process in which solute or particles deposit onto a membrane surface or into membrane pores so that membrane performance is degraded
goniometer	an instrument for the precise measurement of angles

hybrid	a composite consisting of two contitunets at the nanometer or molecular level. Commonly one of these compounds is inorganic and the other one organic in nature
hybrid-*class I*	hybrid materials that show weak interactions between the two phases, such as van der Waals, hydrogen bonding or weak electrostatic interactions
hybrid-*class II*	hybrid materials that show strong chemical interactions between the components such as covalent bonds.
hydraulic fracturing	the propagation of fractures in a rock layer caused by the presence of a pressurized fluid
hydrodynamic	the mechanical properties of a fluid or fluids or of a solute in a fluid or fluids
hydrogen bond	A hydrogen bond is a type of attractive (dipole-dipole) interaction between an electronegative atom and a hydrogen atom bonded to another electronegative atom. This bond always involves a hydrogen atom. Hydrogen bonds can occur between molecules or within parts of a single molecule. A hydrogen bond tends to be stronger that a van der Waals forces, but weaker than covalent bonds or ionic bonds.
hydrophilic	water loving
hydrophobic	water hating
hydroxide	A chemical compound containing one or more hydroxyl radicals (OH)

icosahedral	a polyhedron having 20 faces
interface	a surface regarded as the common boundary of two bodies, spaces, or phases
latent	present and capable of emerging or developing but not now visible, obvious, active, or symptomatic
lepidocrocite	A red to reddish-brown mineral consisting of erric hydroxide, typically occurring as scaly or fibrous crystals
membrane	layer of material which serves as a selective barrier between two phases and remains impermeable to specific particles, molecules, or substances when exposed to the action of a driving force
microfiltration	filtration pertaining to macropores
moiety	a unique part of a molecule
monodisperse	particles of uniform size in a dispersed phase
monomer	a molecular that forms the basic unit for polymers. Monomers may bind to other monomers to form a repeating chain molecule
morphology	the characteristics shape or contour of a surface
nanofiltration	filtration pertaining to micropores
neutron	a subatomic particle which has no net electric charge and a mass slightly larger than that of a proton
neutron scattering	the scattering of free neutrons by matter, it is a physical process and an experimental technique using this process for the investigation of materials. Neutron diffraction (elastic scattering) is

	used for determining structures; Inelastic neutron scattering is used for the study of atomic vibrations and other excitations
octahedra	possessing the symmetry of a regular octahedron. Having a three-dimensional shape with six vertices and eight faces, where each face forms an equilateral triangle
pathogenic	capable of causing disease
permeate	the media which passes through a filter
petrochemical	chemical product derived from petroleum
phase	a physically distinctive form of matter, such as solid, liquid, gas or plasma. A phase of matter is characterized by having relatively uniform chemical and physical properties
polymer	a large molecule made up of chains or rings of linked monomer units
polymerization	the bonding of two or more monomers to form a polymer
pore	a small opening, void, interstice, or also channel within a consolidation solid mass or agglomerate
pore size	the characteristic or equivalent dimensions or range of same (e.g., diameter) of a pore or family of pores in a material
pore volume	the porosity of a solid
purging	removal of volatile substances from a liquid phase by passing a gas such as nitrogen through the liquid
pyrolysis	decomposition of a material by heat

reverse osmosis	filtration due to osmonic pressure gradient through pores < 1nm
sol-gel	solution-gelation
shale	a fine-grained, clastic sedimentary rock composed of mud that is a mix of flakes of clay minerals and and tiny fragments (silt-sized particles) of other materials especially quartz and calcite
shale-gas	natural gas produced from shale
spin coating	a procedure used to apply uniform thin films to flat substrates where an excess amount of a solution is placed on the substrate, which is then rotated at high speed in order to spread the fluid by centrifugal force
sulfonate	a salt or ester of a sulfonic acid. It contains the functional group R-SO_2O^-
surface area	the area, per unit weight of a granular or powdered of formed porous solid, of all external plus internal surfaces that are accessible to a penetrating gas
steady-state	a system in a steady-state has numerous properties that are unchanged in time
thermolysis	heating or dissipation of heat
tribological	interacting surfaces in reletaive motion. It includes the study and application of the principles of friction, lubrication and wear
ultrafiltration	filtration pertaining to mesopores

Zwtter ion	a molecule or ion having separate positively and negatively charged groups

Introduction

The ability to tailor the functional group in order to ensure the desired nanoparticle traits such as solubility is a well-known concept. A nanoparticle's molecular functionalized surface dictates its interaction with the surrounding environment, surface chemistry defines many of its dispersion properties. By understanding nanoparticle interaction, a better picture of the effect a nanoparticle makes on the macromaterial scale can be understood and utilized. Altering the properties of a material over the macro scale by functionalization with a nanoparticle will be displayed in this thesis. Functionalization of a chosen material with nanoparticles will be shown to be due to the properties of an orientated organic molecule coating the nanoparticle.

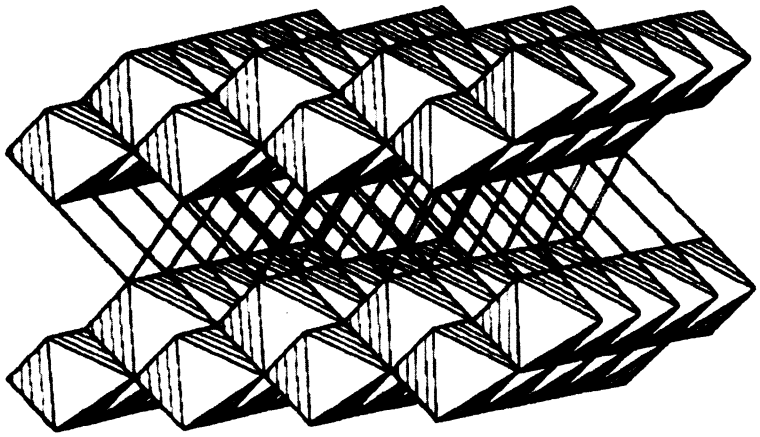

Figure I.1. The topographic structure of boehmite, γ-AlO(OH), showing the continuous chains of edge-shared octahedral stacked in layers and the interconnecting hydrogen bonding (double lines). Adapted from A. Apblett, C. Warren, and A. R. Barron, *Chem. Mater.* 1992, 4, 167.

Investigations by the United States Navy (USN) into non-acute latent hazards affecting field personnel, found numerous ailments via skin irritation, caused by contact with toxic petrochemicals[1] and viral infection caused by inhalation of aspirated viruses.[2] In this thesis I propose to reduce this threat using a simple strategy of functionalizing

current military garments with a nanoparticle, that then forms a barrier against petrochemicals and aspirated viruses. The nanoparticles act as a membrane against toxic petrochemicals and also serve as a viral filter. Alumina and iron oxide nanoparticles, both functionalized with cysteic acid are used in cooperation with existing garments. The garment material used, Nomex©, was made extremely hydrophilic via coating of its surface with hydrophilic functionalized nanoparticles. The lack of a hydrophilic organic coating on the surface of the particle drastically affected the properties of the membrane both for hydrocarbon and viral screening.

The material used to functionalize the garments, alumoxane and ferroxane, are organically surface stabilized nanoparticles. Aluminum and iron the most abundant metals in earths crust (ca. 8, 5%), are used in alumoxane and ferroxane respectively.[3] The aluminum oxides and hydroxides are the most abundant and in most cases the most important class of aluminum compounds, this is due to a combination of physical and chemical properties coupled with relatively low cost raw materials. The principal structural types of aluminum oxides and hydroxides are corundum (α-Al_2O_3), diaspora [α-AlO(OH)], bayerite [α-$Al(OH)_3$], boehmite [γ-AlO(OH)], and gibbsite [γ-$Al(OH)_3$].[4,5] In addition partial dehydration also gives numerous transitional phases.[6] The structure of boehmite is not closed packed, within each layer of AlO_6 octahedra the oxygen atoms are arranged in cubic-close packing (ccp) with arrays of oxygen atoms with continuous chains of edged octahedra stacked in layers and further interconnected by hydrogen bonds, with aluminum atoms in certain octahedrally coordinated sites Figure I.1.[7]

Two primary synthetic processes are employed for the preparation of alumina and doped alumina materials, the traditional ceramic powder approach and the solution-gelation, or "sol-gel" process. The traditional ceramic powder process is used primarily for the manufacture of dense materials, whereas the sol-gel process has been applied to make porous solids and ceramic coatings. Sol-gel involves a four stage process of dispersion, gelation, drying, and firing. A stable liquid dispersion or sol of the colloidal

ceramic precursor is initially formed in a solvent with various other stabilizers. By changing the concentration or pH, the dispersion is "polymerized" to form a sol phase or *gel*. Excess liquid is removed from this gel by drying at higher temperatures which thus produces the ceramic.

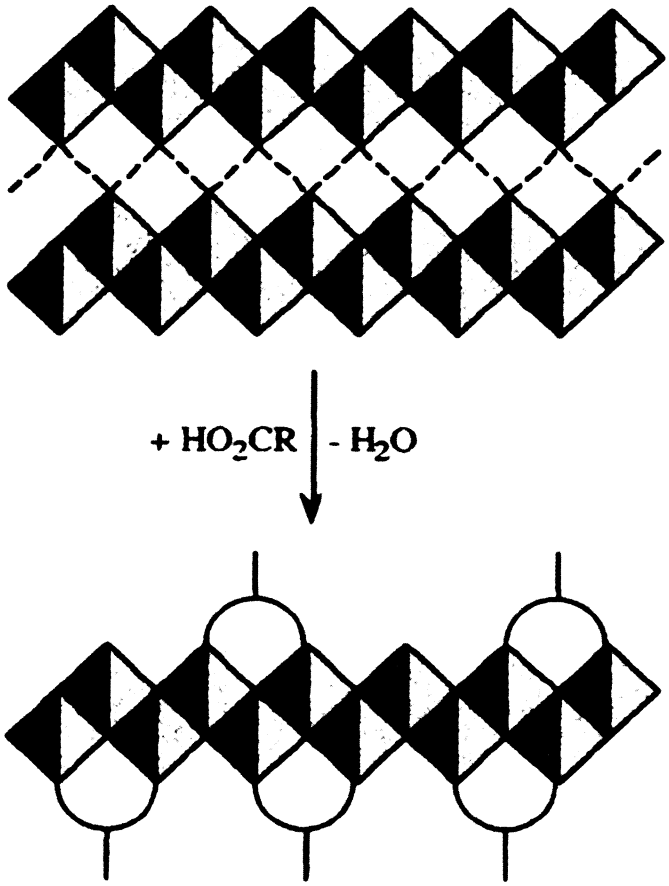

Figure I.2. Pictorial representation of the reaction with boehmite and carboxylic acids to form carboxylate-alumoxanes. The shaded triangles represent a side view of the aluminum-oxygen fused octahedral, while the carboxylate groups are represented by a semicircle with bar. Adapted from R. Callender, C. Harlan, N. Shapiro, C. Jones, D. Callahan, M. Wiesner, B. MacQueen, R. Cook, and A. R. Barron, *Chem. Mater.*, 1997, **9**, 2418.

Sol-gels produced during the hydrolysis of aluminum compounds belong to a type of compound known as alumoxanes which are inorganic-organic *Class II* hybrids.[7] Past research by the Barron group has defined the structure of alumoxanes, revealing they are three-dimensional cage compounds,[8,9] a "top-down" approach was developed based upon the reaction of boehmite Figure I.2, $[Al(O)(OH)]_n$, with carboxylic acids.[10] This reaction resulted in the formation of carboxylate-alumoxane nanoparticles, $[Al(O)_x(OH)_y(O_2CR)_z]_n$. It was determined that the solubility of these carboxylate-alumoxanes are dependent on the identity of the carboxylic acid.

The colloidal properties of the carboxylate-alumoxanes are dependent on the identity of the carboxylate substituent, and so, it is reasonable to assume that any inherent hydrophilicity will be a result of the carboxylic side chain. Alumoxanes are stable over indefinite time periods and are utilized in a wide range of processing techniques such as infiltration, dip-coating, spin coating, and spray-coating onto various substrates. The ease at which it is possible to both coat and deposit alumoxanes and there iron analogues onto a surface means that future coating of desired fabrics is assured. The membranes produced by this process were not pore selective but were instead super-hydrophilic and from as a result of this, obtained their own inherent selectivity.

The ability to trap viruses in an airway designed for breathing is a difficult process, as micron sized water can pass deeply into the vascular system, resulting in infection. However a divers breathable airway must be not be significantly blocked by a small pore size for practical purposes. To overcome this, two things must be achieved: (1) collapsing of the water droplet onto a surface and (2) immobilization of the active virus particle. By introducing a hydrophilic element to the surface of the membrane the collapse of a water droplet onto the surface is possible. The ability of iron oxyhydroxides to bind to viruses has been well documented.[33] With the introduction of these materials onto the surface the iron oxyhydroxide will have the ability to bind to viruses that are on the surface due to collapse by a hydrophilic surface. The toxicity of iron oxide and

oxyhydroxides is negligible and could be easily introduced to a virus filter by incorporation into the alumoxane sol-gel matrix.

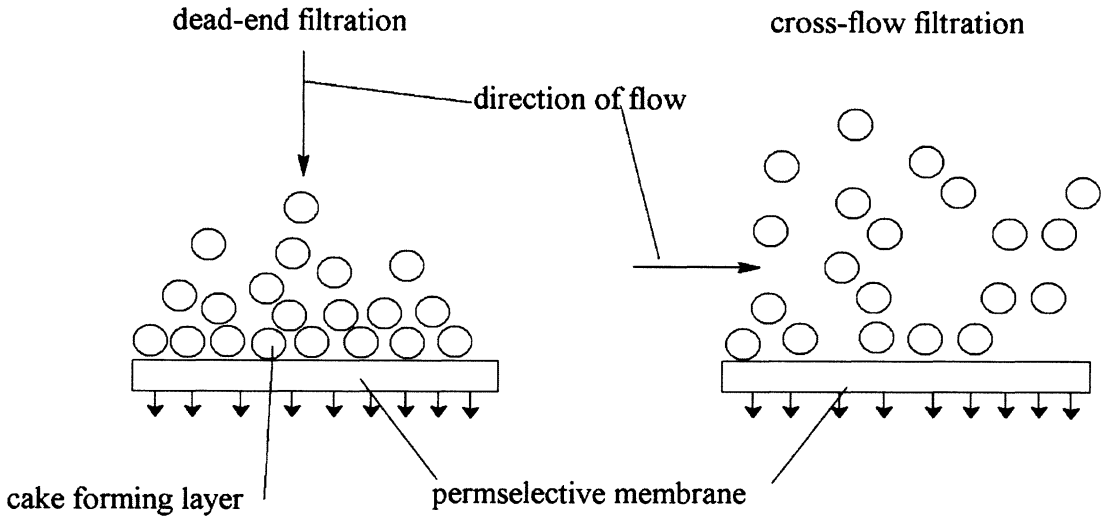

Figure I.3. Illustration of dead-end (left scheme), and cross-flow filtration (right scheme). Adapted from R. R. Bhave, *Inorganic Membranes: Synthesis, Characteristics, and Applications*, Van Nostrand Reinhold, New York, 1991.

Two common processes similar to the production of alumoxanes are used to produce iron oxyhydroxides or ferroxanes. Powder processing, shape forming, and sol-gel processes. The more environmentally benign alternative to the sol-gel process has been reported in the case of Al ceramic synthesis.[31] The process is based upon alumoxanes species containing oxo (O^{2-}) bridges between Al atoms prepared directly from boehmite (γ-AlOOH).[11,12] Using similar techniques lepidiocrocite (γ-FeOOH) is used in conjunction with carboxylic acids to produce ferroxanes. The reaction between lepidocrocite and acetic acid in water results in the formation of carboxylate-FeOOH nanoparticles called ferroxanes. It is well accepted that FeOOH and Fe_2O_3 are resistant to acidic, corrosive, and oxidant conditions.[26,27] Moreover, Fe minerals are found to be more

reactive toward heavy metals than Al minerals.[11,12] Lepiodcrocite particles have generally a monodisperse size distribution around 0.3 μm. The size decrease from the parent material might be attributed to either a dissolution or a cleavage-breakage of the particles. Respectively the cleavage or breakage of the γ-FeOOH mineral is similar to the formation of alumoxane from the γ-AlOOH mineral. The structure of the initial FeOOH mineral is the key factor in producing ferroxane. γ-FeOOH consists of layers made of Fe octahedra, the cohesion is due to weaker hydrogen bonds that can be cleaved by a carboxylic acid. The structure of ferroxane consists of a FeOOH core part with the structure of the lepidocrocite.

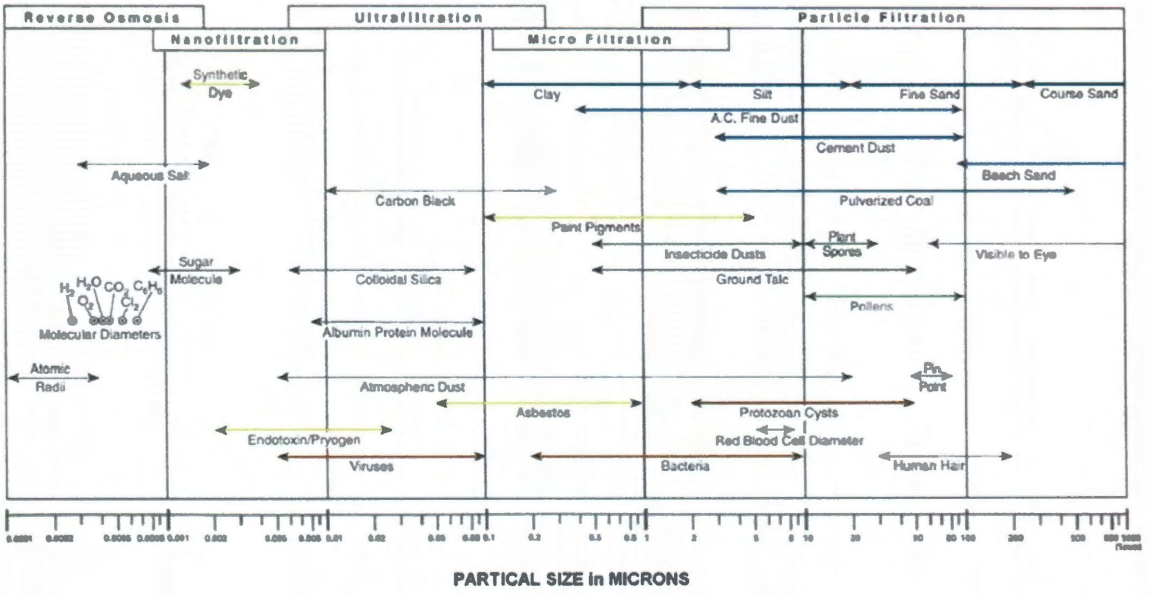

Figure I.4. Chart showing types of filtration and related particle size. Adapted from C. D. Jones, *Controlled ceramic porosity and membrane fabrication via alumoxane nanoparticles.*, Rice University, Houston, Texas, 2000.

Membrane technologies play an increasingly important role in pollution prevention, resource recovery, process development, water purification, and waste

treatment activities.[13,22,24] Polymeric membranes dominate these applications,[14] however, the use of polymeric membranes in separations involving aggressive materials such as many organic solvents, acids, bases, and oxidants is often limited by the tolerance of the polymeric material to extreme conditions.[15] Additionally, polymeric membranes are prone to swelling, gyration, and contortion. These physical movements decrease the ability of a membrane to present a particular organic functionality on a macromaterial scale, as well as introducing uncertainty regarding the physical nature of the membrane that can be undesirable. Compared to polymer membranes ceramic membranes are noted for their excellent mechanical strength and tolerance to solvents, as well as pH stability, oxidation resistance, and extreme thermal durability; However they are limited exclusively to pore size exclusion. By utilizing functionalized alumoxanes and ferroxanes both chemical and pore size selectivity can be achieved without use of polymeric material, with the added benefit of a rigidly orientated organic functionality.[16, 22] Filtration using ceramic membranes has been performed in the past using either dead-end or crossflow configurations Figure I.3.[23] In dead-end filtration, the permeate is forced perpendicular through the filter, while particles are retained. The retained particles eventually concentrate on the membrane surface forming a cake layer, which increases the resistance to filtration and hence, decreases flux.[22] This is a major problem with dead-end filtration because the process must be stopped periodically to remove the cake layer. The crossflow filtration configuration utilizes tangential flow to reduce caking. The feed flow brings both liquid and solid particles to the membrane surface, where they are rejected or allowed to cross the membrane. These particles begin to make a thin cake layer toward the exit.[22] This allows for continuous processing and thus crossflow filtration is increasingly being used for industrial applications. A large reduction in caking can be achieved over both types of membranes by introduction of a hydrophilic surface to the membrane.[17]

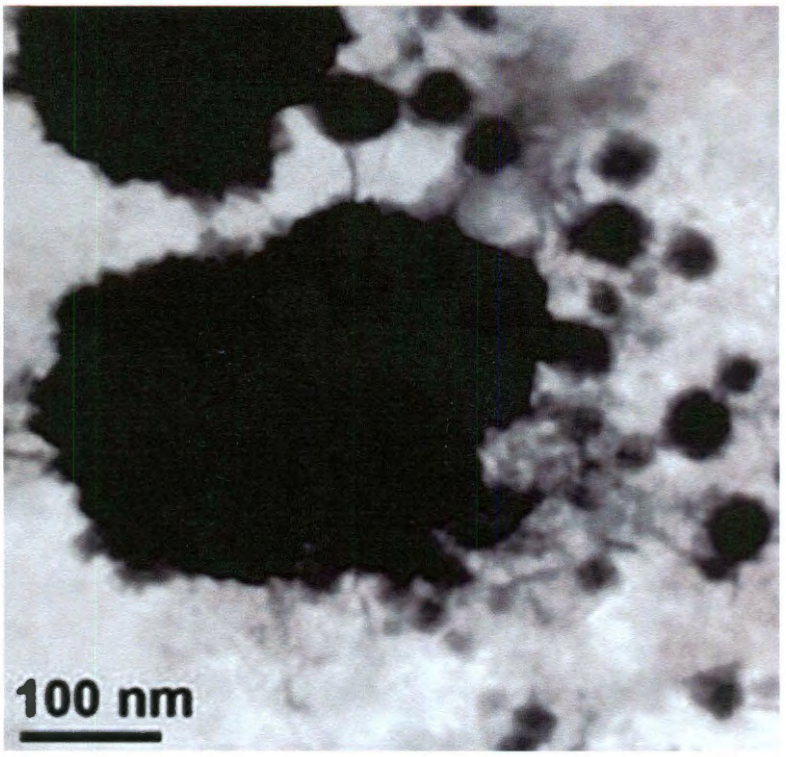

Figure I.5. TEM image showing aggregates of aquatic viruses bound to lepidiocrocite. Taken from C. J. Daughney et al., *Marine Chemistry*, 2004, **91**, 101.

In past instances, membrane processes had been classified according to the driving force and the physical sizes of the separated species.[18,19,20,21] Driving forces include pressure, concentration, or a voltage difference across the membrane. Membranes generally fall into four categories as shown in Figure I.4, (1) Microfiltration membranes, contain the largest pores (macropores) which are greater than 50 nm. (2) Ultrafiltration membranes, contain mesopores in the range of 2 nm to 100 nm in diameter. (3) nanofiltration membranes, contain micropores that are less than 2 nm in diameter. (4) Reverse osmosis membranes, contain pores less than one nanometer in diameter. However, we have now in our own work observed a filtration process which is highly hydro selective, but also screens hydrocarbons with a hydrodynamic size much smaller than the pore size of the fabric. The selectivity of the membrane decreases for molecules

with increasing solubility in water. The membrane therefore can be both physico (pore size) and chemo (charge) selective. This enables the membrane to exhibit latitudes of selectivity not available to other classes of membranes.

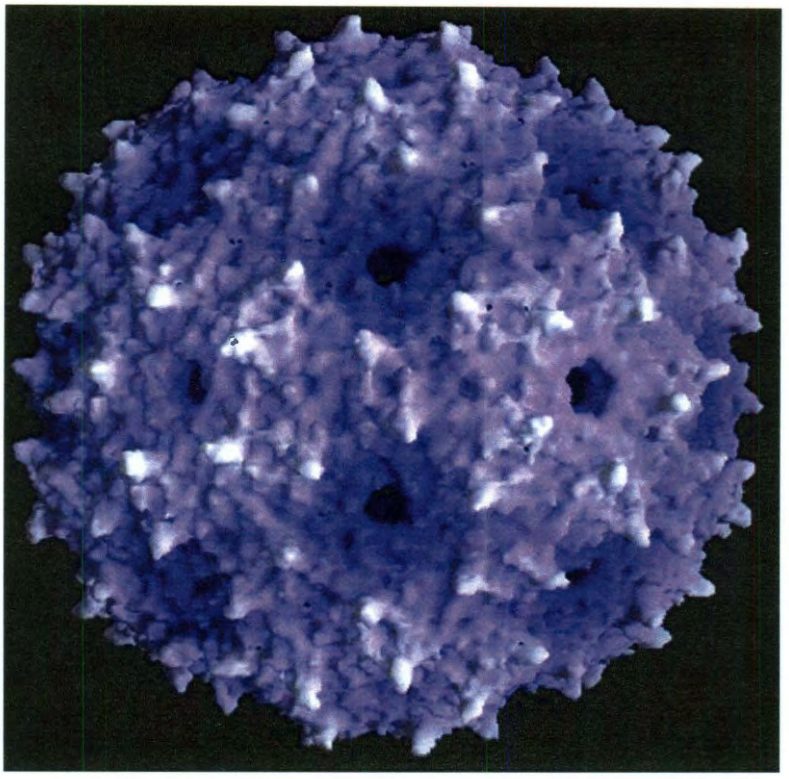

Figure I.6. MS2 bacteriophage capsid space-filling model.[22] Taken from C. M. Fauquet, M. A. Mayo, J. Maniloff, U. Desselberger, and L. A. Ball, *Virus Taxonomy: Eighth Report of the International Committee on Taxonomy of Viruses.*, Elsiver Press, San Diego, California, 2005.

Contamination of water by viral pathogens is endemic in many parts of the world. Sources of contamination include industrial and agricultural wastes, as well as sewage and other forms of pollution. Waste water, containing approximately 7,000 viruses per liter are common, and can be more than 500,000 virus particles per liter.[23] Aspiration by a combat diver of this contaminated water can lead to serious infections and intoxications

through exposure of mucous membranes in the eyes (conjunctiva), nose (rhinal exposure) and mouth. In many cases gastroenteritis, respiratory disease, eye, ear, and nose infections result. However, more serious consequences and life-threatening complications can occur. To overcome this threat a viral filter for aspirated viruses was envisioned. Utilization of a highly hydrophilic filter would allow deposition of aspirated virus contained within the water droplets onto the surface of the filter. Immobilization of the virus would occur through binding to a carboxylic acid functionalized ferroxane nanoparticle. The use of iron oxide nanoparticles in breathing filters was theorized to be useful as iron oxide and oxyhydroxides toxicity is low.[24] It has also been shown that FeOOH and Fe_2O_3 are more resistant to acidic, corrosive, and oxidant conditions.[25]

The affinity for binding of iron nanoparticles to virus pathogens has been observed in nature as shown in Figure I.5.[26] Previous research has shown that viruses interact and act as nucleation sites for the adsorption and precipitation of dissolved metals, especially iron.[27] Up to 50% of "dissolved iron" in sea water is between 30 nm and 100 nm in diameter. Between 90% and 99% is strongly chelated by organic ligands.[28,29] Viral-lepidiocrite binding has been observed in sea water systems. Use of functionalized lepidiocrite also known as ferroxane was thought to enhance its viral binding capacity. The use of carboxylic acid as a functional group on lepidiocrocite would allow tailoring of an interaction with these active sites. Functionalization of leipiocrocite with a carboxylic acid yields the nanoporous iron oxide material ferroxane.[28] This material was used in our studies as a virus binding material. The strategy of synthesis of our filter was to immobilize the nanoparticles onto a fabric porous scaffold. We functionalized a fabric support with hydrophilic alumoxane and hydrophilic ferroxane and subjected this filter to viral screening. Reduction in concentrations of viruses passing through the functionalized filter compared to the un-functionalized filter was four orders of magnitude greater.

Testing of virus filtration was undertaken using bacteriophage MS2 Figure I.6, this is a single stranded (+) RNA virus with an icosahedral capsid about 25 nm in diameter.[30] MS2 is similar to some water borne pathogenic viruses and has been used as a surrogate in several disinfection studies.[31] Compared to other bacteriophage, MS2 has been shown to be more resistant to UV disinfection.[32] In disinfection studies using chlorine and chloramines, MS2 was found to be comparable to or more resistant than Hepatitis A virus[33] and Poliovirus.[34] MS2 has also been recommended by the EPA as an indicator for viral inactivation processes.[35] MS2 is particularly convenient to work with, as its propagation and enumeration are relatively simple when compared to procedures required with pathogenic human viruses.

The organic functionalization of the alumoxane and ferroxane and how that functionalization acts on a macromaterial scale is the key to both filtration projects. In an aquatic environment, nanoparticle behavior is dependent on particle-specific properties (e.g., size, shape, chemical composition, surface charge, and coating), particle state, the surrounding solution chemistry such as pH, ionic strength, ionic composition, and hydrodynamic conditions.[36,37] In turn, the ability for nanoparticles to aggregate or deposit is directly related to its surface chemistry. These factors are important in determining aggregations of particles or deposition onto various surfaces.[40] If the particle is immobile the surface chemistry still dictates its interactions with its surrounding environment. If a surface has a non-repulsive interaction between itself and a mobile surface it is limited in being able to capture that mobile form.[38] This type of transport aggregation also drastically affects toxicity and reactivity in many real world systems.[39]

Particle-particle interactions and particle-surface interactions are usually described by the Derjaguin, Landau, Verwey and Overbeek (DLVO) theory of colloidal stability. However, non-DLVO forces such as steric, magnetic, and hydration forces can also play an important role in the deposition of materials onto a surface. The DLVO

theory[39,40] of colloidal stability describes the total interaction energy experienced by a nanoparticle when approaching another particle, or a surface as, in the case of deposition.

Surfaces that have hydrophilic functionalization have significant amounts of bound water that may play a role in the interaction of particles to that surface. The approach of two particles with hydrated surfaces will generally be hindered by an repulsive interaction, this interaction may occur between MS2 and our surface. However the hydrophilic surface is only one factor in the manipulation of viruses the second factor being the active iron component within the ferroxane nanoparticle.[41]

Virus deposition kinetics to a surface are dependent on the height of the energy barrier to that surface.[41] Virus particles that overcome the energy barrier will deposit on a surface in a deep primary energy minimum. The height of the energy barrier for deposition is directly dependent on the size of the interacting surfaces, with smaller particles exhibiting much lower energy barriers.[41,42] It has been shown that nanoparticles that deposit in primary energy minima onto a surface are less likely to be released from the surface following changes in solution, such as ionic strength and pH.[43] At the ionic strength of typical aquatic systems, the interaction energy of particles is characterized by a high energy barrier and a secondary energy minimum.[44,45]

In aquatic environments, the interactions between nanoparticles and collector surfaces generally described by the DLVO theory of colloidal stability can either be attractive or repulsive. In one example organic functionalization of surfaces with polymers and surfactants impart steric repulsive forces that oppose the long-range attractive magnetic forces between nanoscale zero-valent iron (*n*ZVI) particles. The properties of polymer-coated *n*ZVI are influenced by the chemical composition and structure of the polymer coating.[46] Besides imparting a more negative surface charge due

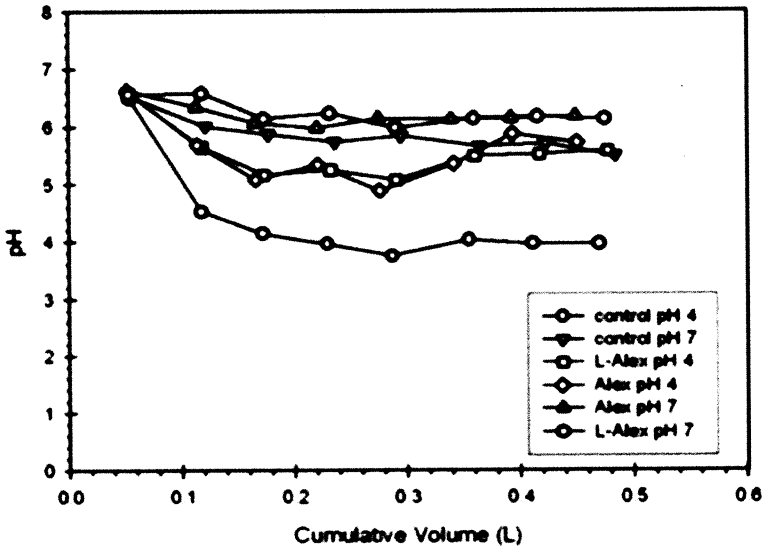

Figure I.7. Difference in transport of organic functionalized particles (L-Alex) compared to un-functionalized particles (Alex). Taken from R. Doshi, W. Braida, C. Christodoulatos, and M. Wazne, *Environ. Res.*, 2008, **106**, 296.

to sorption of, surfactants such as poly(vinyl alcohol-co-vinyl acetate-co-itaconic acid), PV3A, also decrease the isoelectric point.[47] These results collectively suggest that the properties of *n*ZVI are controlled by the characteristics of the surfactant or polymer added, in other words there surface chemistry. A case in point being the deposition behavior of inorganic nanoparticles has shown that bare and surface modified nanoscale aluminum (*n*Al) have demonstrated dissimilar deposition behaviors, even though the core material remains the same.[48]

References

1 J. E. Amsom, *Undersea. Biomed. Res.*, 1991, **18**, 213.

2 G. Zhaneta, K. Lee, K. Hersh, G, Noya, and E. D. Richter, *J. Environ. Engineering and Sci.*, 2003, **111**, 609.

3 N. N. Greenwood and A. Earnshaw, *Chemistry of the Elements*, Pergamon Press, Oxford, 1984, Ch. 7.

4 K. Wefers and C. Misra, "Oxides and Hydroxides of Aluminum." Alcoa Laboratories, 1987.

5 W. H. Gitzen (Ed.), *Alumina as a Ceramic Material*, The American Ceramic Society, Special Publication No. 4, 1970.

6 S. J. Wilson, *J. Solid State Chem.*, 1979, **30**, 247.

7 The term alumoxane is commonly used to describe a species containing an oxo (O^{2-}) bridge (at least) two aluminum atoms, i.e., Al-O-Al.

8 A. W. Apblett, A. C. Warren, and A. R. Barron, *Chem. Mater.*, 1992, **4**, 167.

9 C. C. Landry, J. A. Davis, A. W. Apblett, and A. R. Barron, *J. Mater. Chem.*, 1993, **3**, 597.

10 C. C. Landry, N. Pappe, M. R. Mason, A. W. Apblett, A. N. Tyler, A. N. MacInnes, and A. R. Barron, *J. Mater.Chem.*, 1995, **5**, 331.

11 K. G. Karthikeyan, H. A. Elliott, and J. Chorover, *J. Colloid Interface Sci.*, 1999, **209**, 7278.

12 F. J. Hingston, A. M. Posner, and J. P. Quirk, *J. Soil Sci.*, 1972, **23**, 177.

13 R. W. Baker, *Membrane Separation systems: Recent Developments and Future Directions*, Noyes Data Corp., Park Ridge, NJ, 1991.

14 *Inorganic Membranes: Markets, Technologies, Players*, Business Communications Co., Inc. (Norwalk, CT), Marketing Study GB-112N, 1997.

15 H. D. Hsieh, in *New Membrane Materials and Processes for Separation*, Eds. K. K. Sirkar and D. R. Lloyd, American Instituite of Chemical Engineering, New York, Vol. 84, 1988.

16 A. J. Burgraaf, in *Membrane Science and Technology Series 4, Fundamentals of Inorganic membrane Science and Technology,* Eds. A. J. Burggraff and L. Cot, Elsevier, New York, 1996, p. 21.

17 L. Palacio, J. I. Calvo, P. Pradans, A. Hernandez, P. Vaisanen, and M. Nystrom, *J. Membr. Sci.*., 1999, **152**, 189.

18 R. G. Gutman, *Membrane Filtration: The Technology of Pressure-driven Crossflow Processes*, Adam Hilger, Bristol, 1987.

19 M. Mulder, *Basic Principles of Membrane Technology*, 2nd Ed. Kluwer Academic Publishers, London, 1996.

20 R. R. Bhave, *Inorganic Membranes: Synthesis, Characteristics, and Applications*, Van Nostrand Reinhold, New York, 1991.

21 T. Matsuura, *Synthtic Membranes and Membrane Seperation Processes*, CRC Press, Ann Arbor, 1994.

22 C. M. Fauquet, M. A. Mayo, J. Maniloff, U. Desselberger, and L. A. Ball, *Virus Taxonomy: Eight Report of the International Committee on Taxonomy of Viruses.*, Elsiver Press, San Diego, Caliornia, 2005.

23 W. Renate, W. Macht, J. Dunkop, R. Hecht, U. Hornig, and P. Schulze, *Water Res.*, 1989, **23**, 133.

24 R. M. Cornell and U. Schwertmann, *The Iron OxidesI,* VCH, New York, 1996.

25 M. Pourbaix, *Atlas d'Equilibre Electrochimiques*. Gauthier-Villars, Paris, 1963.

26 C. J. Daughney, X. Chatellier, A. Chan, P. Kenward, D. Fortin, C. A. Suttle and A. D. Fowle, *Marine Chemistry*, 2004, **91**, 101.

27 (a) L. A. Warren and F. G. Ferris, *Environ. Sci. Technol.*, 1998, **32**, 2331. (b) X. Chatellier, D. Fortin, M. M. West, G. G. Leppard, and F. G. Ferris, *Eur. J. Mineral*, 2001, **13**, 705. (c) C. J. Daughney, D. A. Fowle and D. Fortin, *Geochim.*

Cosmochim. Acta., 2001, **65**, 1025. (d) J. B. Fein, S. Scott, and N. Rivera, *Chem. Geol.*, 2002, **182**, 265.

28 (a) M. N. Wells and E. D. Goldberg, *Mar. Chem.*, 1992, **40**, 5. (b) M. N. Wells and E. D. Goldberg, *Mar. Chem.*, 1993, **41**, 353. (c) M. N. Wells and E. D. Goldberg, *Limnol. Oceanogr.*, 1994, **39**, 286. (d) J. Wu and G. W. Luther III, *Limnol. Oceanogr.*, 1994, **39**, 119. (e) J. Wu and G. W. Luther III, *Mar. Chem.*, 1995, **50**, 159 (f) J. Wu and G. W. Luther III *Geochim, Cosmochim. Acta.*, 1995, **60**, 2729. (g) J. Wu, E. Boyle, W. Sunda, and L. –S. Wen, *Science*, 2001, **292**, 847.

29 J. Nishioka, S. Kakeda, C. S. Wong, and W. K. Johnson, *Mar. Chem.*, 2001, **74**, 157.

30 M. T. Madigan and J. M. Martinko, *Brock biology of microorganisms*. Upper Saddle River, N. J., Pearson Prentice Hall, 2006.

31 (a) M. H. Cho and J. Chung, *Applied Environmental Microbiology*, 2005, **71**, 270. (b) M. A. Butkus, *Applied Environmental Microbiology*, 2004, **70**, 5. (c) Y. Koizumi and M. Taya, *Biochem. Eng. J.*, 2002, **12**, 107. (d) E. D. Mackey, *J. Am. Water Works Assoc.*, 2002, **94**, 62.

32 R. Sommer, *Water Res.*, 2001, **35**, 3109.

33 M. D. Sobsey, T. Fuji and P. A. Shields, *Water Sci. and Tech.*, 1988, **20**, 385.

34 J. A. Tree, M. R. Adams and D. N. Lees, *Appl. Environ. Microbiol.*, 2003, **69**, 2038.

35 Pirnie, M. *Guidance manual for compliance with filtration and disinfection requirments for public water systems using surface water sources.* USEPA, 1991.

36 S. J. Klaine, P. J. J. Alvarez, G. E. Batley, T. F. Fernandes, R. D. Handy, D. Y. Lyon, S. Mahendra, M. J. McLaughlin, and J. R. Lead, *Environ. Toxicol. Chem.*, 2008, **9**, 1825.

37 M. R. Wiesner and J. –Y. Bottero, *Environmental Nanotechnology*, The McGraw-Hill Companies: New York, 2007, p450.

38 M. Elimelech, J. Gregory, X. Jia, and R. A. Williams, *Particle Deposition and Aggregation: Measurement, Modeling, and Simulation*, Butterworth-Heinemann, Oxford, 1995.

39 E. J. W. Verwey and J. T. G. Overbeek, *Theory of the Stability of Lyophobic Colloids*, Elsevier, Amsterdam, 1948.

40 B. V. Derjaguin and L. D. Landau, *Acta Physicochim, URSS*, 1941, **14**, 633.

41 T. W. Healy, A. Homola, R. O. James and R. J. Hunter, *Faraday Discuss.*, 1978, **65**, 156.

42 M. Elimelech and C. R. O'Melia, *Langmuir*, 1990, **6**, 1153.

43 K. L. Chen and M. Elimelech, *Langmuir*, 2006, **22**, 10994.

44 N. Tufenkji and M. Elimelech, *Langmuir*, 2005, **21**, 841.

45 M. W. Hahn and C. R. O'Melia, *Environ. Sci. Technol.*, 2004, **38**, 210.

46 T. Phenrat, Y. Q. Liu, R. D. Tilton, and G. V. Lowry, *Environ. Sci. Technol.*, 2009, **43**, 1507.

47 Y. P. Sun, X. Q. Li, W. X. Zhang, and H. P. Wang, *Colloids Surf. A*, 2007, **308**, 60.

48 R. Doshi, W. Braida, C. Christodoulatos, and M. Wazne, *Environ. Res.*, 2008, **106**, 296.

Chapter 1

A new functionalization strategy for oil water separation membranes

Introduction

The information provided in this chapter has been published in the Journal of Membrane Science 2011, **382**, 107.

Oily waste waters pose a significant threat not only to US Navy personnel but also to the environment in general. They are an inconvenient by product of many industries, and cannot be easily processed[1,2,3,4,5] such a hazard was observed recently at the BP oil leak in the Gulf of Mexico. This catastrophe pointed to the need for a readily deployable system for the separation of water (especially salt water) from hydrocarbons and the need for protective garments against these threats. Many techniques exist for the separation of emulsions, however membrane filtration has been shown to be one of the best methods for separation of oily waste waters.[6,7,8] We believe by utilizing membrane technology and incorporating it into USN garments we will be able to negate the threat of toxic petrochemicals.

When designing a membrane three factors need to be accounted for; controlled pore size for exclusion of hydrocarbon molecules,[9,27] high permeate flux of target eluant allowing for fast equilibration that is necessary for diving purposes, and anti-fowling properties.[10,11,12,13] When using a base fabric the pore size is a direct consequence of the weave of the fabric. High permeate flux of water, as well as membrane fouling or lack thereof would be controlled by the hydrophilicity of the functionalized garment. Membrane fouling is a significant factor when ensuring reusability of the proposed garment. Fouling can be due to a number of factors, the interaction between membrane surfaces and solutes plays an important role in determining the extent of membrane fouling. This is explained by the mechanisms[14,15] of pore blocking, cake formation, ligand exchange reactions, charge interaction, or hydrophobic interaction. Of the

aforementioned mechanisms, hydrophobic interaction between solutes and membrane material is frequently accepted as one of the predominant fouling mechanisms. Therefore, membrane fouling is expected to be more severe with hydrophobic than hydrophilic membranes.[16,17] Hydrophilic membranes are less sensitive to adsorption compared to their hydrophobic analogues. They have been shown to overcome many of these negative characteristics, especially with regards to anti-fouling,[18,19,20,21] as well as having high permeate flux for aqueous eluants,[22] and in many ways are superior to hydrophobic membranes.[23] Several methods such as surface segregation,[24]surface coating,[25] and surface graft polymerization,[26] have been utilized for enhancing surface hydrophilicity and thus antifouling properties. However, we believe that our nanomaterial can be added to this list and can provide an excellent alternative.

The fabrication of an alumina membrane using alumina nanoparticles with a hydrophilic side chain functionalization would yield the best possible result with regards to the above criterion. The extent of hydrophilicty would significantly contribute to the success of the membrane. Hydroxyl terminated alumina membranes had been investigated by our laboratory previously.[27,28] These particular membranes are utilized extensively due to their extreme tolerance to adverse effects such as temperature extremes, pH, and oxidation, and tolerance to solvents.[29,30] Carboxylic functionalized inorganic nanoparticles have been synthesized and studied by this group previously.[31,32] It has been shown that the carbonyl and alcoholic oxygen's of a carboxylic moiety bind to hydroxyl terminated alumina, and iron oxides.[33] This leaves the accompanying side chain of the carboxylic acid orientated away from the surface of the nanoparticle, and as such significantly contributes to the material character of that nanoparticle. Carboxylic acids, with a myriad of side chain terminations can be used to promote particular material properties of the functionalized nanoparticle such as selective aggregation, hydrophilicity/hydrophobicity.

The use of an alumina nanoparticle as the functionalization element of the fabric is due to its ability to display on a material scale the functionalities of the surface

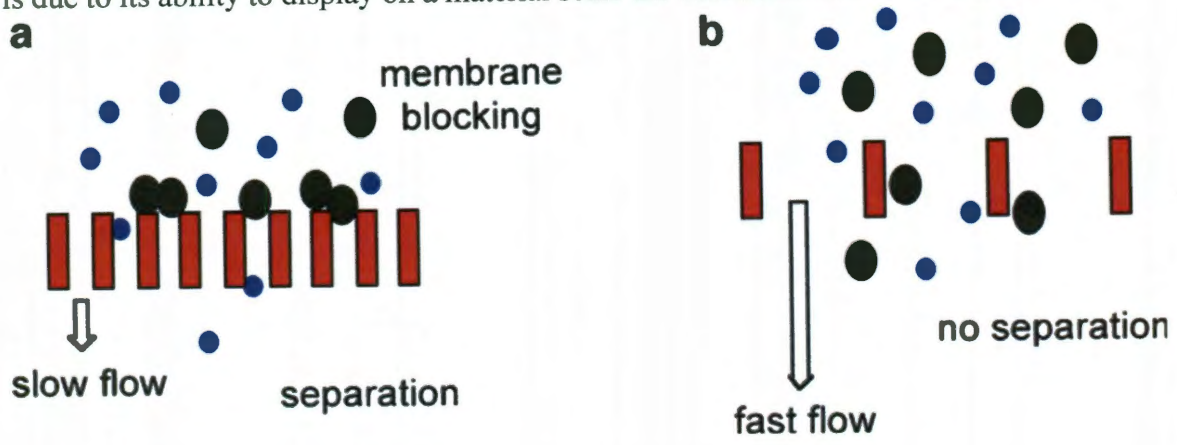

Figure 1.1. Schematic representation of the attributes of membranes with (a) small and (b) large pore size.

stabilized molecular ligand. The nanomaterial can then be easily converted into a desired form such as the coating of a fiber, or deposition on a surface. The coated material can then take on the material properties of the original alumina nanoparticle such as hydrophilicity. This is of significant benefit as the substrate material is now modified on a macro material scale, without alteration of, its chemical substructure. This is something that could not be achieved by chemical alteration of the material alone, and also allows for easy transference of a desired functionality to almost any substrate material.

In this chapter I have screened for super-hydrophilic terminated carboxylic acids, finding the most hydrophilic to functionalize an alumina nanoparticle, the engineer a fabric membrane using these nanoparticles. Unfortunately, small pore sizes (and hence good chemical selectivity, i.e., Figure 1.1a) results in low permeate flux needing high pressures and/or very large systems. Alternatively, while large pore sizes often minimize fouling and allow for a high permeate flux, chemical selectivity is not attainable Figure 1.1b. As it would be desirable to design a membrane with the advantages of both, the

question can be posed: is it possible through chemical control of the surface to design a large pore membrane with the associated high flux, but with the separation characteristics of a small pore membrane?

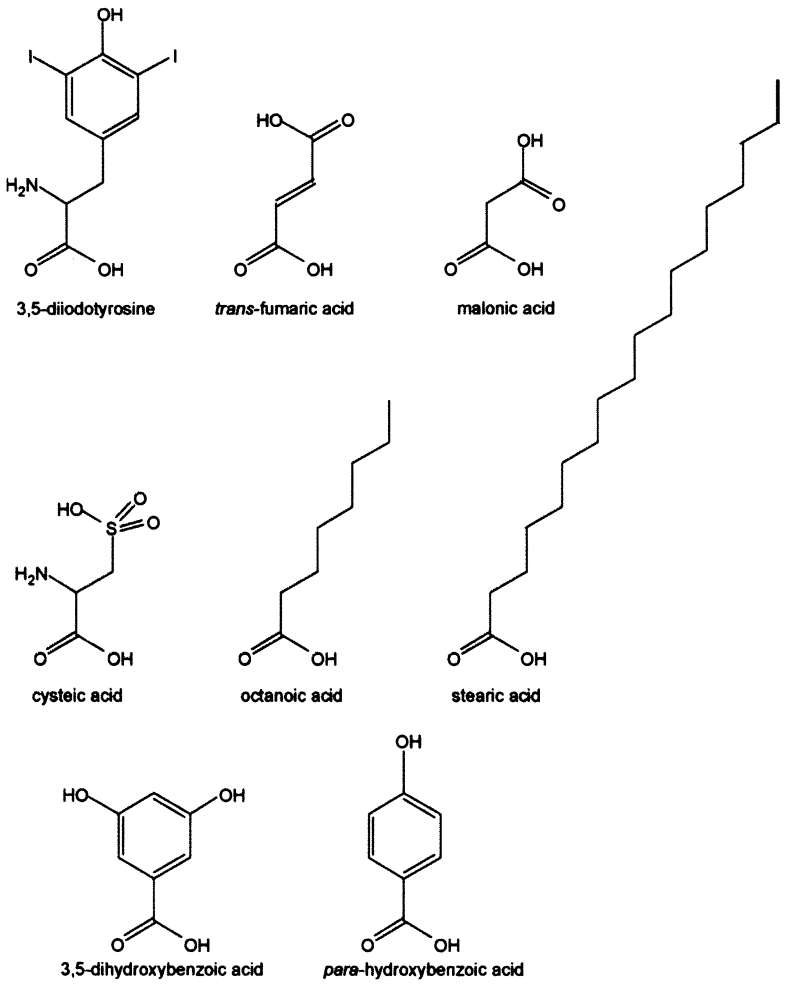

Figure 1.2. Carboxylic acids that were investigated using contact angle measurements.

Results and Discussion

Our previous work has shown that carboxylic acid functionalization of alumina surfaces can change the surface properties of the alumina.[40] For example, reaction of a carboxylic acid with an alumina membrane can alter the flux of the membrane.[27] This effect was related to the hydrophilicity, as indicated by the contact angle of water on the

surface. As our goal is to create a strongly hydrophilic surface on a highly porous substrate, we initially investigated a range of chemical substituents in order to determine structure/property relationships.

Table 1.1. Summary of reaction conditions for carboxylic acid functionalization of alumina surfaces.

Carboxylic acid	Mass (g)	Solvent	Volume (mL)	Molarity (M)	Temperature (°C)	Reaction time (h)
3,5-Diiodotyrosine	1.87	DMSO	20	0.1	160	24
Trans-Fumaric acid	2.32	EtOH	40	0.5	60	24
Malonic acid	2.08	H_2O	40	0.5	105	24
Cysteic acid	3.74	H_2O	40	0.5	105	24
Octanoic acid	2.90	DMSO	40	0.5	160	24
Stearic acid	1.14	$CHCl_3$	40	0.1	61	24
3,5-Dihydroxybenzoic acid	3.08	DMSO	40	0.5	160	24
para-Hydroxybenzoic acid	2.76	DMSO	40	0.5	160	24

Each of the carboxylic acids studied Figure 1.2 was functionalized onto the alumina coated silicon wafers (see Experimental) to allow for ready comparison by contact angle measurements, using goniometer contact angle techniques. XPS analysis was undertaken to ensure that carboxylic acid onto the alumina surface..[40] XPS analysis

of the surfaces all showed the appropriate elemental composition associated with the acid. In addition, high-resolution C1s and O1s spectra Figure 1.3 are consistent with the covalent attachment of the carboxylic acid to the alumina surface.[20,33,34] Our prior work[27] suggested that *para*-hydroxybenzoic acid functionalization would make an alumina surface slightly more hydrophilic than the native oxide. This was therefore used as the basis for our comparison.

Figure 1.4 shows the water contact angle measurements made for the range of acids studied. It may be seen that cysteic acid functionalized alumina coated wafers were extremely hydrophilic, achieving complete wettability when in contact with water. In fact the extent of wetting is such that complete wetting of the surface results Figure 1.5. We attribute the performance of cysteic acid to the hydrogen bonding abilities of both sulfonate and amine moieties, on functionalized cysteic acid and its Zwitter ionic form Figure 1.6. Both moieties can form multiple hydrogen bonds to the solvent, thus making the surface of the alumoxane nanoparticles hydrophilic. Based on these results cysteic acid was chosen as the best candidate for the creation of our highly hydrophilic alumoxane Nomex® composite membrane.

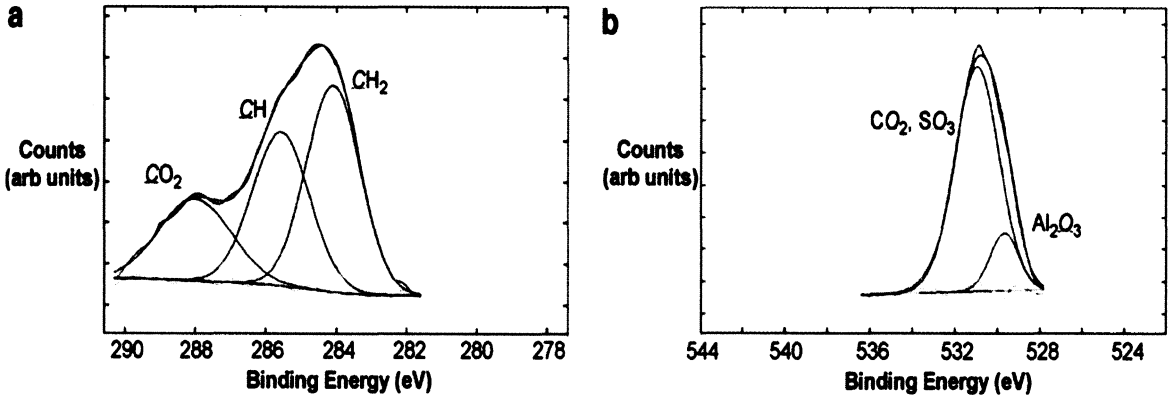

Figure 1.3. The (a) C1s and (b) O1s regions of the XP spectra for cysteic acid functionalized alumina surface.

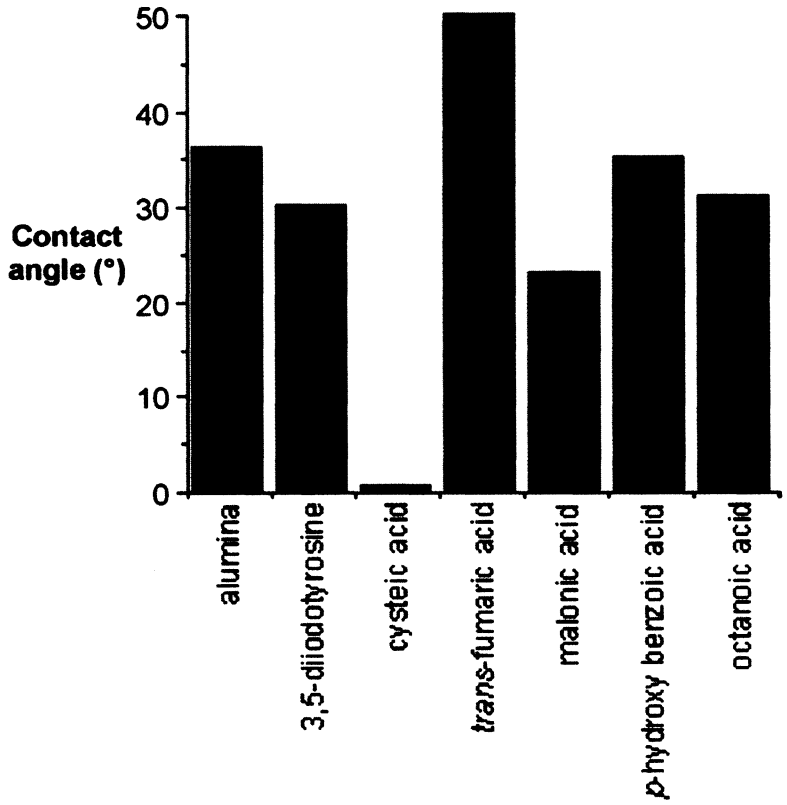

Figure 1.4. Contact angle measurements for water on carboxylic acid functionalized alumina surfaces.

We have previously reported that carboxylic acid functionalized alumina nanoparticles (carboxylate alumoxanes) can be used to coat a range of fabrics and fibers[35] to form a continuous, conformal layer that does not alter either the properties of the fiber or the macroscopic porosity of the fabric. In our previous work we have subsequently converted the alumoxanes to alumina by thermolysis at 400 °C. However, when alumoxanes are heated to 100 °C they lose their solubility (and are thus not removed from the substrate) but retain their surface functionalization.

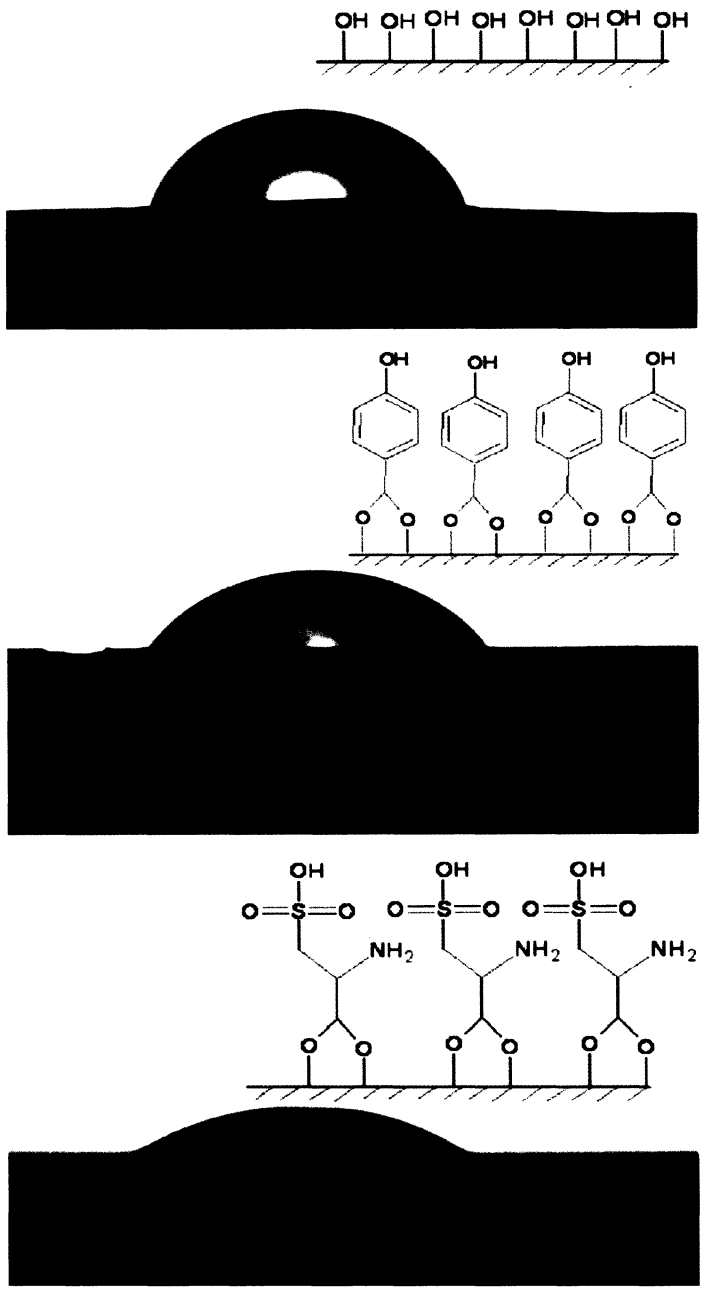

Figure 1.5. Photographic images of water droplet on unfunctionalized alumina surface (top), para-hydroxybenzoic acid functionalized alumina surface (middle), and cysteic acid functionalized alumina surface (bottom). Note the image of the water droplet on the cysteic acid functionalized alumina surface was taken immediately upon dropping on the surface since within a few seconds the droplet completely wets the surface.

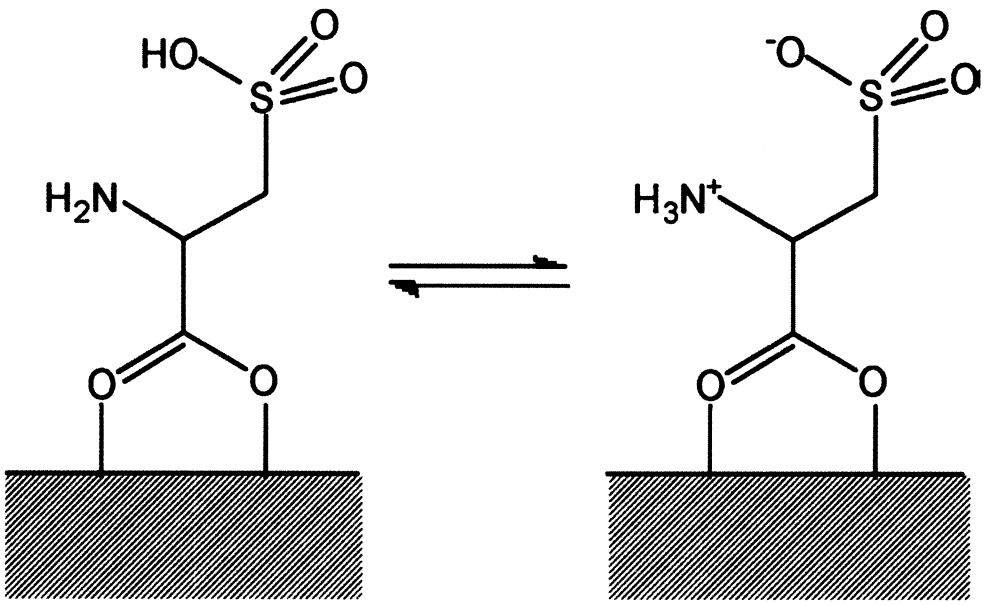

Figure 1.6. Cysteic acid showing Zwitter ionic forms.

Our goal was to deposit a thin layer of cysteic alumoxane onto a suitable highly porous support, anneal to 100 °C to provide a cysteic functionalized alumina surface on the support. In contrast to our previous membrane work,[36] the alumoxane-derived surface is not to act as a nano porous membrane (1 – 10 nm pore diameter), but to act as the sidewalls of a particle filtration membrane (10^3 - 10^6 nm), see Figure 1.7. Thus any differentiation of flux between various compounds will be as a consequence of surface functionalization rather than pore diameter. Furthermore, the fabric support was chosen with pores sufficiently large that no separation or differentiation could be possible Figure 1.8.

Carboxylate functionalized alumina nanoparticles are readily made from the reaction of boehmite with carboxylic acids,[37] and cysteic-alumoxane is made in the same manner (see Experimental). However, the average particle size of the boehmite starting material is nearly two orders of magnitude larger than the cysteic acid alumoxane particles (i.e., 3 μm versus 30 nm).The presence of any un-reacted boehmite can alter the resulting uniformity of films or coatings. Removal of un-reacted boehmite from the

cysteic acid alumoxane solution by centrifugation reduced the average particle size from 120 nm to 18 nm.

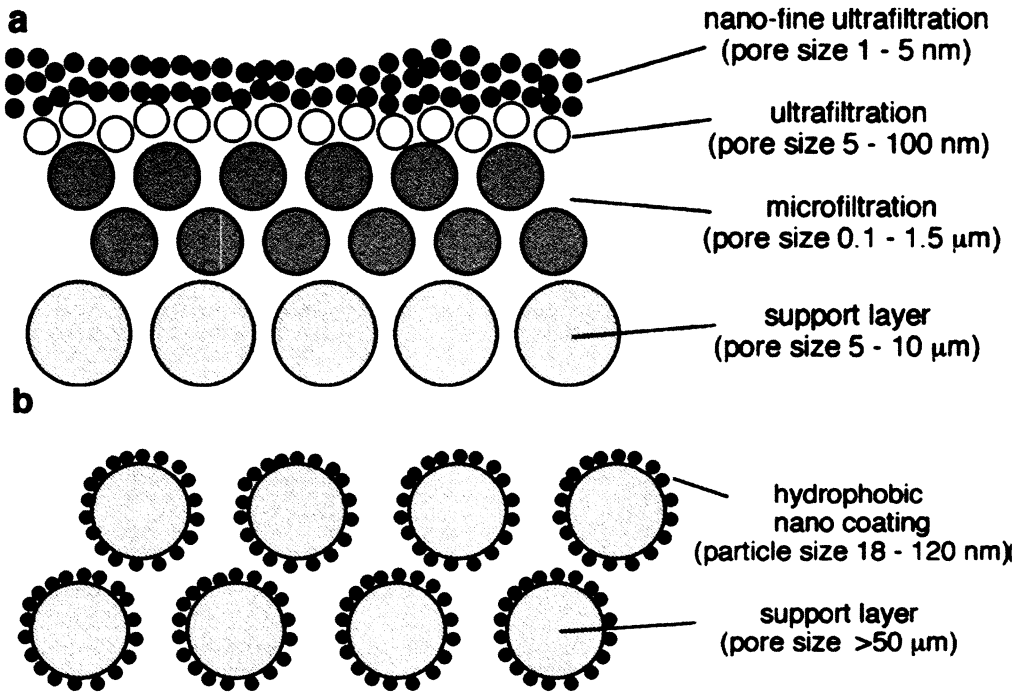

Figure 1.7. Schematic representation of a traditional nano porous membrane (a) and an alumoxane functionalized particle filtration membrane (b).

In order to demonstrate that surface functionalization and not pore size is responsible for any chemical separations we chose to use Nomex® fabric as a support since the large weave i.e., pore-throat size cannot facilitate separation Figure 1.8a. Functionalization of the membrane is achieved by bringing the surface of the support into contact with a solution of cysteic acid functionalized alumoxane. The solution is drawn into the surface pores of the support by capillary forces. The membrane deposited onto the surface of the support should be uniformly thin throughout in order to maximize the flux, and not affect the pore size of the fabric (membrane).

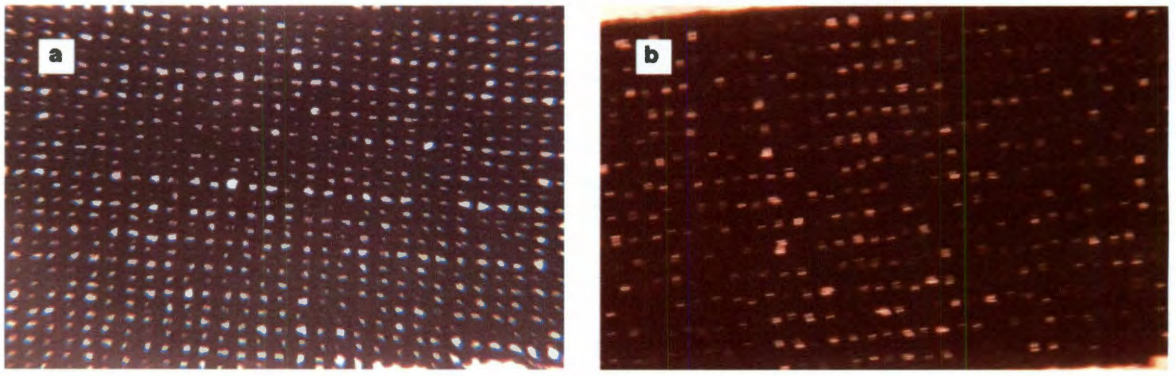

Figure 1.8. Optical images of Nomex© fabric (a) and L-cysteic acid alumoxane functionalized Nomex© fabric (CA-Nomex©) (b).

Figure 1.9. SEM images of un-functionalized Nomex© fabric (a), cysteic acid alumoxane functionalized Nomex© fabric (b), and cysteic acid alumoxane functionalized Nomex© fabric after annealing to 100 °C (c).

The initial pH of the reaction solution for acetic acid alumoxanes was measured to be 4.5 as this was deemed to be important in the synthesis of homogenous 18 nm alumoxane nanoparticles. In the present work, investigation of coating formation was deemed to be important for the application of dip coating a fabric, covering a large surface area. Whereby a uniform coating is required consideration of the effect of pH on

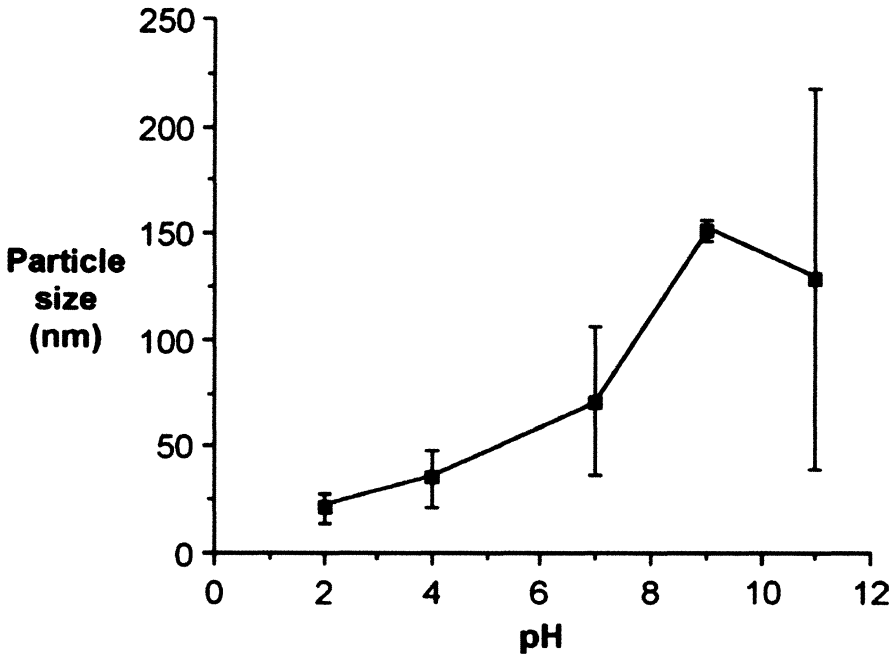

Figure 1.10. A plot of average particle size of cysteic acid functionalized alumoxane as a function of the pH.

the drying pattern was examined. It was found that drying cysteic acid alumoxane solution at different pH levels at 100 °C resulted in significantly different drying patterns. Drying cysteic acid alumoxane at acidic pH resulted in significantly more homogenous drying patterns as well as smaller agglomerations compared to basic pH that can be seen in Figure 1.10. This can also be seen in Figure 1.11, which shows the 3D AFM images of the dried agglomerates of L-cysteic acid alumoxane at pH 4 and 11. This behavior is a significant factor in uniformly coating on our chosen Nomex® scaffold. Uniform coating

of our scaffold occurred at pH 2 as this resulted in fine 25 nm aggregates (see Experimental).

Table 1.2. Dextran molecules used for testing pore size.

Dextran	Average molecular weight (g/mol)	D_s (nm)
T-10	10,500	1.8-3
T-40	37,500	4-6
T-70	67,800	6-9
T-500	413,000	15-19
T-2000	1,652,000	27

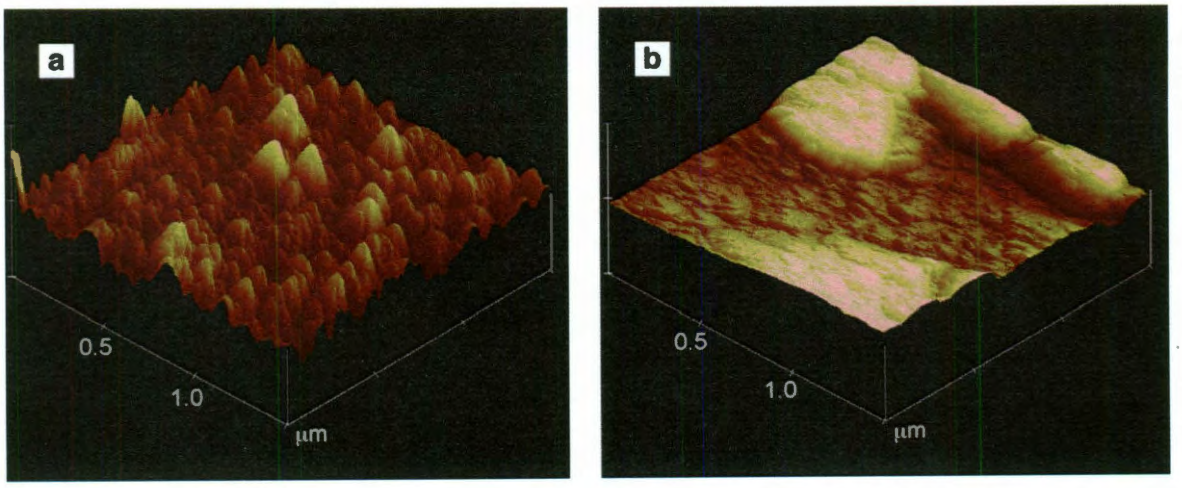

Figure 1.11. AFM image of L-cysteic acid alumoxane dried aggregates, dried at pH 4 (a) and 11 (b). The vertical scale is 50 and 500 nm, respectively.

While there is some webbing in the coated Nomex® Figure 1.9b and c, there is no decrease in the weave (i.e., pore diameter of the fabric) and no pressure drop as compared to the untreated Nomex®. Given the improved synthesis of small, highly uniform, alumoxane particles and their aggregates and the subsequent formation of alumina nanoparticle coated membranes we have prepared a membrane using new cysteic acid

alumoxane nanoparticles which has similar pore size defined by the original Nomex® fabric but with enhanced screening for hydrocarbons. The uniformity of the alumoxane coating and the retention of the L-cysteic acid surface functionalization may be seen by the EDS map for sulfur and nitrogen (see Figure 1.2 and Figure 1.6). Figure 1.12 shows not only the presence of both elements on the entire surface of each individual Nomex® fiber, but the superposition of the elements as expected from the chemical formula of L-cysteic acid. Permeate flux, and permeability measurements were performed as well as size exclusion experiments to determine if the functionalized membrane operates as an entropic barrier or solely by size exclusion dynamics. Given the results presented below

Table 1.3. Time testing of hydrocarbons and hydrocarbon emulsions.

Eluant	Time non-functionalized Nomex© (s)	Time functionalized Nomex© (s)
DI water	48	53
Brine	55	58
Hexadecane	163	278
Oleic acid	1076	14,784
Automotive oil	4381	No elution after 24h
DI water:automotive oil (1:1) emulsion	190	No elution of emulsion
DI water:oleic acid (1:1) emulsion	9699	8954
Brince:automotive oil (1:1)	9699	Only elution of separated brine not emulsion
Brine:oleic acid (1:1)	3228	9240

it was important to demonstrate that the pore size had not changed significantly, i.e., this was still a particle filtration membrane where no selectivity should be observed. Figure 1.13 shows a comparison of the selectivity of the Nomex® fabric with and without treatment as a function of molecular weight. Dextran molecules with defined average molecular weights were used Table 1.2. As may be seen from Figure 1.13, there is a very small amount of selectivity at molecular weights at 1,652 kDa: far in excess of the sizes of organic molecules that would be expected in such polluted waters as frac or production water.

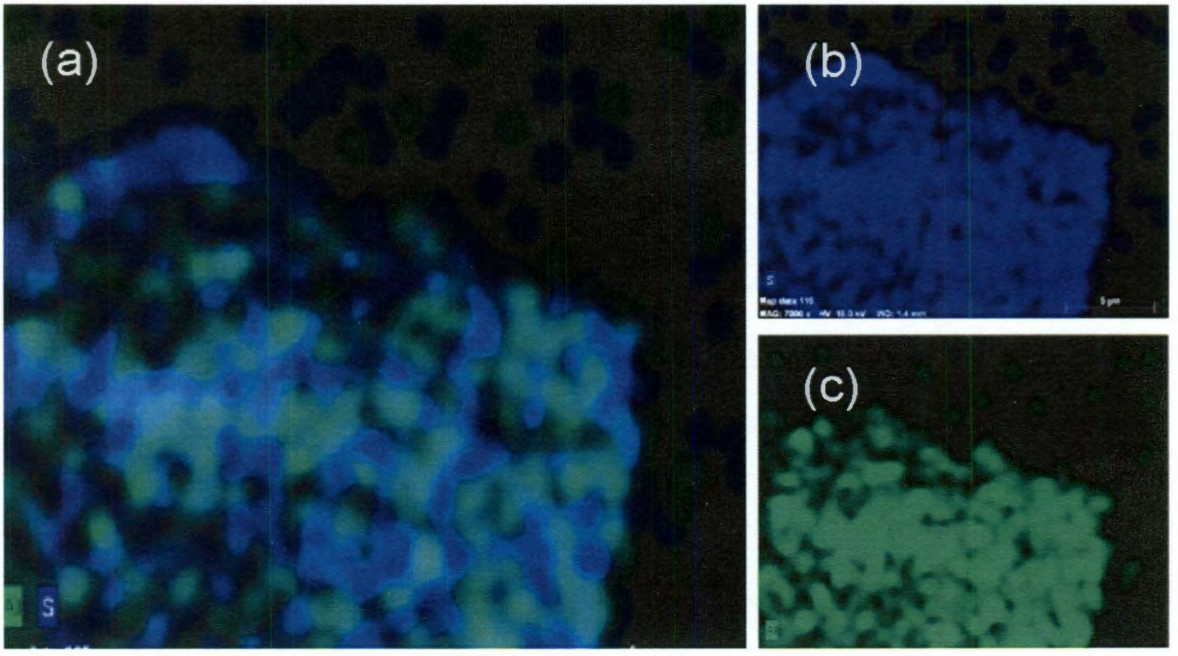

Figure 1.12. EDS images of L-cysteic acid alumoxane functionalized Nomex© fiber showing a composite images of the (a) sulfur (b)and nitrogen maps (c).

We have shown that cysteic alumoxane coated Nomex® shows essentially no differentiation with respect to molecular size except at the very high molecular weights. Thus, the coated materials would not be expected to show differentiation purely on the basis of molecular size. However, based upon our rational, the hydrophilic nature of the

surface should allow differentiation with regard to flux between various compounds. To investigate the effect of the surface treatment on various compounds, the Nomex® fabric (both treated and untreated) was used for end-on filtration (see Experimental) and the time for a set volume to flow was measured Table 1.3. Subsequently, the volumetric flow rates and volumetric flux values were determined for combinations that passed through the functionalized Nomex®

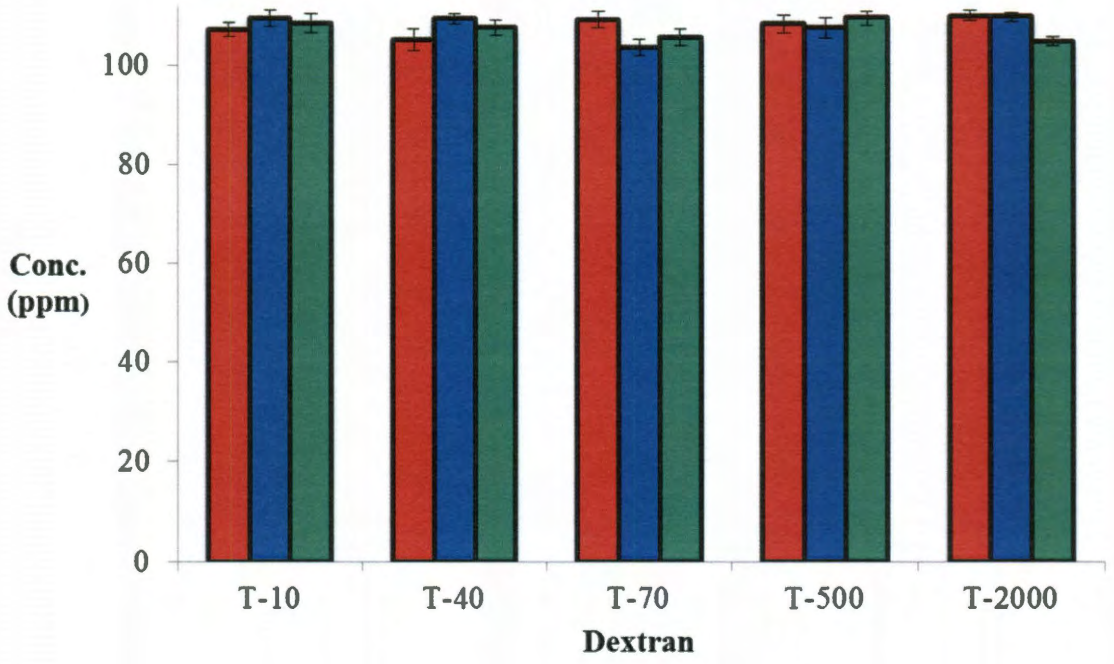

Figure 1.13. TOC measurements of Dextran's through untreated Nomex© fabric (red) as compared to Nomex© dip coated with cysteic acid alumoxane nanoparticle before (blue) and after (green) annealing to 100 °C.

Analysis of relevant eluants was performed using 250 mL of each sample in both pure and mixtured were tested Table 1.3. Emulsions of eluants were made in a 1:1 ratio with DI water and brine. For the DI water emulsion no elution was observed for automotive oil as this formed a stable emulsion, which did not separate. However for

brine emulsions, brine was eluted but oil was not. This is due to the fact that brine does not form stable emulsions and tends to separate organic and aqueous layers, a phenomenon which is used often in organic chemistry to separate aqueous and organic phases. For highly viscous hydrocarbons the ability of the porous material to screen was exemplary, this can be seen in Figure 1.14 where the material retains automotive oil in excess of 12 hr.

Table 1.4 provides a summary of the characteristics of the hydrocarbons and the concentration employed. Standard emulsions of each hydrocarbon were prepared in aqueous solution. The emulsions were passed through a dead-end filtration system. From inspection the volumetric flux and flow rates are exponentially higher for aqueous

Table 1.4. Volumetric flow and flux rate calculations with Nomex© and L-cysteic acid alumoxane functionalized Nomex© (CA-Nomex©) membranes at pH 7.

Membrane	Eluant	Time (s)	Volumetric flow rate ($10^{-6}m^3/s$)	Volumetric flux ($10^{-6}m/s$)
Nomex©	DI water	48	265.4	10,616
Nomex©	Brine	55	231.6	9264.5
Nomex©	Hexadecane	163	78.0	3118.7
Nomex©	Oleic acid	1076	11.8	472.9
Nomex©	Brine:oleic acid	3228	3.9	156.9
CA-Nomex©	DI water	53	240.3	9613.1
CA-Nomex©	Brine	58	219.6	8785.5
CA-Nomex©	Hexadecane	278	45.8	1832.5
CA-Nomex©	Oleic acid	14,784	0.815	32.6
CA-Nomex©	Brine:oleic acid	9240	1.4	55.0

systems compared to hydrocarbons. It is understood that the stability of such a barrier against oil-water emulsions have significant issues with regards to tribological activity. Herein we describe two experiments that demonstrate the stability of the coating applied to the Nomex® fabric and thus the suitability of this membrane for real world use. The ability of the garment to stand up to tribological stress was tested using the MIT fold test where L-cysteic acid functionalized alumoxane coated Nomex® was folded on the same axis 160 times and analyzed using SEM and EDS techniques. It can be seen from

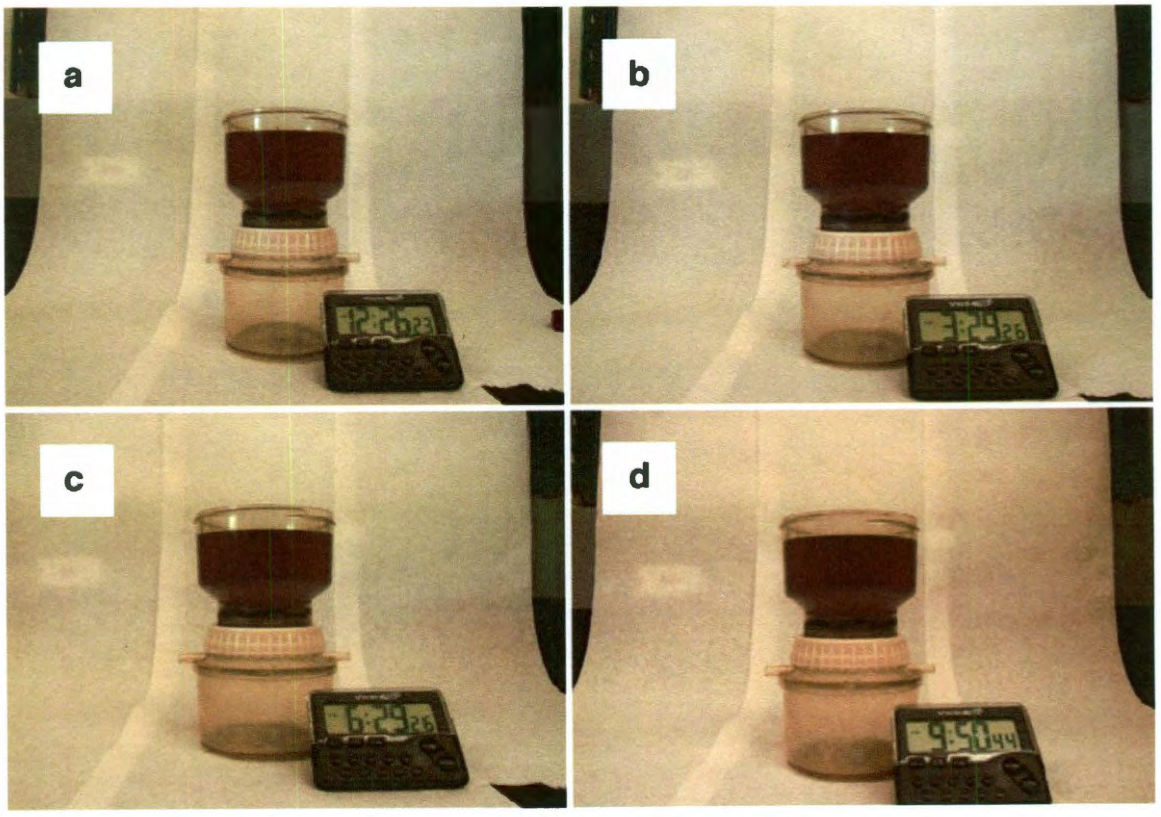

Figure 1.14. Optical images of dead-end filtration of automotive oil at (a) 3, (b) 6, (c) 9, and (d) 12 hrs.

Figure 1.15 that there is negligible loss of alumoxane coating from the Nomex® fabric at the inside crease where there is great physical wear as opposed to out of crease where

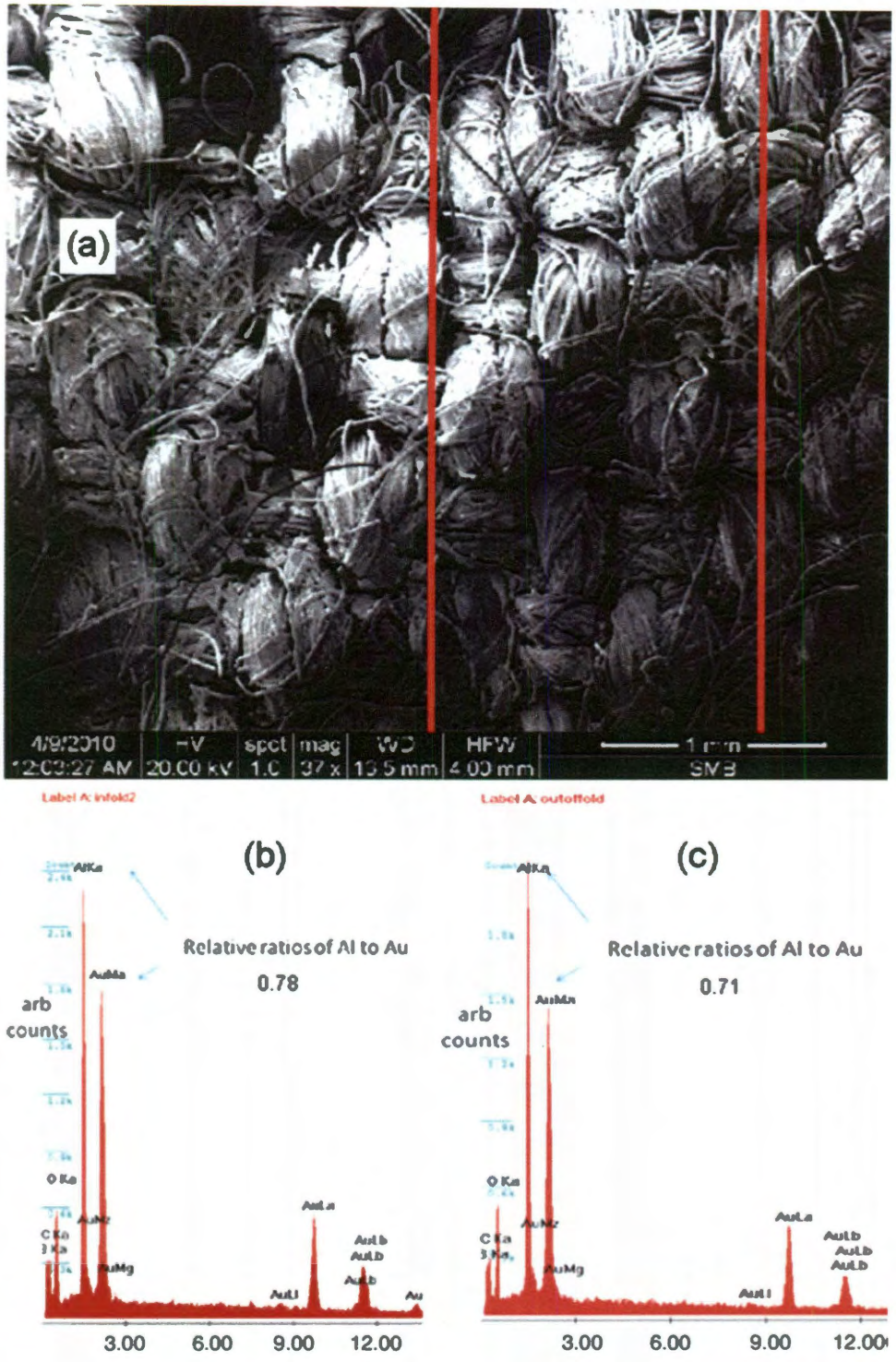

Figure 1.15. SEM images of L-cysteic acid alumoxane coated Nomex© fabric after 160 folds (a) with associated EDS of (b) the crease (left red line) and (c) outside the crease (right red line).

there is the least amount of physical wear. The relative amounts of aluminum to gold were compared after 160 successive folds using EDS line techniques, both inside the crease and outside. It can be seen that the amounts do not vary significantly both on inspection and as a comparison between gold and aluminum. As a second experiment the shedding of aluminum was measured to ensure that there is not excess loss of coating from normal operation. Successive titers of DI H_2O were passed through a 5.5 cm^2 diameter circle of functionalized membrane. These titers were analyzed for aluminum using ICP-OES techniques. It is interesting to note that after eight liters of washing only 0.1 ppm of aluminum was detected Figure 1.16.

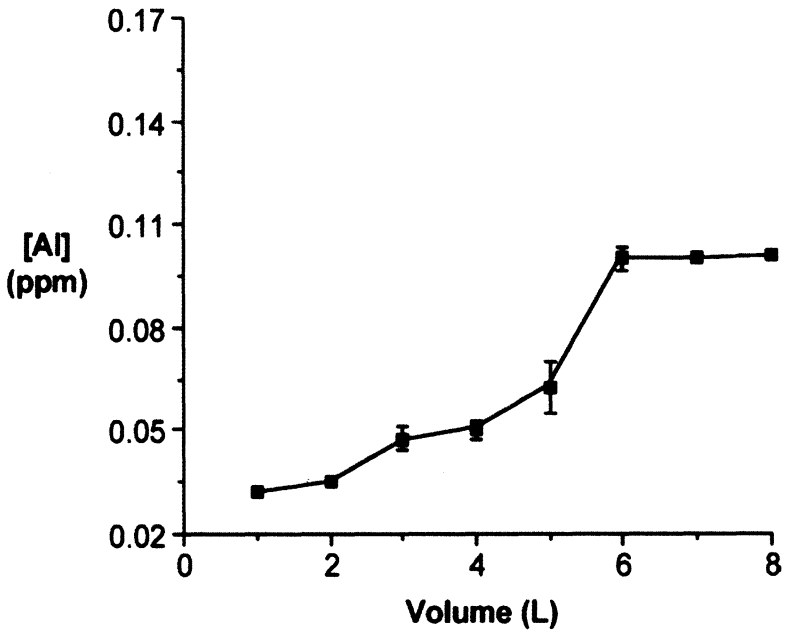

Figure 1.16. Graph of accumulated aluminum content from washings of L-cysteic acid alumoxane functionalized Nomex© fabric.

Conclusion

We have demonstrated that it is possible to synthesize a highly hydrophilic membrane that is capable of screening hydrocarbons from hydrocarbon/water emulsions

with high tribological endurance. The membranes are stable between pH 2 and 12. The reason of which is due to the functionalized alumoxane nanoparticles, the sulfonate and amine moieties and the ionic adducts provide the Zwitter ionic functionalities that allows efficient hydrogen bonding to the water droplets within the emulsions studied. This interaction allows formation of an aqueous layer on the surface of the filter which helps prevent fouling and more importantly provides an entropic barrier for which the oil droplets contained within the emulsions cannot cross. The meniscus of the aqueous layer may in fact decrease the pore size for hydrophobic material, however leaving the pore size sufficiently large enough for the crossing of hydrophoilic material such as the the dextran's studied.

Experimental

Pseudoboehmite Catapal B was provided by Sasol North America Inc. All carboxylate acids were obtained commercially (Aldrich) and were used as received. Nalgene filtration cells (#300–4000) were obtained from Fisher Scientific. Nomex© fabric was obtained from Pegasus Auto Racing Supplies, Inc. EDS studies were performed on a Hitachi HD-2700 STEM scanning microscope. The samples were attached to a metal mount using carbon tape. A 5 nm layer of gold was sputtered onto the samples to provide a conducting surface. Thermogravimetric/differential thermal analyses (TG/DTA) were obtained on a Q-600 Simultaneous TGA/DSC TA Instruments using a carrier gas of either dry nitrogen or air. SEM microscopy studies were performed on a FEI Quanta 400 ESEM. A 5 nm layer of gold was sputtered onto the samples to provide a conducting surface. The samples were mounted on carbon tape. TEM microscopy studies were performed on a Jeol 1230 HC-TEM 120kV. XPS studies were conducted on a PHI Quantera XPS machine. Atomic force microscopy (AFM) measurements were conducted on a multimode AFM in tapping mode. The microscope was equipped with a Nanoscope IIIa scanning probe microscope controller and an

Optizoom microscope from Digital Instruments. AFM tips were from K-TEK nanotechnology which were SPM probe model TETA/Au (15) with an Au conductive coating and a resonant frequency of 300 Hz.

Synthesis of carboxylic acid alumina surfaces. Using a modification of the literature method,[38] silicon wafers were coated with a thin layer of alumina (5 nm) via e-beam deposition. In order to remove impurities on the alumina surface, the coated wafers were sequentially washed in a 1:1 solution of conc. H_2SO_4 and 30% H_2O_2 for 5 min. The wafer was then washed with 2-propanol and air dried. The alumina coated silicon wafer was then gently refluxed at various temperatures depending on the functionalizing carboxylic acid Figure 1.2 as outlined in Table 1.1. After the reaction was completed the wafers were washed with IPA and air dried.

Synthesis of cysteic acid alumoxane. In a modification of the literature procedures,[31, 39,40] pseudoboehmite (100 g) was vigorously stirred in DI H_2O (80 mL) to this was slowly added an aqueous 1 M solution of cysteic acid (80 mL). The resulting solution was allowed to stir overnight, and then centrifuged at 4500 rpm for 1 h. The supernatant was evaporated under vacuum and the resulting solid was used for coatings. The ceramic yield (55%) and the average particle size (18 nm) were determined by TGA and TEM, respectively. The hydrated solid was used in future dip coatings of Nomex® material.

Formation of alumoxane coated Nomex®. Nomex© fabric (18 cm^2) was washed sequentially with EtOH and acetone to remove excess dye and surface contaminants. The fabric was then vacuum-dried and then dip-coated in a 20 wt% aqueous solution of cysteic acid-alumoxane solution (10 g in 50 mL DI H_2O) and held there for 2 - 5 s. The

dip-coat was allowed to oven dry (100 °C) before repeating the procedure. The fabric was loaded with 5 g of cysteic acid alumoxane per 18 cm^2.

Retention studies by gravity filtration. The cysteic acid functionalized alumoxane Nomex® composite membrane was cut to 5.5 cm diameter circle and fitted into the Nalgene filtration cell. The desired solution/emulsion (250 mL) was poured on top of the mounted support. The concentration of the initial feed was compared to the concentration of permeate overtime, to determine the percentage of retention. Initially this was achieved through inspection for larger M_w hydrocarbons but for smaller weight hydrocarbons (including Dextrans) GC-mass spectral analysis was used. This methodology was used for all solution studies presented herein.

References

1 A. Fakru'l-Razi, A. R. Pendashteh, A. Luqman Chuah, A. B. Dayang Radiah, S. S. Madaeni, and Z. A. Zurina, *J. Hazard Mater.*, 2009, **170**, 530.

2 S. Rocca, S. Muller, and M. J. Stebe, *J. Control. Rel.*, 1999, **61**, 251.

3 D. Attwood, and A. T. Florence, *Surfactant Systems*, Chapman and Hall. New York, 1983.

4 H. Isihida, and A. Iwama, *Combust. Sci. Technol.*, 1984, **37**, 79.

5 C. Solans, J. Esquena, and N. Azemar, *Curr. Opin. Colloid Interface Sci.*, 2003, **8**, 156.

6 E. W. Allen, *J. Environ. Engineering and Sci.*, 2008, **7**, 499.

7 V. Quintana, R. Luz, M. Love, J. A. Love, P. J. White, and L. A. Johnson, *J. Food Lipids*, 2003, **10**, 53.

8 L. Lin, and S. S. Koseoglu, *Membrane processing of fats and oils. Bailey's Industrial Oil and Fat Products.* 2005.

9 C. D. Jones, D. A. Bailey, M. R. Weisner, and A. R. Barron, *Adv. Sci. Technol.*, 1999, **16**, 413.

10 S. Boributh, A. Chanachi, and R. Jiraratananon, *J. Membr. Sci.*, 2009, **342**, 97.

11 J. –H. Li, Y. –Y. Xu, L. –P. Zhu, J. –H. Wang, and C. –H. Du, *J. Membr. Sci.*, 2009, **326**, 659.

12 Z. Dai, L. –S. Wan, and Z. –K. Xu, *J. Membr. Sci.*, 2008, **325**, 479.

13 L. Li, G. Yan, J. Wu, X. Yu, and Q. Guo, *J. Macromol. Sci. Part A: Pure and Applied Chemistry.* 2008, **45**, 828.

14 W. Scholtz, and W. Fuchs, *Water Res.*, 2000, **34**, 3621.

15 S. Judd, and S. W. Till, *Desalination*, 2000, **127**, 251.

16 H. Y. Yu, *Sep. Purif. Technol.*, 2005, **45**, 8.

17 Q. Sun, Y. Su, X. Ma, Y. Wang, and Z. Jiang, *J. Membr. Sci.*, 2006, **278**, 285.

18 Z. Yi, Y. –Y. Xu, L. –P. Zhu, H. –B. Dong, and B. –K. Zhu, *Chinese J. of Poly. Sci.*, 2009, **27**, 695.

19 J. –N. Shen, D. –D. Li, F. –Y. Jiang, J. –H. Qiu, and C. –J. Gao, *Sep. and Purif. Tech.*, 2009, **66**, 257.

20 Y. –H. Zhao, B. –K. Zhu, L. Kong, and Y. –Y. Xu, *Langmuir,* 2007, **23**, 5779.

21 L. Zhu, Y. –Y. Xu, H. –B. Dong, Z. Yi, and B. –K. Zhu, *Mater. Chem. Phys.*, 2009, **115**, 223.

22 J. –P. Mericq, S. Laborie, and C. Cabassud, *Desalination and Water Treatment,* 2009, **9**, 287.

23 D. S. Kim, J. S. Kang, and Y. M. Lee, *Sep. Sci. Tech.*, 2004, **39**, 833.

24 Y. –L. Su, W. Cheng, C. Li, and Z. Jiang, *J. Membr. Sci.*, 2009, **329**, 246.

25 C. Ba, D. A. Ladner, and J. Economy, *J. Membr. Sci.*, 2010, **347**, 250.

26 K. –S. Chen, H. –R. Lin, S. –C. Chen, J. –C. Tsai, and Y. –A. Ku, *Poly. J. (Tokyo, Japan).*, 2006, **38**, 905.

27 K. A. DeFriend, M. R. Wiesner, and A. R. Barron, *J. Membr. Sci.*, 2003, **224**, 11.

28 K. A. DeFriend, and A. R. Barron, *J. Membr. Sci.*, 2003, **212**, 29.

29 R. W. Baker, *Membrane Seperation Systems: Recent Developments and Future Directions.* Park Ridge, N.J., Noyes Data Corp., 1991.

30 A. J. Burggraaf, *Fundementals of Inorganic Membrane Science and Technology, Membrane Science and Technology Series 4*. New York: Elsevier, 1996.

31 R. L. Callender, C. J. Harlan, N. M. Shapiro, C. D. Jones, D. L. Callahan, M. R. Wiesner, R. Cook, and A. R. Barron, *Chem. Mater.*, 1997, **9**, 2418.

32 R. L. Callender, and A. R. Barron, *J. Mater. Sci.*, 2001, **36**, 4977.

33 C. E. Bethly, C. L. Aitken, C. J. Harlan, Y. Koide, S. G. Bott, and A. R. Barron, *Orgometallics*, 1997, **16**, 329.

34 C. T. Vogelson, Y. Koide, L. B. Alemany, and A. R. Barron, *Chem. Mater.*, 2000, **12**, 795.

35 R. L. Callender, and A. R. Barron, *J. Mater. Res.*, 2000, **15**, 2228.

36 J. Rose, J. -Y Bottero, C. Levard, A. Masion, M. M. Cortalezzi, A. R. Barron, and M. R. Wiesner, *Actualite Chimique*, 2009, **331**, 36.

37 A. W. Apblett, A. C. Warren, and A. R. Barron, *Chem. Mater.*, 1992, **4**, 167.

38 C. T. Vogelson, A. Keys, C. L. Edwards, and A. R. Barron, *J. Mater. Chem.*, 2003, **13** 291.

39 R. L. Callender and A. R. Barron, *J. Am. Ceram. Soc.*, 2000, **83** 1777.

40 N. Shahid and A. R. Barron, *J. Mater. Chem.*, 2004, **14**, 1235.

Chapter 2

Alumoxane/Ferroxane Nanoparticles for the Removal of Viral Pathogens: The importance of Surface Functionality to Nanoparticle Activity

Introduction

The information provided within this chapter has submitted to the Journal of Materials Chemistry.

Contamination of water by viral pathogens is endemic in many parts of the world. Sources of contamination include industrial and agricultural wastes, sewage and other forms of pollution. Sewage levels of approximately 7,000 viruses per liter are common, and can be more than 500,000 virus particles per liter.[1] Exposure of mucous membranes in the eyes (conjunctiva), nose (rhinal) and mouth to aerosolized viruses from contaminated water poses a serious risk of gastroenteritis, respiratory diseases, or eye, ear and nose infections. However, more serious consequences and life-threatening complications can occur. To overcome this, a viral filter for aspirated viruses would be of great utility.

The use of iron oxide nanoparticles in breathing filters was theorized to be useful as the human toxicity of iron oxides and oxyhydroxide is low.[2] It has also been shown that Fe(O)OH and Fe_2O_3 are more resistant to acidic, corrosive, and oxidant conditions than other antiviral materials (e.g., silver).[3] The affinity for binding of iron nanoparticles to virus pathogens was envisaged as it has been observed in nature.[4] Previous research has shown that viruses interact and act as nucleation sites for the adsorption and precipitation of dissolved metals especially iron.[5] Up to 50% of "dissolved iron" in sea water is between 30 nm and 100 nm in diameter.[6,7,8] Between 90% and 99% of iron particulates are strongly chelated by organic ligands.[7,8] Viral-lepidocrocite binding has been observed in sea water systems. Since virus adsorption is a function of surface area as well as surface activity, nanoparticles should show enhanced performance. However,

an important question to answer is whether any such performance is simply a function of the "nano" nature of the iron oxide nanoparticle, or a consequence of the surface functionality in concert with the nano scale.

Despite the efficacy of iron oxides and the potential of nanocrystaline iron oxides to bind to viruses, there is a second important component of any trap for aspirated viruses; it is necessary to provide a surface onto which water droplets will collapse. We have previously shown that coating Nomex® or similar fabric with cysteic acid [$HO_2CCH(NH_2)CH_2SO_3H$] functionalized alumina nanoparticles (cysteic-alumoxane) results in a superhydrophilic surface that allows for the passage of water,[9] but not hydrocarbons. In the present application the function of the superhydrophilic surface as measured by an extremely low contact angle (< 3°) is to "collapse" airborne water droplets onto that surface. If this hydrophilic surface is combined with functionalization

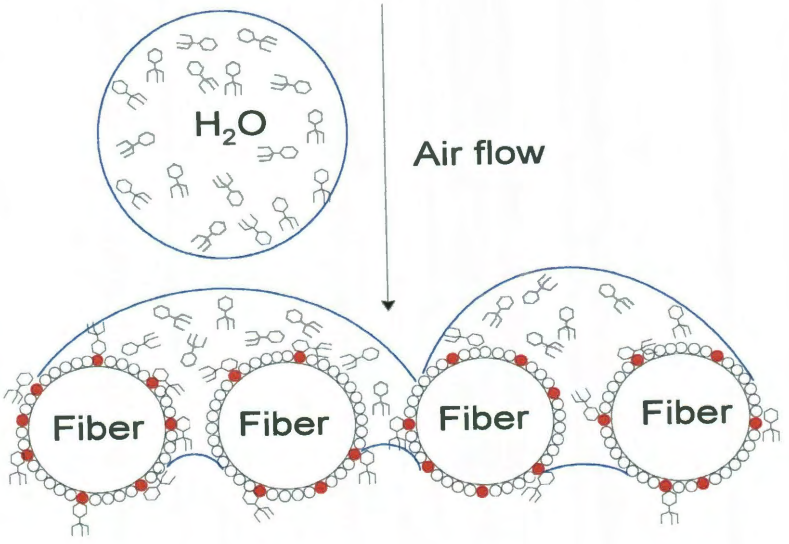

Figure 2.1. Schematic diagram of alumoxane/ferroxane viral trap showing the fibers coated with both ferroxane (iron oxide) nanoparticles (shown in red) and alumina nanoparticles.

to trap and immobilize viruses, then a combined system for removal of airborne or aspirated viruses may be achieved. As noted above, binding efficiency of iron oxides for viruses has been well documented suggesting that an iron oxide containing surface should be ideal as the immobilization agent. Thus, we propose that the creation of a bi-functional nano-composite coating on a porous support should provide a suitable test bed as a trap for aspirated virus contaminated water. Nomex® fabric, our chosen nanoparticle scaffold is utilized extensively in protective garments and by many professionals working in hazardous locations,[10] Nomex® is also tolerant of many harsh conditions.[11]

We have shown previously that carboxylic acid functionalized iron oxide nanoparticles (ferroxanes) are readily prepared from rust-like materials, and we propose that the combination of a hydrophilic surface alumoxane nanoparticles and viral binding functionalization ferroxane nanoparticles should make an effective composite material for the filtration of aspirated virus in an airway.[12]

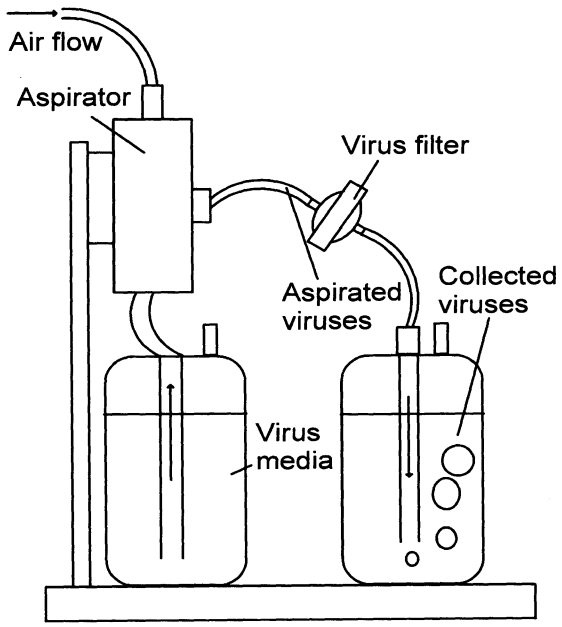

Figure 2.2. Schematic diagram of the viral adsorption apparatus.

Results and Discussion

The strategy of our filters was to immobilize the nanoparticles onto a porous fabric scaffold Figure 2.1. To accomplish this, a fabric support onto which hydrophilic alumoxane and hydrophilic ferroxane nanoparticle were functionalized and then subjected to viral screening. A five orders of magnitude reduction in concentrations of viruses passing through the functionalized filter, compared to the un-functionalized filter was observed.

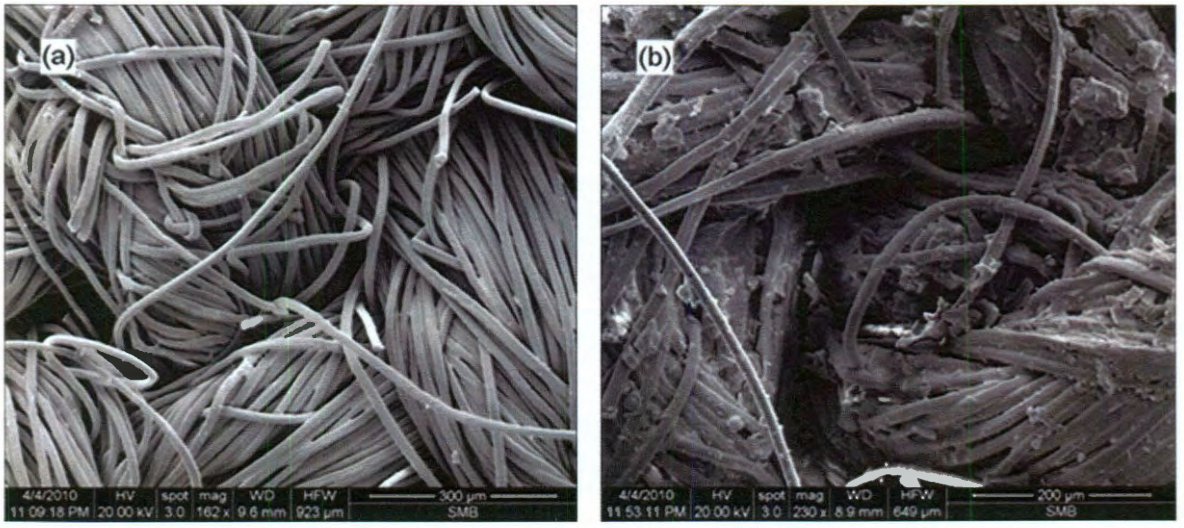

Figure 2.3. SEM image of (a) uncoated Nomex fabric and (b) alumoxane/ferroxane composite coated fabric (NPN-2).

Our previous work has shown that carboxylic acid functionalization of alumina surfaces can change the surface properties of the alumina.[9] We have previously undertaken the study of many carboxylic acid functionalized hydrophilic surfaces. These effects were related to the hydrophilicity, as indicated by the contact angle of water on the surface. It was observed that cysteic acid functionalized alumina coated wafers were extremely hydrophilic, achieving complete wettability when in contact with water.[9] In fact, the extent of wetting is such that complete wetting of the surface is

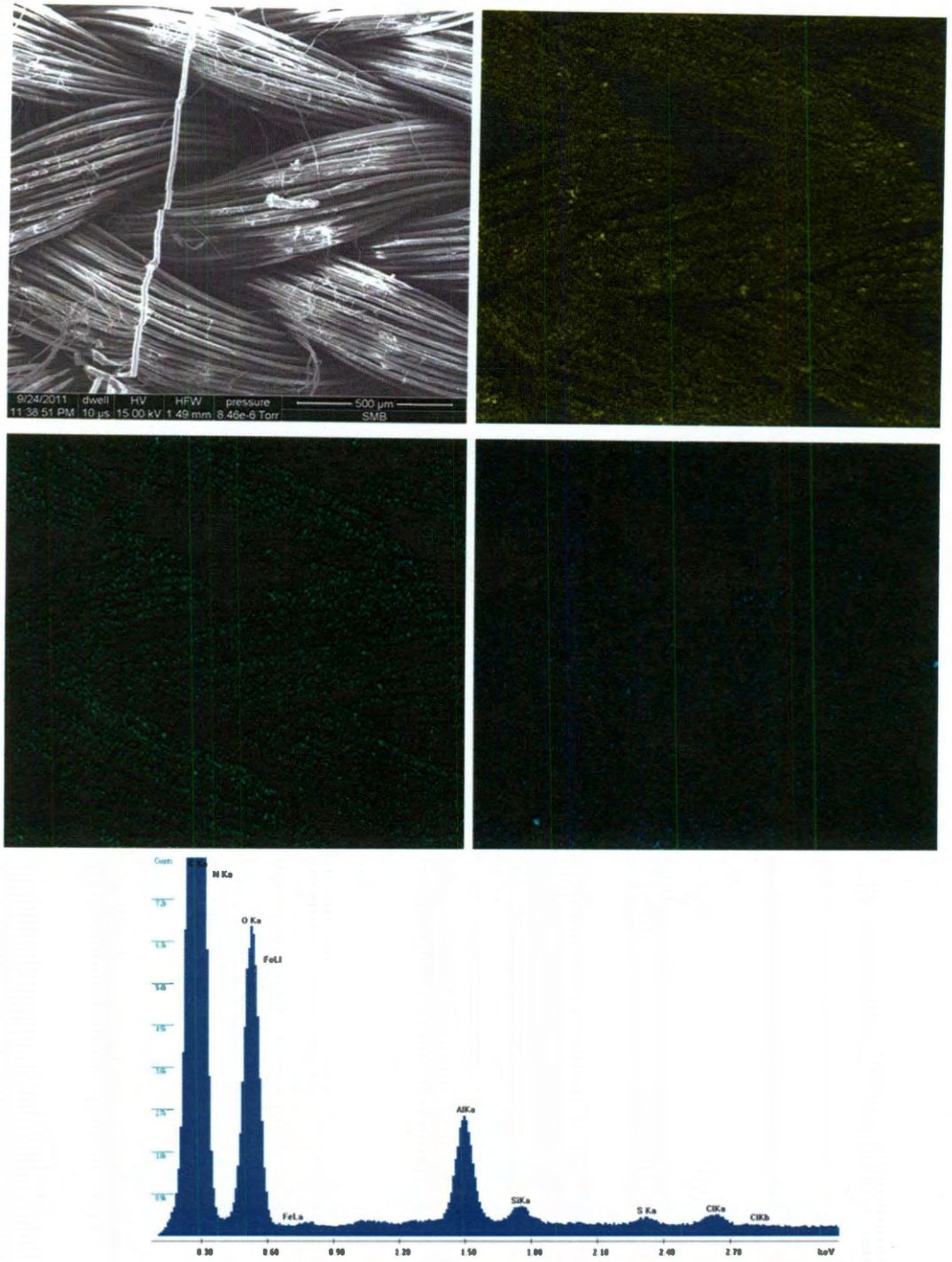

Figure 2.4. SEM and associated EDS map and spectrum of alumoxane/ferroxane nanoparticle coated fiber (NPN-2): (a) SEM image, (b) aluminum, (c) nitrogen, (d) sulfur, and (e) spectrum.

attributed to the hydrogen bonding abilities of both sulfonate and amine moieties on functionalized cysteic acid and its Zwitter ionic form. Based on these results, cysteic acid was chosen as the best candidate for the creation of our highly hydrophilic alumoxane-ferroxane Nomex® composite membrane.

We have previously reported that carboxylic acid functionalized alumina and lepidiocrocite nanoparticles (carboxylate alumoxanes and ferroxane) can be used to coat a range of fabrics and fibers.[13] Our goal was to deposit a thin layer of cysteic acid alumoxane onto a suitable support and anneal to 100 °C to provide a cysteic functionalized alumina surface on the support, followed by the same process with ferroxane. In contrast to our previous membrane work,[14] the resulting nanoparticle coated fabric (NPN) surface is not to act as a membrane, but to be the sidewalls of a particle filtration membrane (10^3 - 10^6 nm). SEM images indicated that deposition of the hydrophilic alumoxane and the viral active ferroxane nanoparticle occurred evenly across the fibers Figure 2.3. (This observation is confirmed by EDS mapping of individual fibers Figure 2.4 showing a continuously uniformly coated single fiber, as shown by the exact mapping Figure 2.4b, c, d) Uniform layering allows for passages of air with deposition of water droplets containing the target virus

Furthermore, from Figure 2.3 it can be seen that there is no extensive webbing that would preclude flow through the filter or act such that the fabric pore sizes are decreased. The reason we chose to use Nomex® fabric as a support was that the large weave of the fabric cannot facilitate screening and thus it must be the surface of the fibers, and not pore size of the fabric that is responsible for virus separation. Fabrication of the filter is achieved by first bringing the surface of the support into contact with a solution of cysteic acid functionalized alumoxane. The solution is drawn into the surface pores of the support by capillary forces. The surface coating thickness is controlled by the concentration of the cysteic acid alumoxane and ferroxane precursors and the pH of the solution. Size exclusion experiments using Dextrans determined that pore throat size of

the functionalized membranes were sufficiently large as to not be an issue,[9] especially when considering that the Brownian motion of an aspirated water droplet in its aerodynamic motion, if less than 1 μm in diameter is significantly larger than its diameter.[15] This ensures that in the application of our membrane for aspirated virus removal within an air-way, the air flux is large while still ensuring capture of the aerosol water droplet.

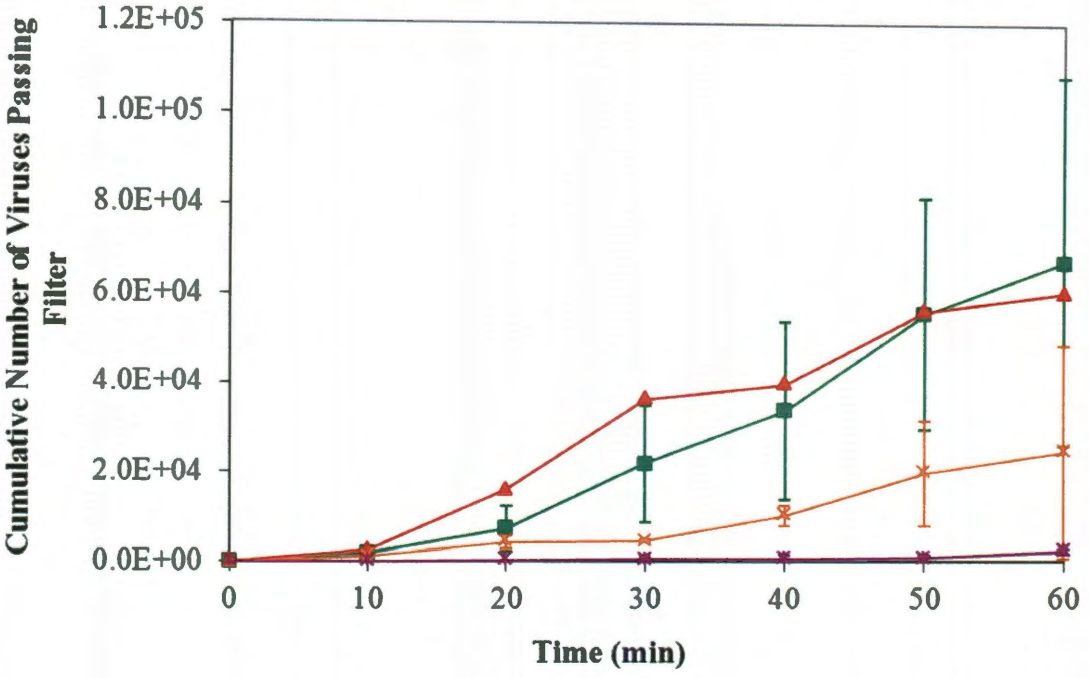

Figure 2.5. Plot of cumulative number of viruses passing through the Nomex® derived filters as a function of exposure time for MS2 bacteriophage adsorption studies. NPN-160 (red), Nomex (green), NPN (orange), NPN-2 (purple).

Testing of virus filtration was undertaken using bacteriophage MS2; this is a single stranded (+) RNA virus with an icosahedral capsid about 25 nm in diameter.[16] In water treatment processes, MS2 behaves similarly to some waterborne pathogenic viruses and is frequently used as a surrogate in disinfection studies.[17] Compared to other

bacteriophages, MS2 has been shown to be more resistant to UV disinfection.[18] In disinfection studies using chlorine and chloramines, MS2 was found to be comparable or resistant compared to Hepatitis A virus[19] and Poliovirus.[20] MS2 has also been

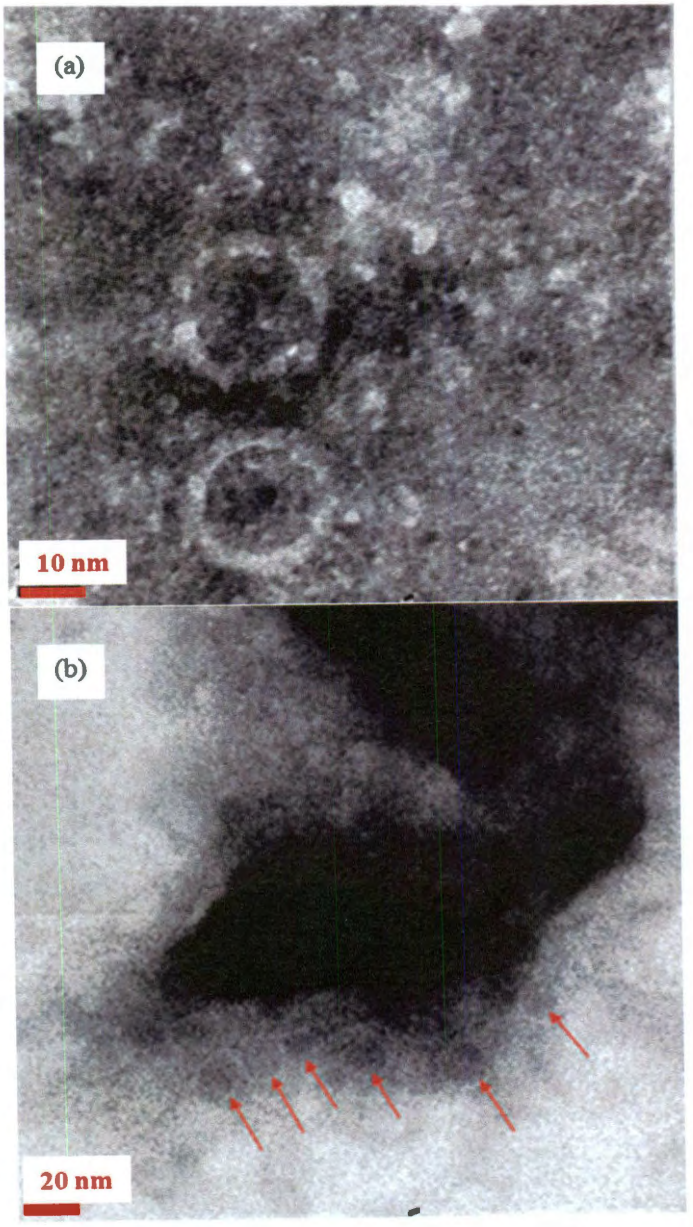

Figure 2.6. TEM of (a) MS2 bacteriophage and (b) MS2 (arrowed) bound to cysteic acid functionalized ferroxane nanoparticle.

recommended by the EPA as an indicator for viral inactivation processes.[21] MS2 is particularly convenient to work with, as its propagation and enumeration are relatively simple when compared to procedures required for human pathogenic viruses. All virus trapping measurements were repeated to give statistical reliability.

Figure 2.5 shows a plot of the cumulative number of viruses passing through each coated fabric as a function of time. It may clearly be seen that the alumoxane/ferroxane nanoparticle coated fabrics (NPN and NPN-2) show a large decrease as compared to Nomex® alone. It is particularly noteworthy that an increase in the ferroxane content (i.e.,

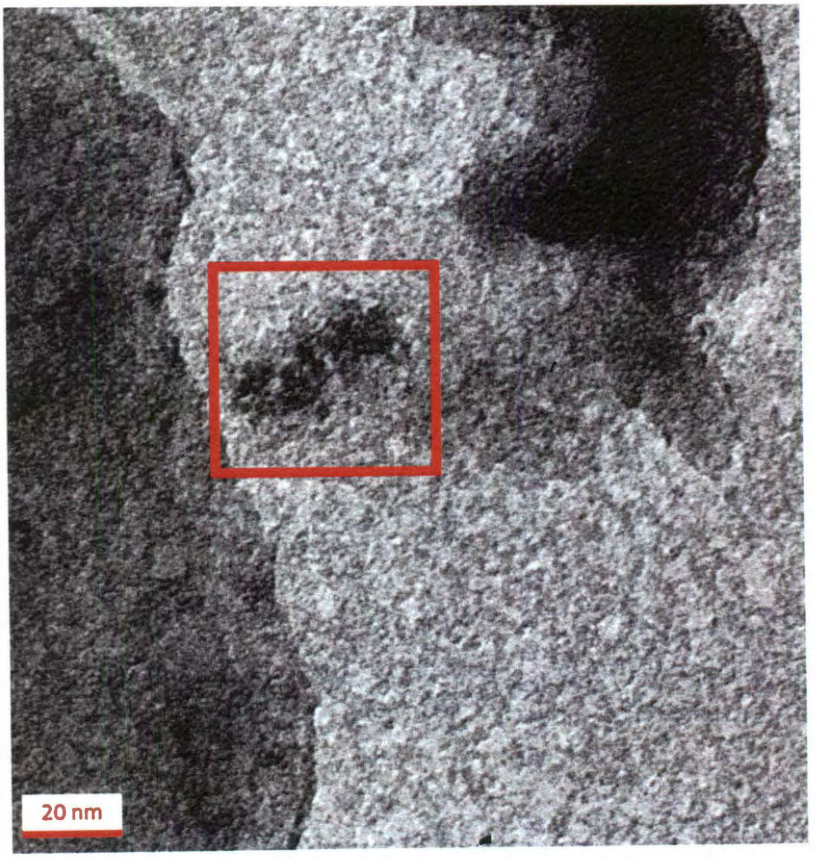

Figure 2.7. TEM of MS2 bacteriophage bound to cysteic acid functionalized ferroxane fired to 160 °C for 2hrs.

sample NPN-2 versus sample NPN) results in an equivalent increase in virus retention. This suggests that it is the ferroxane that has an active role in either deactivating or binding to the virus. In order to confirm this result we have investigated the interaction of MS2 with individual ferroxane particles by TEM. Figure 2.6a shows a TEM image of two MS2 viruses, while in the center of Figure 2.6b is a representative example of a ferroxane particle to which is associated at least one MS2 virus. In the entire TEM sample ferroxane nanoparticles were observed "binding", i.e., being in close proximity to at least one if not multiple MS2 viruses. From Figure 2.5 it may be seen that the Nomex® fabric alone provides some barrier to transport of aspirated MS2 bacteriophage in comparison to no fabric at all. This provides a simple measure of the physical barrier that any porous fabric would provide.

Although previous work has suggested that iron oxides should act as efficient traps for viruses such as MS2, the coated fabric that was heated to 160 °C (NPN-160) shows essentially the same results as for untreated Nomex®. This result is indicative of two issues. First, the nanoparticle coating process does not significantly alter the porosity/flow through the fabric, and thus the results discussed below are not a consequence of smaller pore/weave sizes. Second, annealing the cysteic acid alumoxane and ferroxane to 160 °C Figure 2.7 results in the partial loss of functional groups on the nanoparticles without sintering of the individual nanoparticles (which lower the surface area). This suggests that the surface functionalization of the nanoparticles is vital for the surface collapse of aspirated water droplet and/or the absorption and immobilization of the MS2 viruses. Thus, we can conclude that a nanoparticle surface functionalization is far more important in the present process than the actual nanoparticle nature of the coating per se.

Conclusion

We have synthesized and characterized a permeable hydrophilic fabric-based filter with high flux for air flow and high virus binding capabilities, derived from simple hydrophilic principles and natural virus binding mechanisms found in nature. The benign nature of synthesis of the membrane composite ensures that future functionalization of any component within an air-way system is possible with regards to virus inactivation. The concept of this membrane may be utilized in the future for functionalizing multiple components. The detailed nature of the ferroxane-MS2 interaction needs greater investigation, but, it is reasonable to propose that the interaction is essentially the same as in nature with regards to virus binding to lepidiocrocite. However, the important result from this work is that it is not sufficient to have nanoparticles per se, but that their surface functionality is important in ensuring functionality of the membrane. In the present case, this means the use of hydrophilic surface functionalization that ensures the collapse of aspirated water droplets and the wetting of the surface to allow exposure of the viruses to the "active" component on the surface.

Experimental

Cysteic acid, $FeCl_2.4H_2O$, EtOH and acetone (Sigma-Aldrich) were used as received. Pseudoboehmite Catapal B was provided by Sasol North America Inc. Nomex® fabric was obtained from Pegasus Auto Racing Supplies and was washed sequentially with EtOH and acetone to remove excess dye molecules. Energy dispersive spectroscopy (EDS) studies were performed on a Hitachi HD-2700 STEM scanning microscope. The samples were attached to a metal mount using carbon tape. A 5 nm layer of gold was sputtered onto the samples to provide a conducting surface. Thermogravimetric/differential thermal analyses (TG/DTA) were obtained on a Q-600 Simultaneous TGA/DSC TA Instruments machine using a carrier gas of either dry argon or air. Scanning electron microscopy (SEM) studies were performed on a FEI Quanta 400

ESEM. (A 5 nm layer of gold was sputtered onto the samples to provide a conducting surface.) Transmission electron microscopy (TEM) studies were performed on a JEOL 1230 HC-TEM 120kV. Dilute solutions of nanoparticles were solicited in DI water and drop cast onto 300 mesh copper grids, the excess solution being wicked away. The grids were received from Ted Pella with amorphous carbon surface and Formvar coating with the Formvar being removed by immersion of the grid in chloroform for thirty seconds and air drying just before drop casting. X-ray photoelectron spectroscopy (XPS) studies were conducted on a PHI Quantera XPS machine. Samples were mounted onto platen using double sided carbon tape. Atomic force microscopy (AFM) measurements were conducted on a multimode AFM in tapping mode. The microscope was equipped with a Nanoscope IIIa scanning probe microscope controller and an Optizoom microscope from Digital Instruments. AFM tips were from K-TEK nanotechnology, which were scanning probe microscopy (SPM) probe model TETA/Au (15) with an Au conductive coating and a resonant frequency of 300 Hz. Bacteriophage MS2 (ATCC 15597-B1) and the bacterial host, *E. coli* (ATCC 15597) were obtained from the ATCC. LB-Lennox media and sodium bicarbonate were purchased from Fisher Scientific, and Bacto™ agar was purchased from Difco Laboratories. Ultrapure water was obtained from a Barnstead E-Pure system. All materials were sterilized by autoclave, 70% EtOH, or filtration through a 0.22 □M membrane. MS2 was used as a surrogate pathogenic virus in this study. MS2 phages were propagated in LB-Lennox media. 200 μL of MS2 stock solution was combined with 800 μL of an incubation of *E. coli*. This was combined with 3 mL of molten (45 °C) LB-Lennox media containing 0.7% Bacto™ Agar and poured onto a Petri dish containing solid LB-Lennox media with 1.5% Bacto™ Agar. The plates were incubated overnight and subsequently filled with 15 mL of 100 mM $NaHCO_3$ solution and gently rocked for 3 hours.[22] The buffer containing the MS2 particles was withdrawn, centrifuged at 10,900 x g for 15 minutes, and the supernatant passed through a 0.22 μM-pore-size syringe filter. The virus concentration in the filtered solution (~7 x 10^9

PFU/mL) was measured by the agar overlay method,[23] and the solution was stored at 4 °C until use in the virus removal experiments.

Synthesis of cysteic acid alumoxane nanoparticles. In a modification of literature procedure,[24] pseudoboehmite (100 g) was vigorously stirred in DI H_2O (80 mL) to which a 1 M aqueous solution of cysteic acid (80 mL) was slowly added. The resulting solution was stirred overnight, and then centrifuged at 4500 rpm for 1 h. The supernatant was evaporated under vacuum and the resulting solid was used for coatings. Ceramic yield: (55%). Average particle size: (18 nm).

Synthesis of cysteic acid ferroxane nanoparticles. In a modification of the literature procedure,[12] a 1M solution $FeCl_2 \cdot 4H_2O$ (100 mL) was mixed with 1.67 M solution of NaOH (100 mL). The molar ratio R = $[FeCl_2.4H_2O]/[NaOH]$ = 0.6 favors the formation of a pure lepidocrocite in an aqueous 1M solution of cysteic acid (80 mL) was slowly added. The resulting suspension was centrifuged at 4400 rpm for 30 mins and the volatiles were removed in a vacuum at 90 °C. The resulting solid was used for subsequent coating experiments. Ceramic yield: 30%. Average particle size: 100 nm.

Formation of alumoxane/ferroxane composite membrane. A sample of Nomex® fabric (18 cm^2) was washed sequentially with EtOH and acetone to remove excess dye molecules. The fabric was then vacuum dried to remove all volatiles. The fabric was dip-coated in an aqueous solution L-cysteic acid-alumoxane solution 20 wt% (10 g in 50 mL) and held there for 2 – 5 s. The dip-coat was allowed to oven dry (100 °C) before repeating the procedure three times. Loading of L-cysteic acid functionalized ferroxane 5 wt% (1.0 g in 20 mL DI H_2O) onto the L-cysteic acid alumoxane coated Nomex® resulted in the nanoparticle coated fabric (NPN), which was tested against aspirated MS2 bacteriophage for virus filtration. In order to limit potential nanoparticle

shedding a similar sample was annealed to partially convert the nanoparticles to ceramic by heating the filter to 160 °C for 2 hrs in an argon atmosphere (NPN-160). Increased loading of cysteic ferroxane 20 wt% (5.0 g in 20 mL) was undertaken onto an alumoxane functionalized 18 cm^2 piece of Nomex® fabric (NPN-2). The above membranes were characterized via XPS, SEM-EDS and tested as a virus filter against MS2 bacteriophage.

Viral absorption studies. The virus filtration experiments were conducted by generating an aerosolized virus stream, passing the output through a Nomex® fabric composite membrane the synthesis of which is outlined above, and collecting and enumerating the viruses that are completely transported through the system Figure 2.2. The aerosolized virus stream was generated using a TSI Constant Output Atomizer (model 3076, Shoreview, MN) operating in recirculation mode. The system was sterilized with 70% EtOH followed by thorough rinsing with sterile ultrapure water prior to each experiment. To conduct an experiment, the virus stock was combined with 300 mL ultrapure water (final titer ~10^6 PFU/mL) in the feed reservoir, which was placed in an ice bath and connected to the atomizer. A 25 mm diameter piece of fabric was cut and placed in a reusable Swinnex® filter holder (Millipore, Billerica, MA) which was then attached to the discharge of the atomizer. The output of the filter holder was connected to a tube, which discharged through a stone diffuser into 150 mL of ultrapure water in a tall glass jar. The discharge water was sampled before each test and every 10 minutes up to 1 hour. Viruses in the samples were enumerated by the agar overlay method.[25]

References

1 W. Renate, W. Macht, J. Durkop, R. Hecht, U. Hornig, and P Schulze, *Water Res.*, 1989, **23**, 133.

2 R. M. Cornell and U. Schwertmann, *The iron oxides*, VCH, New York, 1996.

3 M. Pourbaix, *Atlas d'Equilibre Electrochimiques*, Gauthier-Villars, Paris, 1963.

4 C. J. Daughney, X. Chatellier, A. Chan, P. Kenward, D. Fortin, C. A. Suttle, and D. A. Fowle, *Mar. Chem.*, 2004, **91**, 101.

5 (a) L. A. Warren and F. G. Ferris, *Environ. Sci. Technol.*, 1998, **32**, 2331. (b) X. Chatellier, D. Fortin, M. M. West, G. G. Leppard, and F. G. Ferris, *Eur. J. Mineral.*, 2001, **13**, 705. (c) C. J. Daughney, D. A. Fowle, and D. Fortin, *Geochim. Cosmochim. Acta.*, 2001, **65**, 1025. (d) J. B. Fein, S. Scott, and N. Rivera, *Chem. Geol.*, 2002, **182**, 265.

6 (a) M. L. Wells and E. D. Goldberg, *Mar. Chem.*, 1992, **40**, 5. (b) M. L. Wells and E. D. Goldberg, *Mar. Chem.*, 1993, **41**, 353. (c) M. L. Wells and E. D. Goldberg, *Limnol. Oceanogr.*, 1994, **39**, 286.

7 (a) J. Wu and G. W. Luther III, *Limnol. Oceanogr.*, 1994, **39**, 119. (b) J. Wu and G. W. Luther III, *Mar. Chem.*, 1995, **50**, 159. (c) J. Wu and G. W. Luther III, *Geochim. Cosmochim. Acta.*, 1996, **60**, 2729. (d) J. Wu, E. Boyle, W. Sunda, and L. –S. Wen, *Science*, 2001, **292**, 847.

8 J. Nishioka, S. Kakeda, C. S. Wong, and W. K. Johnson, *Mar. Chem.*, 2001, **74**, 157.

9 S. J. Maguire-Boyle and A. R. Barron, *J. Membr. Sci.*, 2011, **382**, 107.

10 (a) R. S. Villar, A. A. Martinez, and J. M. D. Tascon, *J. Therm. Anal. Calorim.*, 2005, **79**, 529. (b) L. T. Hasty, *Engineer.*, 2003, **33**, 37. (c) H. Gu, *Proc. Inst. Mech. Eng. S.*, 2009, **30**, 4324.

11 (a) Y. Sun and G. Sun., *Ind. Eng. Chem. Res.*, 2004, **43**, 5015. (b) A. Akdag, H. B. Kocer, S. D. Worley, R. M. Broughton, T. R. Webb, and T. H. Bray, *J. Phys. Chem. B*, 2007, **111**, 5581.

12 (a) J. Rose, M. M. Cortalezzi-Fidalgo, S. Moustier, C. Magnetto, C. D. Jones, A. R. Barron, M. R. Wiesner, and J. –Y. Bottero, *Chem. Mater.*, 2002, **14**, 621. (b) M. M. Cortalezzi-Fidalgo, J. Rose, G. F. Wells, J. –Y. Bottero, A. R. Barron, and M. R. Wiesner, *J. Membr. Sci.*, 2003, **227**, 207.

13 (a) R. L. Callender and A. R. Barron, *J. Mater. Sci.*, 2001, **36**, 4977. (b) R. L. Callender and A. R. Barron, *Ceramic Trans.*, 2000, **115**, 435. (c) R. L. Callender and A. R. Barron, *J. Mater. Res.*, 2000, **15**, 2228.

14 (a) C. D. Jones, M. Fidalgo, M. R. Wiesner, and A. R. Barron, *J. Membr. Sci.*, 2001, **193**, 175. (b) D. A. Bailey, C. D. Jones, A. R. Barron, and M. R. Wiesner, *J. Membr. Sci.*, 2000, **176**, 1. (c) K. A. DeFriend, M. R. Wiesner and A. R. Barron, *J. Membr. Sci.*, 2003, **224**, 11. (d) K. A. DeFriend and A. R. Barron, *J. Membr. Sci.*, 2003, **212**, 29.

15 S. –S. Lu, X. Wang, H. Hirano, T. Tagawa, and H. Ozoe, *J. Appl. Phys.*, 2005, **98**, 1.

16 M. T. Madigan and J. M. Martinko. *Brock Biology of Microorganisms*. Pearson Prentice Hall, Upper Saddle River, New Jersey 1996.

17 (a) M. A. Butkus, *Appl. Environ. Microbiol.*, 2004, **70**, 2848.
(b) Y. Koizumi and M. Taya, *Biochem. Eng. J.*, 2002, **12**, 107.
(c) E. D. Mackey, *J. Am. Water Works Assoc.*, 2002, **94**, 62.

18 R. Sommer, *Water Res.*, 2001, **35**, 3109.

19 M. D. Sobsey, T. Fuji, and P.A. Shields, *Water Sci. Technol.*, 1988, **20**, 385.

20 J. A. Tree, M. R. Adams and D. N. Lees, *Appl. Environ. Microbiol.*, 2003, **69**, 2038.

21 M. Pirnie, *Guidance manual for compliance with the filtration and disinfection requirements for public water systems using surface water sources.* USEPA (1991).

22 M. Cho, H. Chung and J. Yoon, *Appl. Environ. Microbiology*, 2005, **71**, 270.

23 M. H. Adams *Bacteriophages*; Interscience: New York, **1959**.

24 R. L. Callender, C. J. Harlan, N. M. Shapiro, C. D. Jones, D. L. Callahan, M. R. Wiesner, D. B. MacQueen, R. Cook, and A. R. Barron, *Chem. Mater.*, 1997, **9**, 2418.

25 M. H. Adams *Bacteriophages*; Interscience: New York, **1959**.

Chapter 3.

Organic functionalization of porous ceramic membranes

Introduction

The information supplied within this chapter has been published in the patent application "Methods, Systems, and Membranes for Separation of Organic Compounds from Liquid Samples", Inventors: Andrew R. Barron, Samuel J. Maguire-Boyle, A provisional patent application has been filed for this invention (application number 13/087, 706, filed on April 15, 2011)

Shale gas will be the dominant source of energy over the next 40 years.[1] Currently this energy comes at a very high price, both in terms of production costs and possible environmental hazards. The low permeability of shale rock until relatively recently meant that cost of extraction was too high. However introduction of horizontal drilling coupled with hydraulic fracturing or 'fracing' has allowed cost effective access to this resource. Fracing normally uses on average 20 million liters of water per well. The post frac water, also called production water cannot be used down well again. The recovery of water from production water for reuse has been viewed in the past by industry as being economically untenable as it is notoriously difficult to purify.[2] Since water is an extremely valuable commodity it cannot continually be wasted on a scale such as this. Recyclability of the frac water is the only viable option if shale gas is to be utilized over the next 50 years.

Recyclability of many types of industrial wastes such as production water has been undertaken using ceramic filtration membranes for many years.[3] The use of these membranes have been utilized by industry primarily for their robust nature and the ability to have select pore sizes with narrow distributions.[4,5] However their ability to purify or otherwise separate material has under the current art many drawbacks, such as membrane fouling and permeate flux.[6] Until now these drawbacks have proven to be economically unviable to shale gas drilling companies.

The ability of traditional ceramic membranes to screen undesirable molecules from a sample has relied solely on its pore size, the smaller the pore size the smaller the molecule that can be screened. However a smaller pore size in turn represents a myriad of operational technicalities, such as higher operating pressures, lower flux, membrane fouling and thus the need for maintenance which all multiply into substantial costs for an operating company. If a membrane could be synthesized that could negate these issues then it could be economically viable to utilize filtration as a cost effective treatment of production water.

One of the largest hurdles facing the current state of art for ceramic membranes is membrane fouling. The interaction between membrane surfaces and solutes plays an important role in determining the extent of membrane fouling explained by the mechanisms[7,8] of pore blocking, cake formation or hydrophobic interaction. Of the aforementioned mechanisms, hydrophobic interaction between solutes and membrane material is frequently accepted as one of the predominant fouling mechanisms. Therefore, membrane fouling is expected to be more severe with hydrophobic than hydrophilic membranes.[9,10]

It had been noted in literature that hydrophilic membranes display less sensitivity to adsorption compared to their hydrophobic analogues. Hydrophilic membranes have been shown to overcome many of these negative characteristics especially with regards to anti-fouling[11,12,13,14] as well as having high permeate flux for aqueous eluants,[35] and in many ways are superior to hydrophobic membranes.[15] There have been a myriad of ways at which the ceramic membrane surfaces have been altered to a more hydrophilic state thus overcoming fouling, such as surface segregation,[15] surface coating,[16] and surface graft polymerization.[17] However the direct covalent functionalization of the surface of a porous ceramic membrane with an organic molecule has never been attempted.

The covalent organic functionalization of a ceramic surface is not a new concept as it has been observed for years in the nanotechnology sector, such as the

functionalization of alumina,[18] also just recently our lab has published work where ceramic nanoparticles organically functionalized with cysteic acid were used as a coating on a fabric fiber which was in turn used as a membrane.[19] These same simplistic techniques used in the above experiments were then applied to the more ordered ceramic porous membranes. The resulting organo-ceramic membranes with large pore sizes of 0.22 μm were used to remove organic matter from waste water. In this thesis production water was used as a qualitative test to evaluate the rejection of organic compounds as well as the permeate flux and trans-membrane pressure.

In our previous work it was found that surfaces functionalized with cysteic acid had a significant ability to repel hydrocarbons. A ceramic membrane functionalized with cysteic acid was prepared, and analyzed for its ability to filter organics. The permeate from this process observed initially under inspection was significantly clearer than the non-functionalized membrane. Further tests outlined herein display the unique ability of the membrane to reject organics of a smaller hydrodynamic diameter far smaller than the native ceramic membrane with the same pore size.

The functionalization of the ceramic membrane could only occur through one pathway, where the carboxylic acid binds to the hydroxylated surface.[20] The aligned orientation of the sulfonate and amine moieties away from the membrane surface results in the membrane displaying significant hydrophilicity. However the pore size of the functionalized membrane compared to the un-functionalized membrane is very similar as the length of the functionalizing molecule from carboxylic acid to sulfonate is minuscule compared to the pore size of the functionalized membrane. The significant improvement in hydrocarbon screening was initially baffling. To use an analogy it was the equivalent of a tennis ball returning to someone who had just thrown it through an open doorway.

However the drastic improvement did have some clues, the retention of water in the pores of the functionalized alumina was significant. Hydrophilic surfaces on filtration membrane had been shown to be superior throughout the literature,[8,9,10] obviously for the

rejection of organics as well as a lack of membrane fouling. Hydrogen bonding could therefore be assumed to play a significant role in this process both with regards to anti-fouling mechanisms and hydrocarbon screening. However none of the functionalization techniques had the benefit of ordering and aligned orientation of our direct covalent functionalization.

It had been observed through molecular modeling calculations[23] and neutron scattering[21,22] that the density of the water phase at the liquid-solid interface and from the surface into the bulk solution differs significantly depending on the hydrophilicity of the surface.[23]

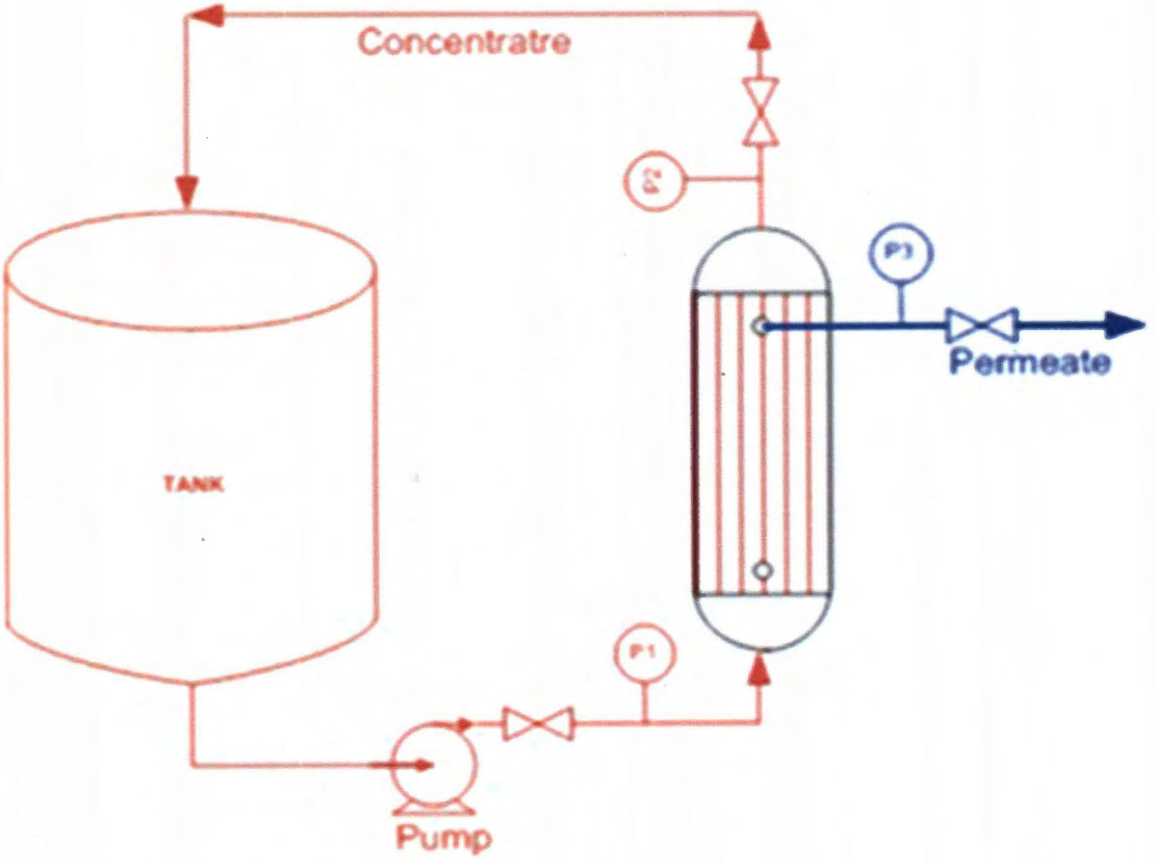

Figure 3.1. Schematic representation ceramic membrane filtration assembly.

It may be that the ordering of water from a surface to the bulk is a function of the hydropilicity of that surface. The molecular modeling for this phenomenon was only calculated for hydrophobic to semi-wetting surfaces. If this was extrapolated to hydrophilic or superhydrophilic surface it could be assumed that the perpendicular distance in ordering from the surface would extend further into the bulk. If it is assumed that this is what's occurring within the pore volume of the functionalized ceramic membrane then it can also be inferred that the ordering could represent a significant entropic barrier for a hydrocarbon or hydrocarbon colloid to overcome when passing through a pore that traditionally would be considered far too large to screen that molecule.

Results and Discussion

The unique ability of this membrane to exclude hydrocarbons from passing through its pores while still retaining a significant water flux had been initially conceived from previous work,[19] it had been observed in these studies that retention of hydrocarbons was possible even with membranes of very large pore size. The active component in the previous studies was L-cysteic acid, which was used to functionalize and synthesize alumoxane nanoparticles. The material outcome of functionalizing the nanoparticles was to create superhydophilic nanoparticles, the chemical reason involved orientation of the Zwitter ionic moieties of cysteic acid away from a surface.[19] Figure 3.3 It was envisioned that the same functionalization could be achieved on a ceramic porous membrane, as organic functionalization of ceramics had previously been undertaken in our group.[5]

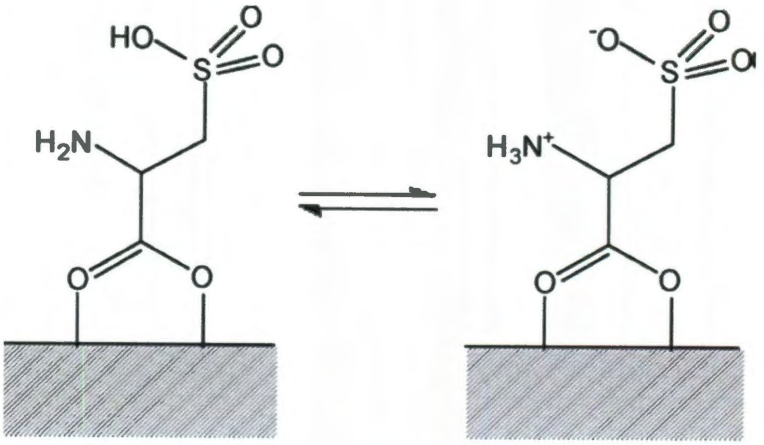

Figure 3.2. Cysteic acid showing zwitter ionic forms.[19]

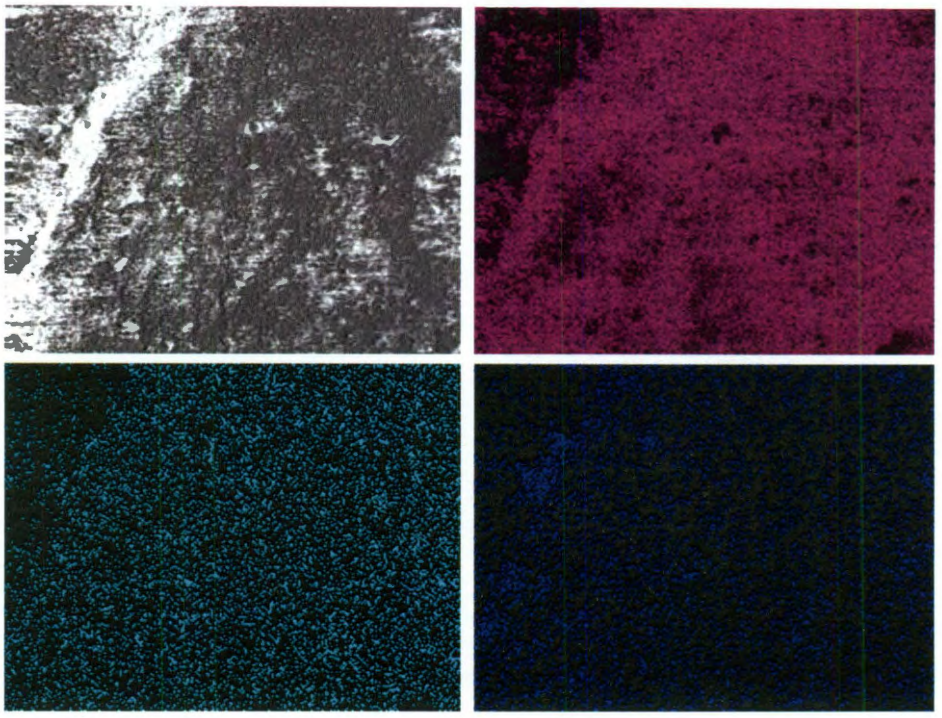

Figure 3.3. SEM image of cysteic acid functionalized membrane (top left), EDS mapping of cysteic acid functionalized membrane of aluminum (top right), sulfur (bottom left) and nitrogen (bottom right).

The close proximity of the two zwitter ion moieties on the same molecule is not significant in itself although as a free molecule the ability of cysteic acid to totally solvate

in water is substantial, it is the orientation of the molecule which is covalently bound to the surface via its carboxylic moiety which allows the surface to become superhydrophilic. The total functionalization of the surface can be seen from the SEM-EDS spectrums and mapping which was performed Figure 3.4.

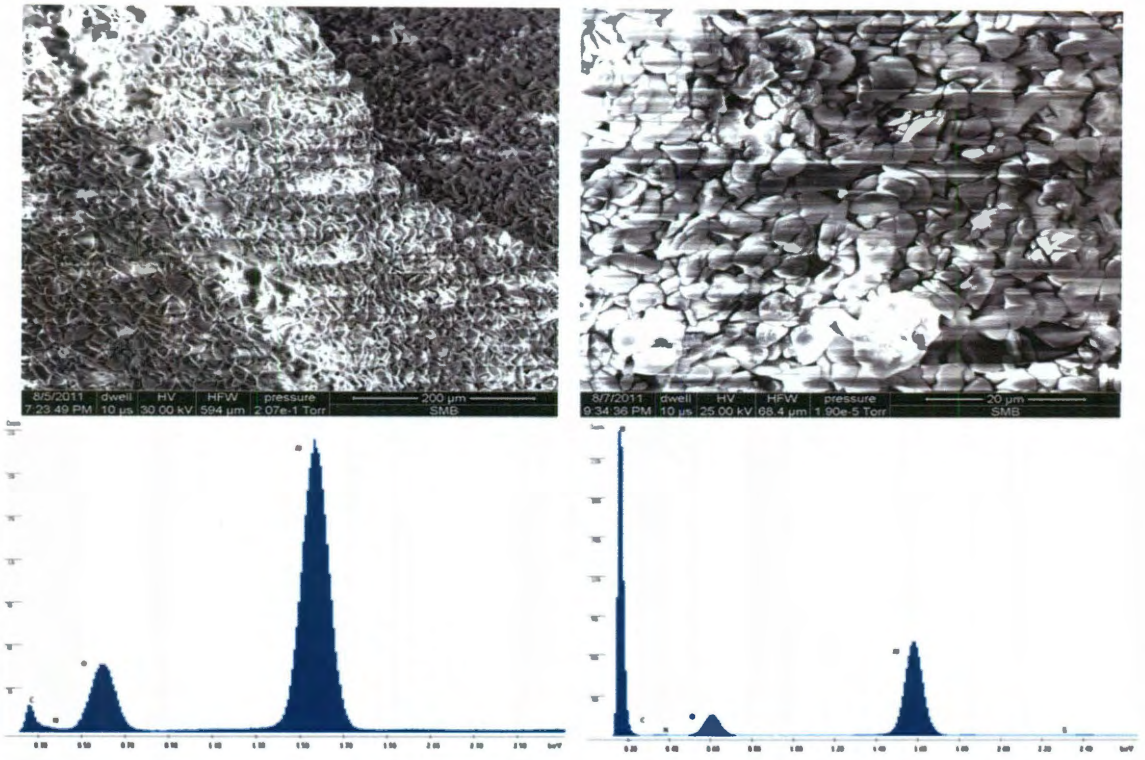

Figure 3.4. SEM images of un-functionalized alumina membrane (top left), and cysteic acid functionalized membrane (top right). EDS spectrum of un-functionalized alumina membrane (bottom left), and cysteic acid functionalized membrane (bottom right).

Particular note must be taken in comparison of the EDS spectrum of both functionalized membrane and un-functionalized membrane Figure 3.4. Where it can be seen that no sulfur or nitrogen peak exists for the un-functionalized membrane compared to the functionalized membrane. Mapping of the functionalized membrane for nitrogen

and sulfur, showed even coverage across the entire cross section, even though of a relatively poor signal compared to bulk aluminum and oxygen Figure 3.3.

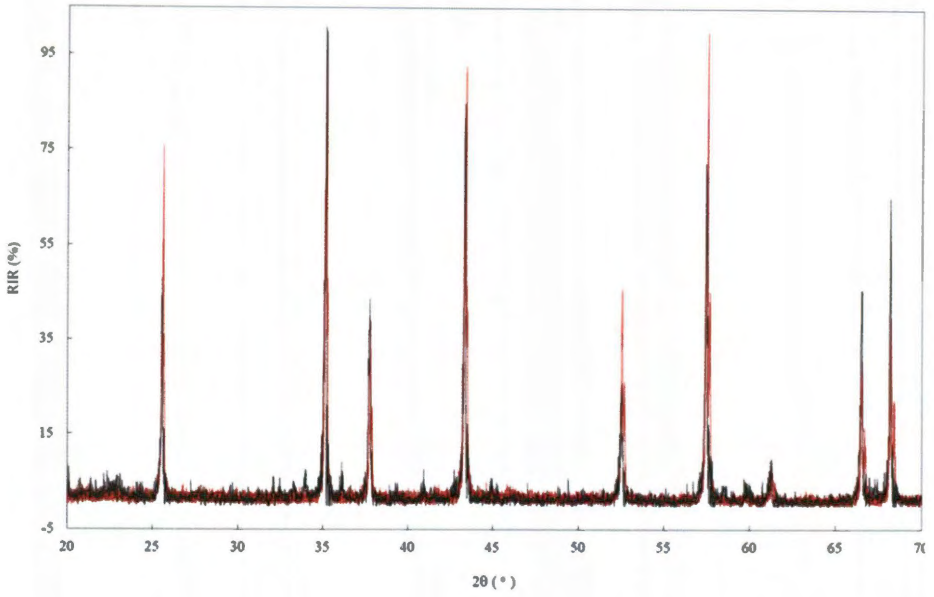

Figure 3.5. Powder XRD comparison of cysteic acid functionalized (red), and un-functionalized α-Al_2O_3 porous membrane.

Alteration of the pore size, surface morphology or bulk crystal structure did not occur by functionalization of the membrane. Comparison by inspection using SEM of the surface of both the functionalized and un-functionalized membranes reveals no obvious changes, significant charging was observed as the samples were analyzed in their native state with no conductive coating so as to get an unaltered EDS elemental spectrum. A comparison of both the crystal structure of both functionalized and un-functionalized membrane reveals the distinct pattern of bulk α-Al_2O_3 has not changed with the functionalization Figure 3.5.

This observation reveals how minute the alteration of the membrane compared to the total bulk is. This can again be seen when calculating total weight gain of the membrane, if 100% coverage of the membrane is assumed, and assuming that the square

surface area footprint for cysteic acid was 36979 pm^2 and a cubic packing is also assumed, an over-all percent weight gain for the porous alumina ceramic membrane such as ours with a surface area of 0.358 m^2/g would have a weight gain when functionalized with cysteic acid of approximately 0.18%. This tiny amount accounts for the small weight loss observed with TGA analysis Figure 3.6. When this functionalization is

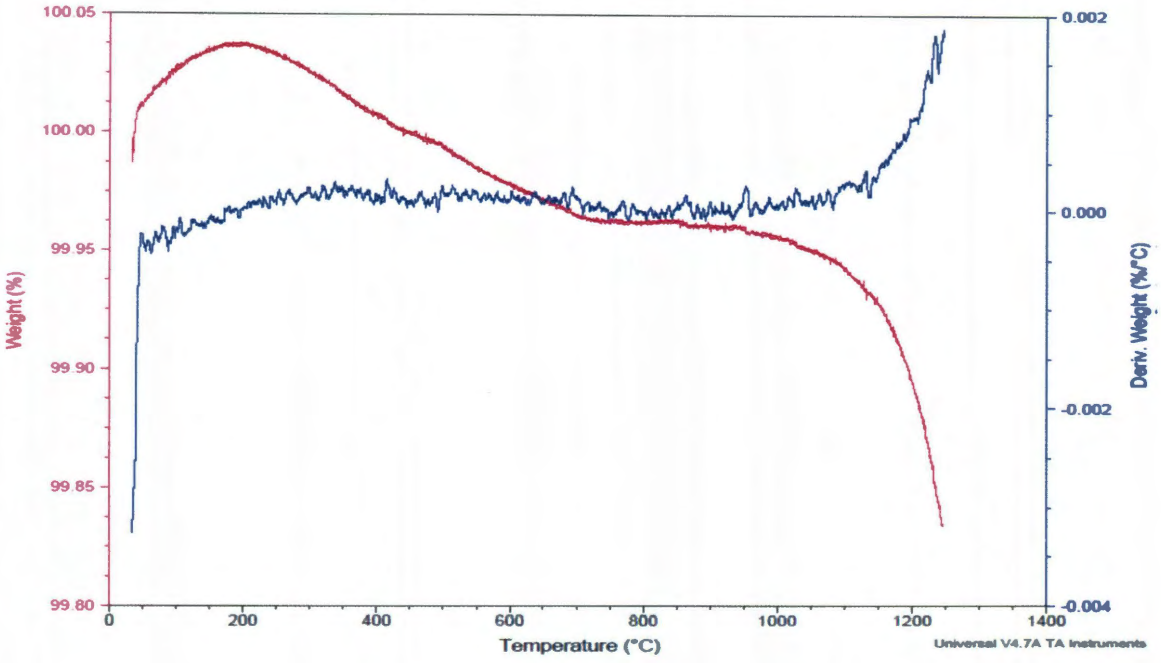

Figure 3.6. TGA of cysteic acid functionalized membrane of porous α-Al_2O_3.

performed on a porous surface the porous material imbues water to a larger extent than the un-functionalized material. This is evident by the FTIR spectrum of functionalized/un-functionalized material. The un-functionalized porous membrane Figure 3.7 shows no absorbance in the same region or indeed any region on the sample which is indicative of water impurity usually seen as a broad band in the 3000 cm^{-1} region. But instead only displays Al-O stretching at 656, 898 cm^{-1} and Al-OH bending modes at 1096 cm^{-1} with the broad weak stretching of the hydroxylated surface at 2995,

3130 cm^{-1}, weak peaks could be indicative of the low hydroxylated area of the ceramic surface compared to bulk.

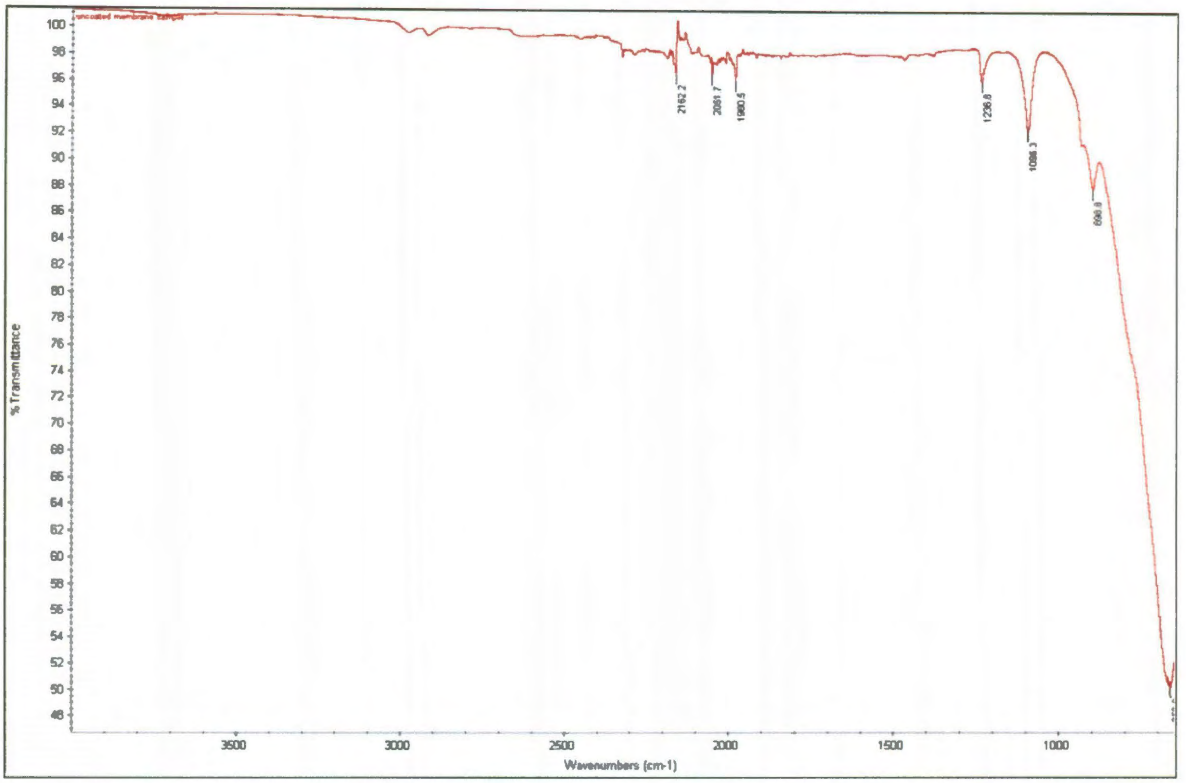

Figure 3.7. FTIR of powdered α-Al_2O_3 porous membrane.

The FTIR of crystalized cysteic acid monohydrate bulk sample Figure 3.8 again shows no water impurity and displays peaks at 1700 cm^{-1} and 1240, 1163, 1032 cm^{-1} which are assigned to ν(C=O) and $\nu(SO_3^{2-})$ absorption, respectively. The sulfonate group and amine group participating in hydrogen bonding $\nu(SO_3^{2-})$ vibrations appears at 1237, 1192 and 1043 cm^{-1}, with the $\nu(NH_2)$ vibration appearing at 3158, 3006 and 2961 cm^{-1} these being drowned out by hydrogen bonding and O-H stretching in the functionalized membrane.

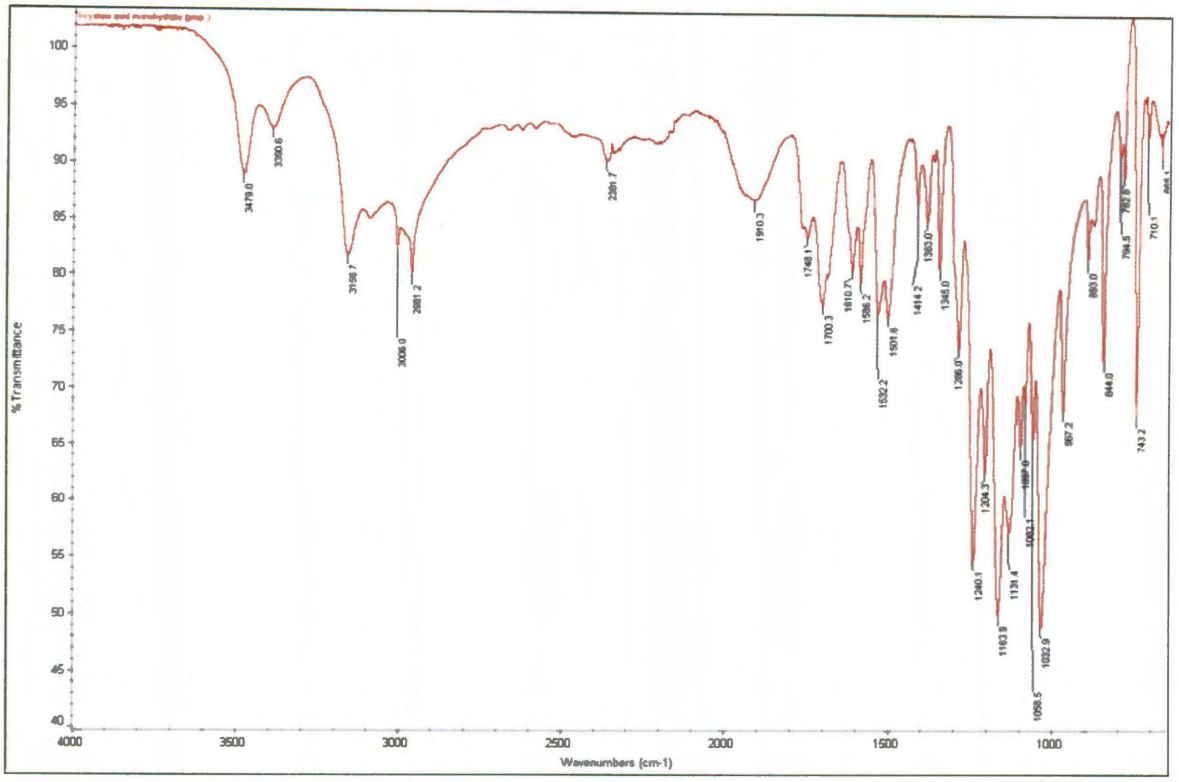

Figure 3.8. FTIR of L-cysteic acid monohydrate.

The functionalized membrane FTIR signal is totally dominated by water Figure 3.9. From the IR analysis of the functionalized membrane it can be seen that there is an extremely large broad peak which is not concurrent with any moiety either of the native cysteic acid or un-functionalized alumina membrane. This broad peak at 3372 cm^{-1} corresponds to the O-H stretch in water. In the functionalized membrane ν(C=O) appears at 1635 cm^{-1} similar to an amide frequency, and maybe due to electron density alteration due to the changing bonding with regards to functionalization onto the ceramic surface of the carboxylic moiety covalently bound to it. However it must be understood that the small fraction of organic functionalization compared to the bulk of the organic covalent functionalization means that exact characterization can be difficult.

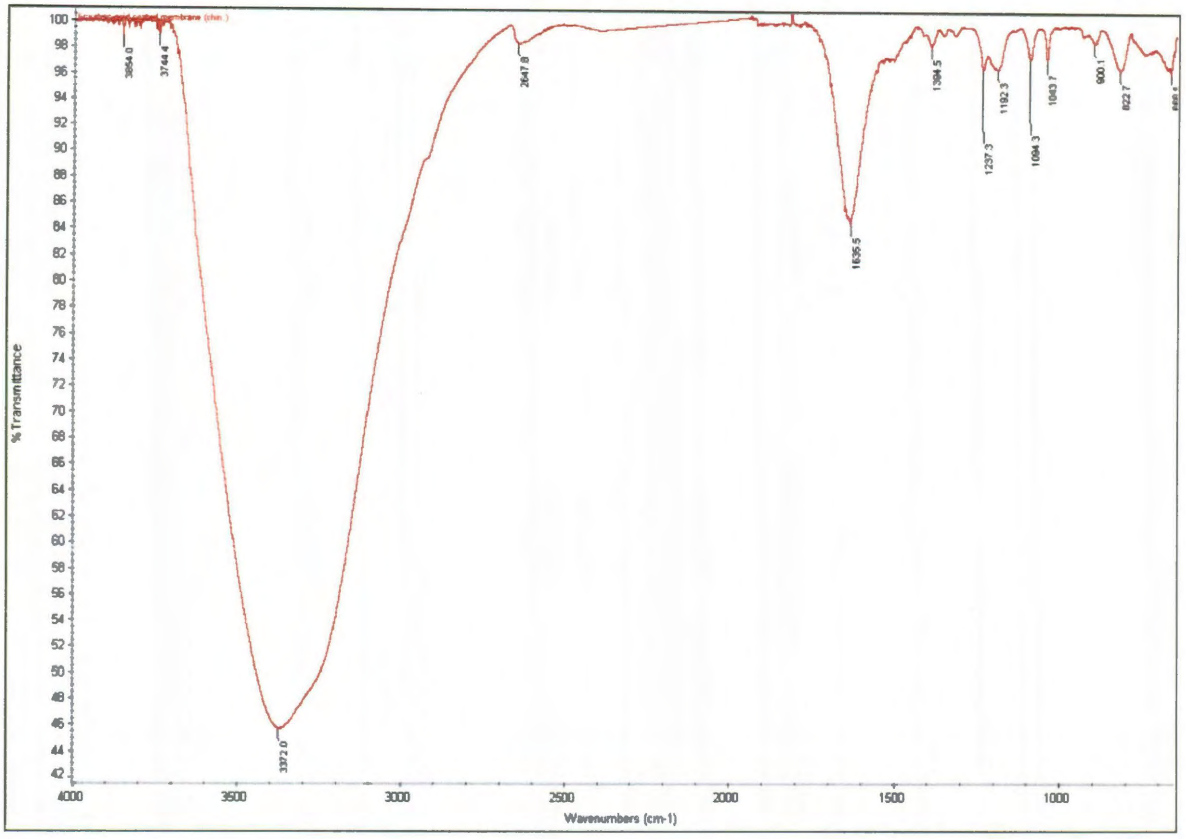

Figure 3.9. FTIR of L-cysteic acid functionalized α-Al_2O_3 membrane.

Functionalization and qualitative and qunatitaive analysis was undertaken using a setup similar to the schematic Figure 3.1 on a pilot plant scale. The production water taken from Pure Stream Corporation well was initially used. Analysis of both carbon amount, molecular content and the elemental composition were analyzed. Initial analysis by inspection clearly demonstrated the ability of the membrane to screen hydrocarbons. The clarity of the permeate sample compared to the original feed sample and the concentrated sample was promising. Figure 3.10

Analysis of the carbon content of both permeate, concentrate and feed samples showed that there was significant retention of carbon material in the production water. The carbon of the permeate sample was in the low ppm range of a few per liter. Figure 3.11 GC-MS analysis on the Pure Stream corporation production water of the chloroform

Figure 3.10. Visual inspection of original (left), concentrate (center), and permeate (right) samples of a functionalized alumina membrane 0.22 μm pore size.

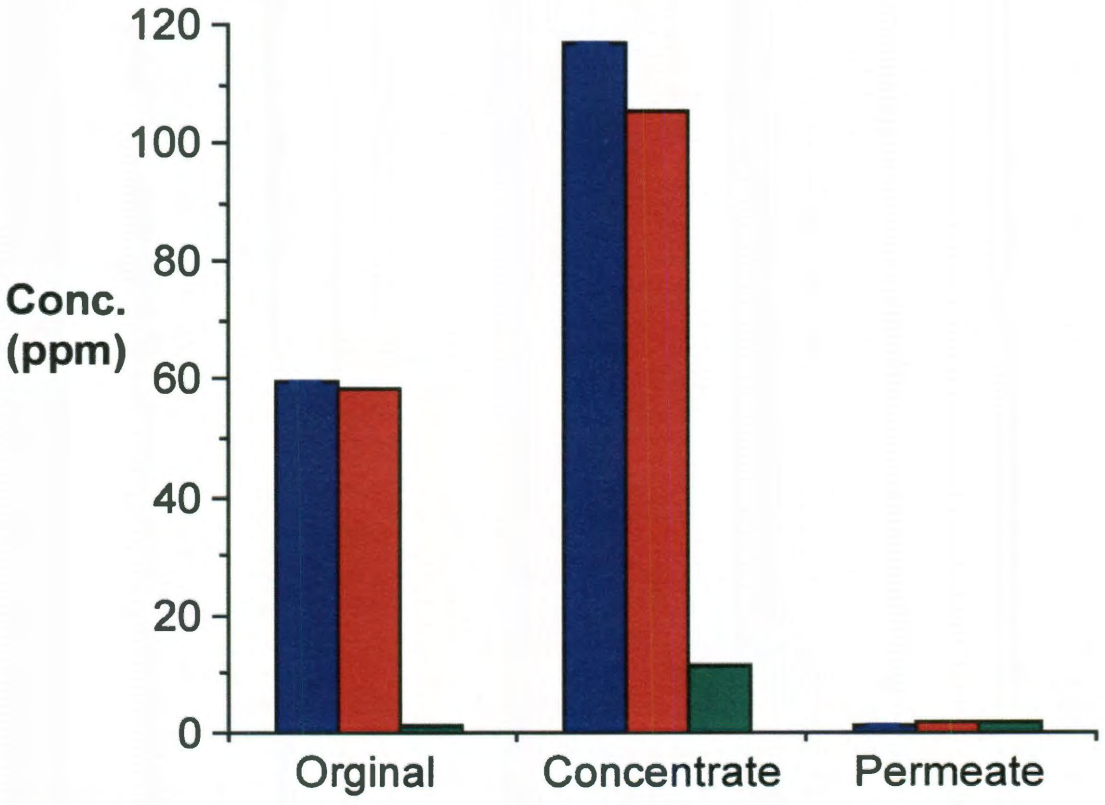

Figure 3.11. Carbon analysis of Frac water. TC (blue), NPOC (red), TIC (green).

liquid-liquid extraction of both the feed, concentrate and permeate samples showed that screening of extremely low M_w hydrocarbons was achieved. Figure 3.12, Figure 3.13. In the permeate feed there is the presence of hydrocarbons however the detection limit is too low for statistically reliable identification. Figure 3.14. Please view Appendix A for supplementary information on hydrocarbon identification.

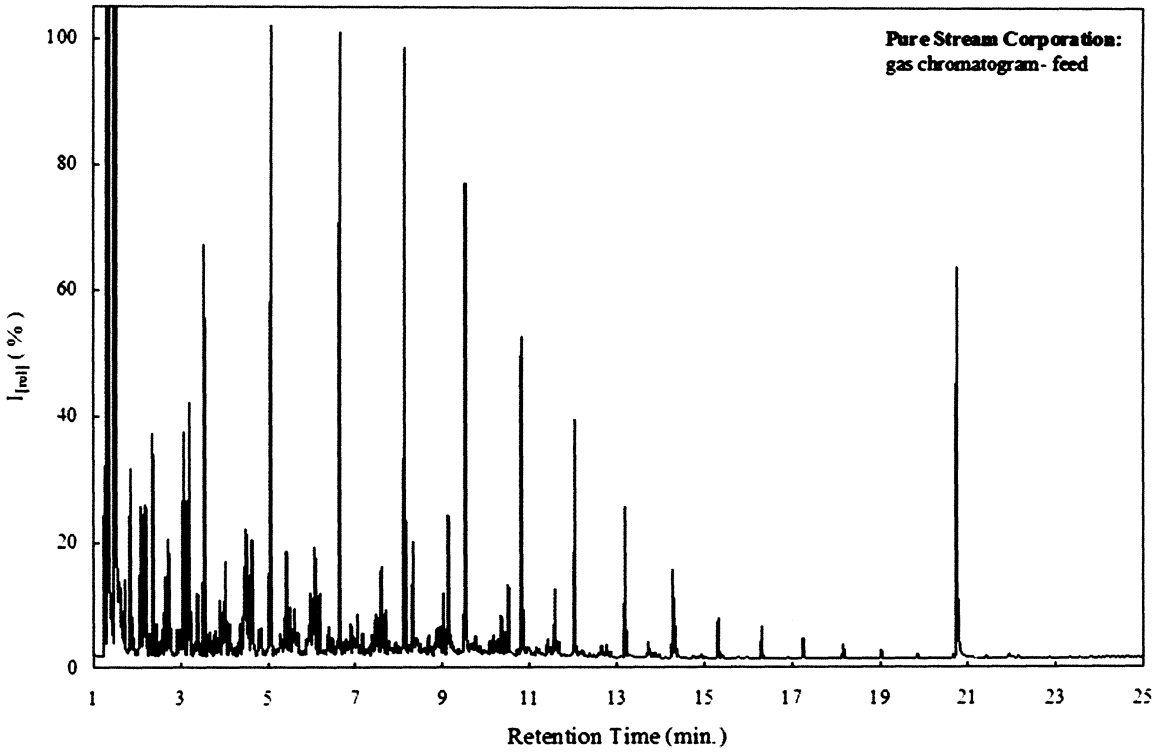

Figure 3.12. GC-MS chromatogram of liquid-liquid extraction in chloroform of feed sample.

The retention of extremely low molecular weight hydrocarbons was observed. The molecular weight hydrocarbons under the same pore size of 0.22 μm of an un-functionalized membrane would pass through easily.

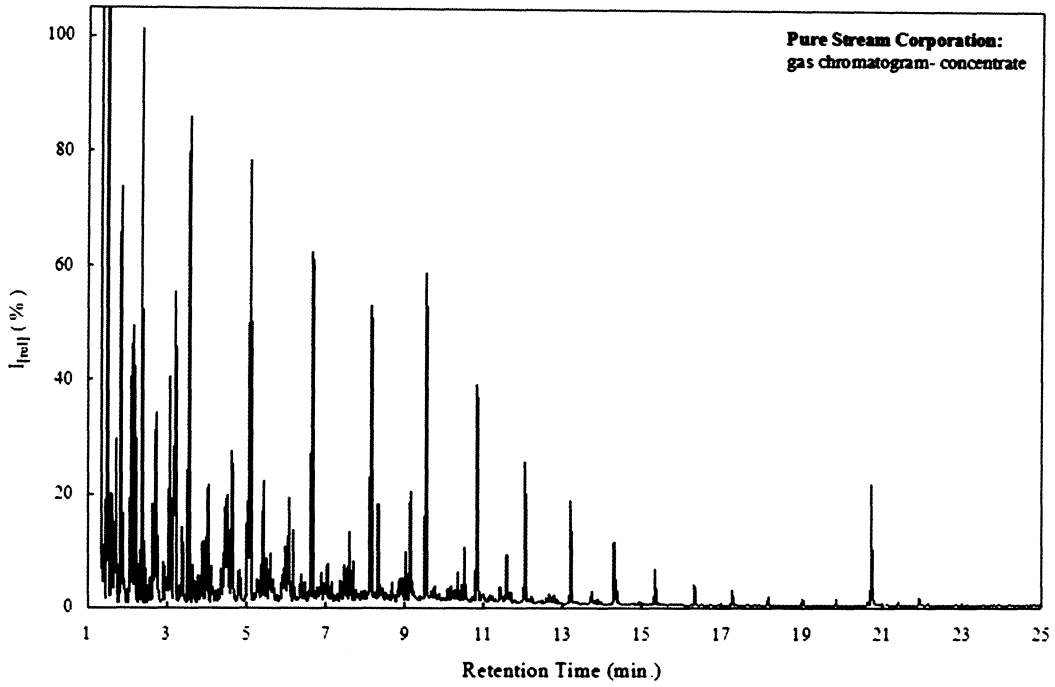

Figure 3.13. GC-MS of liquid-liquid extraction in chloroform of concentrated frac water.

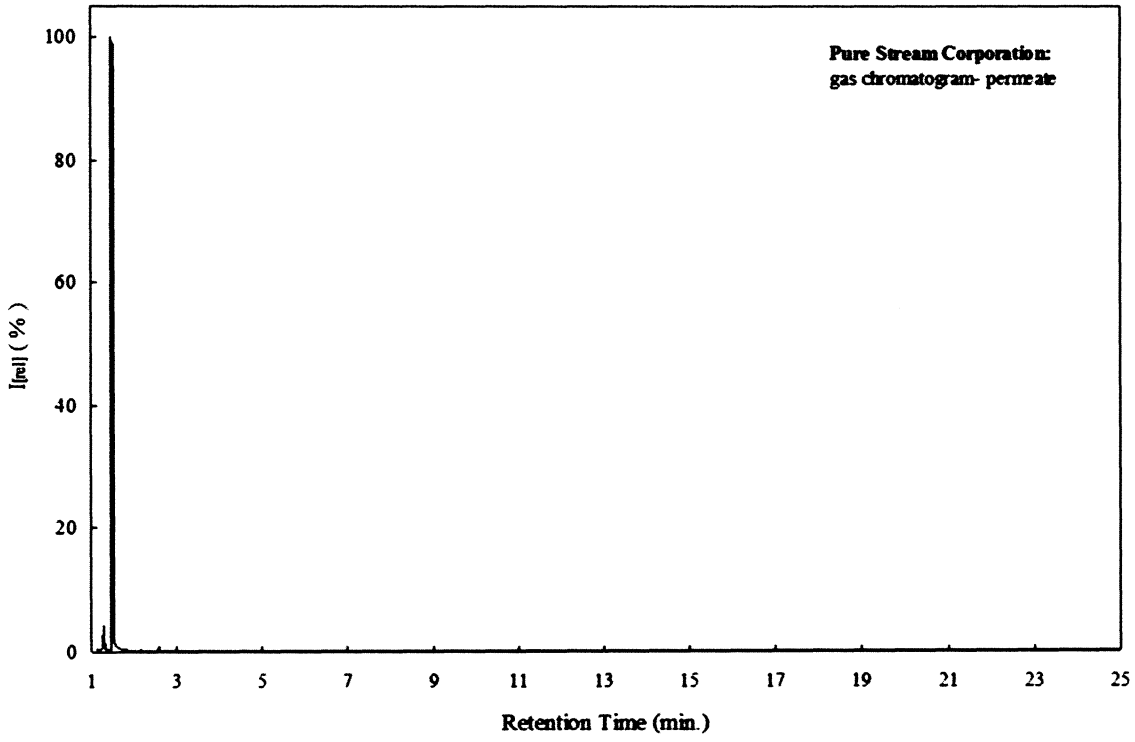

Figure 3.14. GC-MS of liquid-liquid extraction of permeate frac water.

Elemental analysis of each of the samples by ICP-OES indicates that inorganic content remains more or less unaffected by the separation process. Figure 3.17

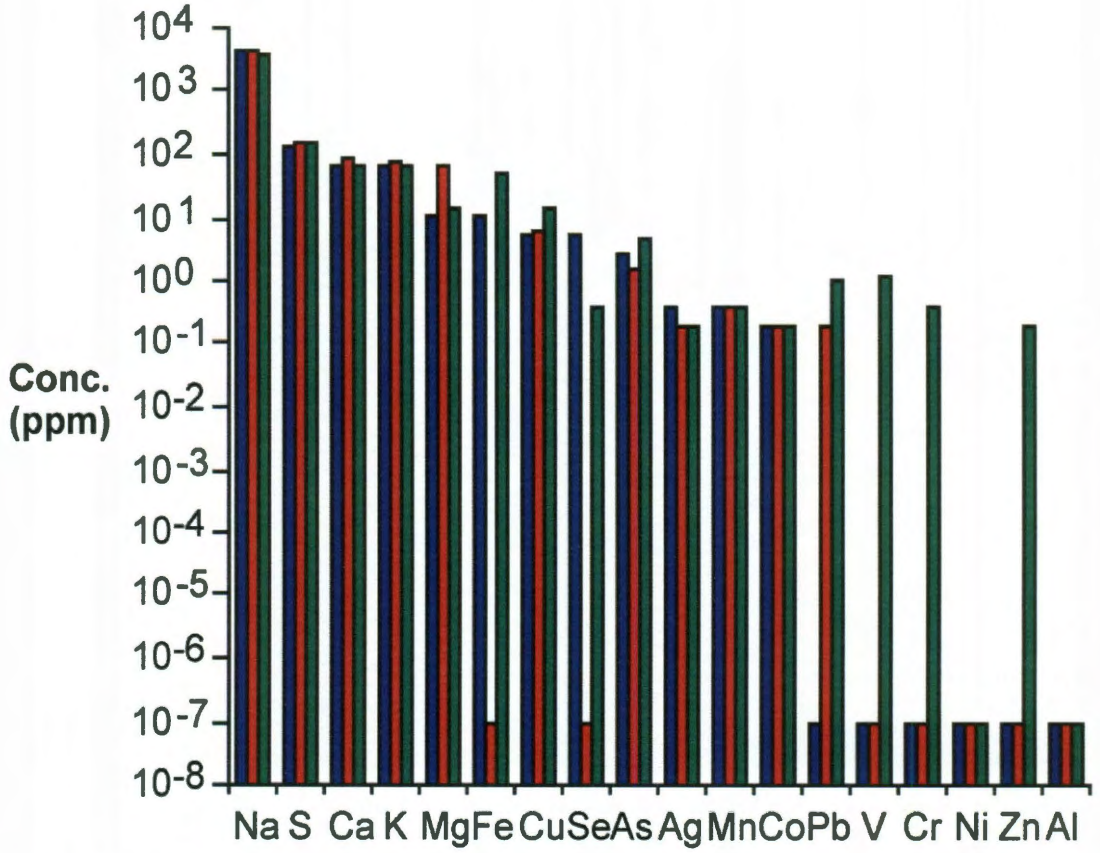

Figure 3.15. ICP-OES analysis for feed (blue), concentrate (red) and original (green) of Utah Frac water.

Not surprisingly, the early alkaline and alkali earth metals sodium, calcium, potassium, and magnesium make up four of the top five elements, followed somewhat distantly by iron, copper, selenium, and arsenic, with a handful of other metals in trace amounts. Interestingly, sulfur exhibits the second highest concentration of all elements examined, likely as a result of the wide-range of compounds, both organic and inorganic, in which sulfur can exist.

The initial promising results from the pilot size filtration of Pure Stream Corp production water of these initial tests led to testing in Utah on an industrial scale of

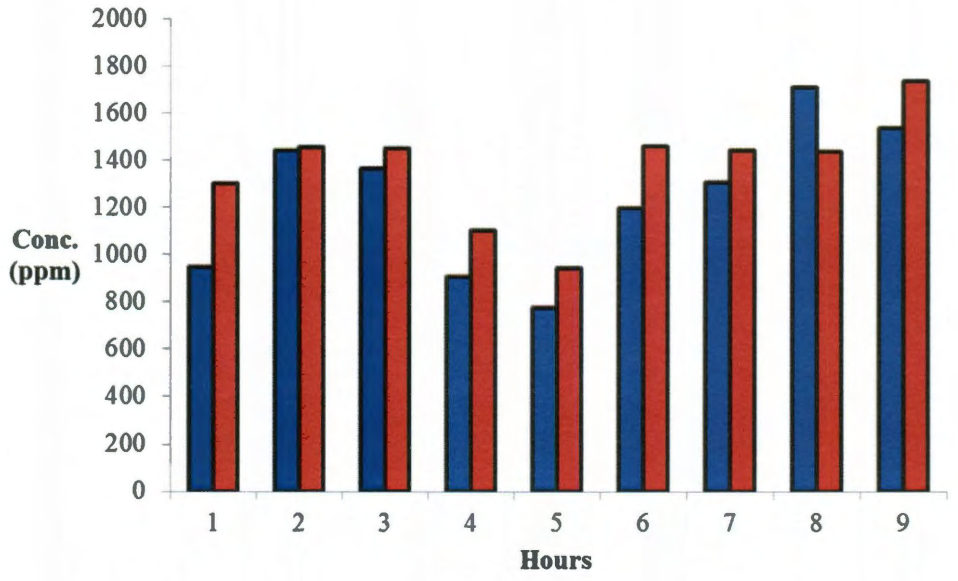

Figure 3.16. TC content of Utah production water, in permeate (blue), and concentrate (red) of Utah frac water.

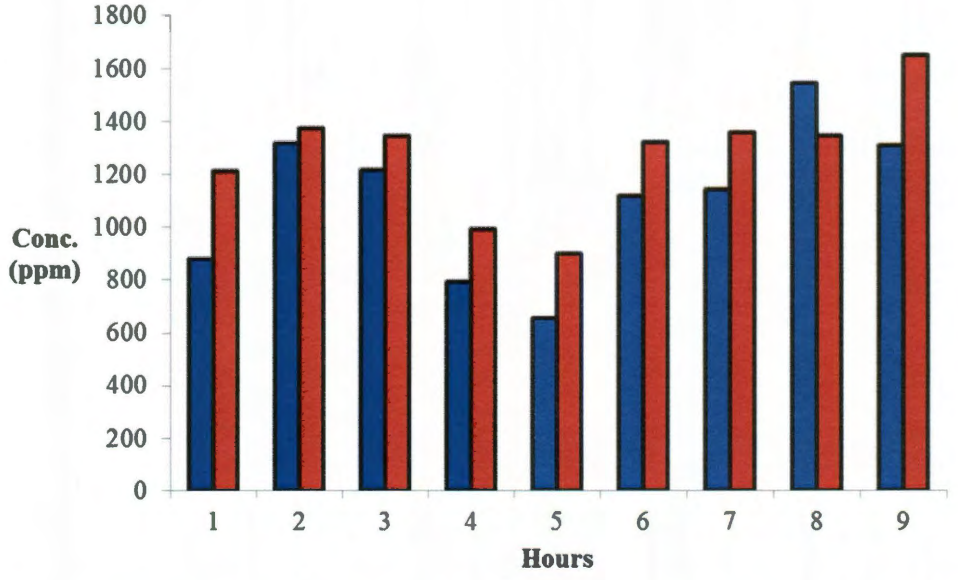

Figure 3.17. TIC content of Utah production water for permeate (blue), concentrate (red) of Utah frac water.

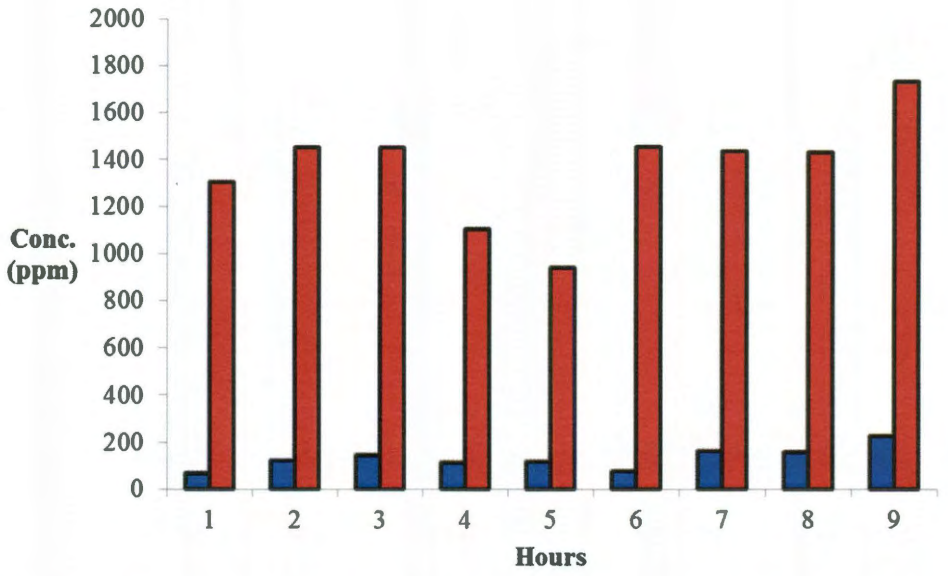

Figure 3.18. NPOC content of Utah production water, permeate (blue), concentrate (red) of Utah frac water.

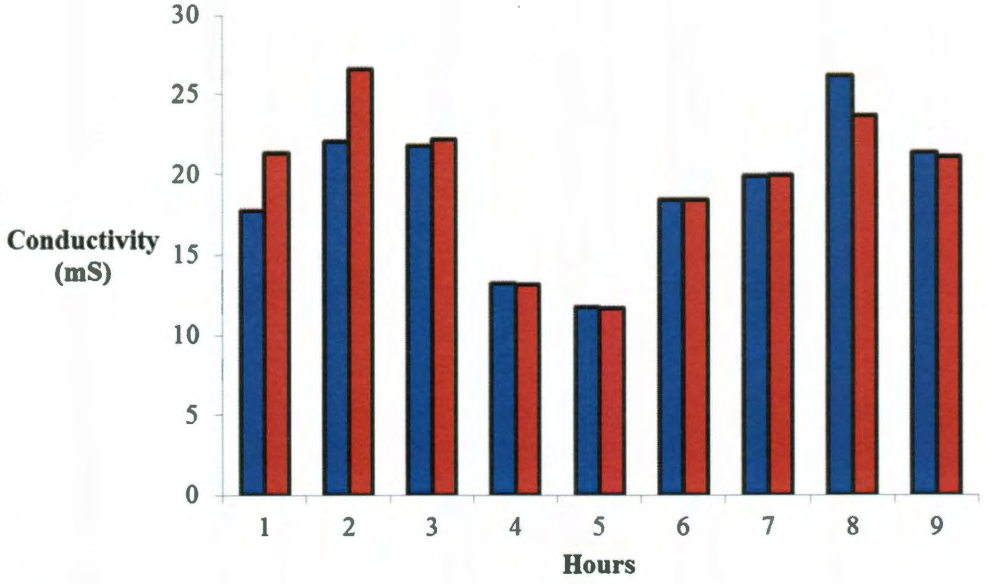

Figure 3.19. Conductivity of Utah production water, permeate (blue) and concentrate (red) of Utah frac water.

production water taken straight from a post frac well. Analysis of the carbon content of the concentrate and permeate samples over the course of several hours as well as the

membrane performance was undertaken. Investigation of the carbon content revealed that significant retention occurred, Figure 3.18. The purity of the permeate is in the low ppm scale and again is a significant improvement over pure ceramic membrane of this pore size.

The carbon analysis shows that screening for NPOC by the functionalized membrane is significant with on average 95% retention of NPOC. The eluted hydrocarbons are expected to be low M_w polar compounds. However total carbon and calculated inorganic carbon remain similar both for feed and permeate. Figure 3.18. This corresponds well with the conductivity data Figure 3.19, which shows that the conductivity also remains the same both for feed and permeate signifying that the inorganic content consists mainly of carbonate salts and dissolved CO_2.

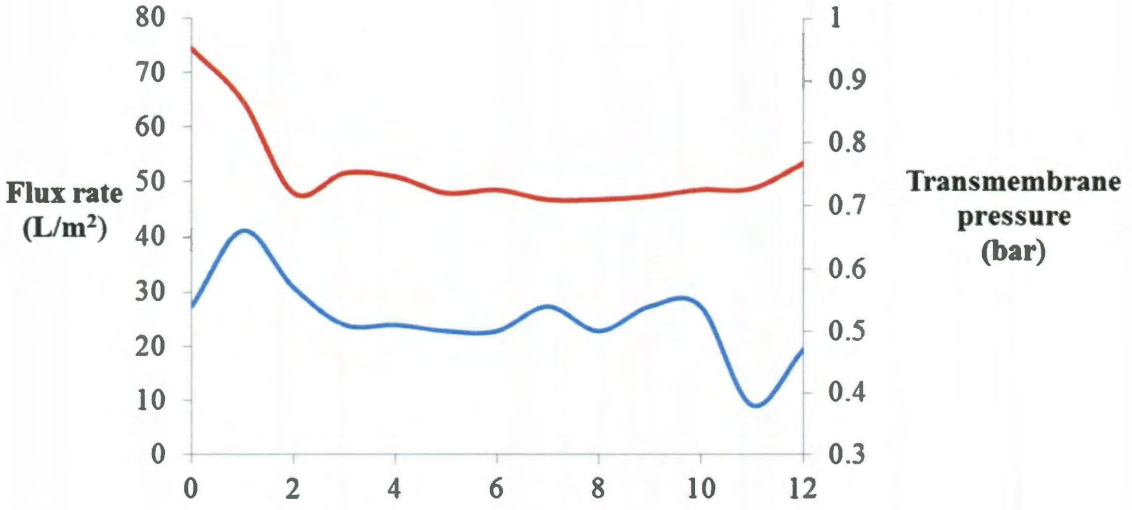

Figure 3.20. Evolution of permeate in relation of transmembrane pressure (blue line), and permeate flux (red line).

One of the initial discoveries with the cysteic acid optimized ceramic membrane was the fact that the membrane hardly suffers from fouling or flux decline as compared to an un-functionalized membrane which suffers a decay on the permeate flow due to the

fouling of organics. This advantage means that the membranes can run longer and are more effective over a longer period of time. As shown in Figure 3.20, evolution of permeate flux rate (Qp) as a function of time permeate flux decreases initially but then stabilizes and remains so for the duration of the measurement.

This decrease in flow is a phenomenon which has been observed in many of our tests to date of the functionalized membranes especially when initial testing of a dry membrane has occurred. Due to the incorporation of water into the pore, there is an initial steady-state that the water/membrane surface must achieve. The trans-membrane pressure shows an initial build-up of pressure which then subsides. The pressure then remains steady for the period of the measurement. This initial build up is a result of 'charging' of the membrane with water and can be attributed to two factors. Firstly purging of the pores of air which can block a pore and result in a lower area for permeate to pass through across the membrane length thus resulting in higher pressures and secondly the establishment of steady-state water layers on the membrane surface. These water layers are the reason for the extended lifetime of the functionalized membrane and its ability to avoid surface fouling. This steady trend is significant when considering that most membranes display a creeping upward trend over the course of their lifetime in trans-membrane pressure and a downward trend for flux. It is also interesting to note that the average permeate flux at which we have run this membrane under these conditions almost always generates an exponential curve for trans-membrane pressure.

Conclusion

The high performance of this large pore size membrane both with regards to hydrocarbon screening, high flux, low operating pressures, anti-fouling properties as well as ease of synthesis point to a new generation of *class II* hybrid inorganic membranes. These membranes have been already used to purify production water on an industrial

scale with excellent results which overcome many obstacles which current membrane technology poses to industry.

The fixed orientation of the functionalized organic molecule points to significant alteration of the properties of the membrane on the macro-material scale. The ease of functionalization and the wealth carboxylic acids which may be available ensure tailoring to particular industrial processes in the near future with regards to many interfacial processes.

The ability of this membrane to screen hydrocarbons of hydrodynamic diameters smaller than the pore size is extremely interesting and deserves more insight into the hydro-dynamic properties on surfaces and in pores which may lead to significant alteration in how filtration is used in industry.

Experimental

All chemicals and solvents were received from Sigma-Aldrich and were used without further purification unless otherwise stated. Porous membranes were received from Molecular Filtration Inc. and were purified with DI water. Thermogravimetric anaylsis (TGA) analysis was conducted on a TA Instruments Q-600 simultaneous TGA/DSC machine, under argon using platinum cups. Analysis was conducted on TA Instruments analysis software. Fourier transform infrared spectroscopy (FTIR) of functionalized and un-functionalized membranes were analyzed on a Nicolet FTIR Infrared Microscope with diamond window. Analysis was undertaken on a Nicolet software package. Scanning electron microscopy (SEM) analysis was conducted on FEI Quanta 400 a multiple stage high resolution field emission environmental scanning electron microscope (ESEM), both in scanning electron (SE) mode and energy dispersive X-ray scattering (EDS) mode, analysis was undertaken where stated either in Hi-Vac or Low-Vac mode. An acceleration voltage of 30 KeV was used as well as a spot size of 4.0 to ensure a dwell time of approximately 30% for the EDS detector and to reduce

charging. Samples were immobilized on an aluminum stub with contact occuring between a carbon tape. Powder X-ray Diffraction (XRD) was conducted on a Rigaku D/Max Ultima II diffractometer, equipped with a vertical θ/2θ goniometer configuration and graphite monochromated Cu-k□ radiation. Data were collected using a 0.005° step width at a fixed-time of 2.0 sec./step, over a 2θ range 20-90°. The slit settings were set at Div Slit = 2°, Div HLSlit = 5 mm, Sct Slit = 2.20 mm, and Rec Slit = 0.15 mm. A cross-section of a membrane was ground into a fine powder by mortar and pestle followed by "wiggle-bug" pulverization. The sample was placed appropriately on a glass slide, which was mounted onto a goniometer. Bruaneaur-Emmet-Teller (BET) analysis Quantachrome Autosorb-3B Surface Analyzer. Samples were broken from the membrane and heated under vacuum at 80 ^{o}C for 24 hrs to remove any excess water. The samples were then purged with helium and analyzed at liquid nitrogen temperature under nitrogen.

Functionalization of membranes with L-cysteic acid. Porous membranes were placed in an airtight glass container this container was filled with DI and placed under vaccum until the membrane stopped effervescing. Vaccum was then removed and the column was heated to 80 ^{o}C for 24 hrs. This water was allowed to totally drain away. The membrane was again covered in a 1M aqueous cysteic acid solution, again vacuum was placed on the container until the membrane stopped effervescing. The solution was brought to gentle reflux for 3 days. The membrane was then allowed to return to room temperature. The membrane was again covered with DI and pumped down until the membrane stopped effervescing and gently heated to 50 ^{o}C then allowed to completely drain from the mmebrane. This process was repeated three times, or until the waste water displayed pH 6.

Frac water sampling. Filtration experiments were conducted on the apparatus as shown in Figure 3.1, single pass-closed loop batch system, the membranes were

subjected to 'real world' filtration of waste frac water also called production water in the oil industry. Filtration occurred at different geographical locations listed below. The flow rates of permeate, concentrate and original samples as well as assembly pressures and substituent temperatures were monitored on site. Sampling of the original frac water, permeate and concentrate were taken at specified times. These samples were analyzed at a later date under laboratory conditions for carbon content, conductivity, elemental composition and finally molecular composition.

Frac water analysis. All samples were filtered three times with Whatman filter paper No. 40 before analysis to remove any non-dissolvable matter. Total carbon (TC) and non-purgable organic coarbon (NPOC) was analyzed on a. Total organic content analysis was performed using a Shimadzu TOC_{VSH} analyzer. The solutions were diluted using HPLC-grade purified water to an approximate concentration of 20 ppm. The dilution factors listed in. Conductivity was measured on a Oakton analyzer using the conductivity stetting the samples were also diluted with milipore water with a conductivity of 18 MΩ. Elemental analysis of the samples were conducted on an inductively coupled plasmon optical emmisson spectroscopy (ICP-OES) machine. Sample preparation for the ICP-OES analysis was performed diluting 0.5 mL sample to 10 mL with concentrated nitric acid. Samples were allowed to 'digest' in acidic solution for 48 hours before further dilution of 0.5 mL acidified sample to 10 mL in HPLC-grade purified water. ICP-OES analyses were performed using an Optima 4300 DV spectrometer equipped with an AS-93+ autosampler. Gas chromatography mas spectroscopy (GC-MS) samples were prepared for analysis using the extraction guidelines that follow. The organic phase of samples acquired from Pure Stream Corp. separations trials (feed, permeate, and concentrate) were extracted from the as-received mixtures using toluene and chloroform. In spite of permeate samples having been examined using identical methods, the characterization thereof proved far more difficult

regarding the identification of organic constituents, which were found to predominantly reside below the minimum detection limits of the instrument. GC-MS analyses were performed using Agilent Technologies 5973 network mass selective detector, equipped with 6890 N network GC system using helium as the carrier gas.

References

1 R. W. Howarth, A. I. and T. Engelder, *Nature*, 2011, **477**, 271.

2 D. V. S. Gupta, B. T. Hlidek, *SPE Production & Operations,* 2010, **25**, 65.

3 C. Guizard, and P. Amblard, *Research on inorganic ceramic membranes applied to water. Handbook of Membrane Seperations,* 2009, 139.

4 M. Abbasi, M. R. Sebzari, A. Salahi, S. Abbasi, and T. Mohammadi, *Desalination and Water Treatment*, 2011, **28**, 1.

5 K. A. DeFriend, M. R. Wiesner, and A. R. Barron, *J. Membr. Sci.*, 2003, **224**, 11.

6 S. Silalahi, and T. Leiknes, *Desalination and Water Treatment*, 2011, **28**, 137.

7 W. Scholtz, and W. Fuchs, *Water Res.*, 2000, **34**, 3621.

8 S. Judd, and S. W. Till, *Desalination*, 2000, **127**, 251.

9 H. Y. Yu, *Sep. Purif. Technol.* 2005, **45**, 8.

10 Q. Sun, Y. Su, X. Ma, Y. Wang, and Z. Jiang, *J. Membr. Sci.*, 2006, **285**, 299.

11 Z. Yi, Y. –Y. Xu, L. –P. Zhu, H. –B. Dong, and B. –K. Zhu, *Chinese J. of Poly. Sci.*, 2009, **27**, 695.

12 J. –N. Shen, D. –D. Li, F. –Y. Jang, J. –H. Qiu, and C. –J. Gao, *Sep. and Purif. Tech.* 2009, **66**, 257.

13 Y. –H. Zhao, B. –K. Zhu, L. Kong, and Y. –Y. Xu, *Langmuir*, 2007, **23**, 5779.

14 L. –P. Zhu, Y. –Y. Xu, H. –B. Dong, Z. Yi, and B. –K. Zhu, *Mater. Chem. Phys.*, 2009, **115**, 223.

15 Y. –L. Su, W. Cheng, C. Li, J. Chao, and Z. Jiang, *J. Membr. Sci.*, 2009, **329**, 246.

16 C. Ba, D. A. Ladner, and J. Economy, *J. Membr. Sci.*, 2010, **347**, 350.

17 K. –S. Chen, H. –R. Lin, S. –C. Chen, J. –C. Tsai, and Y. –A. Ku, *Poly. J. (Tokyo, Japan).* 2006, **38**, 905.

18 S. Santra, G. Srinarayan, and P. Pramanik, *Transactions of the Indian Ceramic Society,* 2010, **69**, 115.

19 S. J. Maguire-Boyle, and A. R. Barron, *J. Membr. Sci.*, 2011, 382, 107.

20 J. Rose, M. M. Cortalezzi-Fidalgo, S. Mostier, C. Magnetto, C. D. Jones, A. R. Barron, M. R. Wiesner, and J. –Y. Bottero, *Chem. Mater.*, 2002, **14**, 621.

21 A. K. Soper and A. Luzar, *J. Chem. Phys.*, 1986, **97**, 1320.

22 S Okazaki, H Touhara, and K Nakanishi, *J. Chem. Phys.* 1984, **81**, 890.

Appendix A

Supplimentary Information for Chapter 3.

Table 3.1. Analysis of selected peaks from GC-MS chromatogram for frac water feed.

R.T. (min)	$A_{[Tot]}$ (%)	Compound name	Qual. (%)
1.852	2.01%	Methylcyclohexane	97
2.094	1.44%	(4-methyl)heptane	72
2.155	1.49%	Toluene	70
2.2	1.32%	(*cis*-1,3-dimethyl)cyclohexane	97
2.367	2.14%	Octane	64
2.731	1.83%	Ethylcyclohexane	89
3.079	2.04%	(2-methyl)octane	90
3.215	2.05%	(1,3-dimethyl)benzene	97
3.549	4.03%	Nonane	97
4.033	1.63%	(2,6-dimethyl)octane	97
4.458	1.30%	(4-methyl)nonane	93
4.503	1.81%	(2-methyl)nonane	81
4.624	2.06%	(1,2,3-trimethyl)benzene	95
5.079	6.79%	Decane	96
5.427	1.34%	(4-methyl)decane	93
6.079	1.29%	(2-methyl)decane	97
6.654	6.54%	Undecane	96
8.139	5.64%	Dodecane	93
9.139	1.83%	(4,6-dimethyl)dodecane	74
9.533	4.99%	Tridecane	98
10.821	3.14%	Tetradecane	98

12.048	2.23%	Pentadecane	96
20.759	4.73%	bis(2-ethylhexyl)hexanedioic acid	99

Table 3.2. Analysis of selected peaks from GC-MS chromatogram for frac water concentrate.

R.T. (min)	$A_{[Tot]}$ (%)	compound name	Qual. (%)
1.599	1.09	Cyclohexane	55
1.721	1.51	Heptane	90
1.857	3.31	Methylcyclohexane	96
2.099	1.95	(4-methyl)heptane	87
2.16	2.15	Toluene	70
2.205	2.27	(*cis*-1,3-dimethyl)cyclohexane	97
2.372	4.01	Octane	81
2.736	2.16	Ethylcyclohexane	93
3.084	2.38	(2-methyl)octane	81
3.22	4.39	p-xylene	97
3.569	4.91	Nonane	97
4.039	1.69	(2,6-dimethyl)octane	95
4.478	1.32	(4-methyl)nonane	94
4.523	1.80	(2-methyl)nonane	59
4.645	2.08	Mesitylene	95
5.114	6.39	Decane	96
5.432	1.15	(2,6-dimethyl)nonane	90
6.675	4.80	Undecane	96
8.175	4.13	Dodecane	97
9.553	3.25	Tridecane	97

10.841	2.01	Tetradecane	98
12.053	1.37	Pentadecane	96
20.749	0.98	bis(2-ethylhexyl)hexanedioic acid	95

Table 3.3. Analysis of ICP-OES for feed, permeate and concentrate.

Analyte	Feed	σ_{feed}	Permeate	σ_{perm}	Concentrate	σ_{conc}
Na	4308.0	37.80	4442.0	50.80	3992.0	34.68
S	135.8	6.20	159.4	5.24	159.4	14.86
Ca	69.6	0.76	83.8	1.56	67.4	0.82
K	64.6	1.24	72.0	2.12	62.6	2.90
Mg	10.6	1.20	64.2	0.68	14.8	2.76
Fe	10.2	0.52	0.0	1.44	49.4	1.50
Cu	5.4	1.72	5.8	1.36	14.0	2.20
Se	5.0	5.66	0.0	11.08	0.4	10.56
As	2.6	0.92	1.6	3.12	4.8	2.08
Ag	0.4	0.06	0.2	0.12	0.2	0.10
Mn	0.4	0.00	0.4	0.04	0.4	0.04
Co	0.2	0.20	0.2	0.48	0.2	0.34
Pb	0	2.36	0.2	1.84	1.0	1.98
V	0	3.16	0	5.36	1.2	1.86
Cr	0	0.20	0	0.08	0.4	0.22
Ni	0	0.76	0	0.60	0	0.66
Zn	0	0.96	0	0.44	0.2	0.12
Al	0	4.84	0	8.76	0	0.52

Appendix B

Publications

1. S. J. Maguire-Boyle, and A. R. Barron, *J. Membr. Sci.*, 2011, 382, 107.

Appendix C

Patents

1. "Analyzing the Transport of Plasmonic Particles through Mineral Formations", Inventors: Andrew R. Barron, Samuel J. Maguire-Boyle, Alvin White Orbeak, A PCT application has been filed for this invention (application number PCT/US2011/038925, filed on June 2, 2011).

2. "Magnetic Particles for Determining Reservoir Parameters", Inventors: Andrew R. Barron, Samuel J. Maguire-Boyle, Alvin White Orbaek, Arfan Ali, Lauren Harrison, David Keith Potter., A PCT application has been filed for this invention (application number PCT/US2011/038912, also filed June 2, 2011.)

3. "Methods, Systems, and Membranes for Separation of Organic Compounds from Liquid Samples", Inventors: Andrew R. Barron, Samuel J. Maguire-Boyle, A provisional patent application has been filed for this invention (application number 13/087, 706, filed on April 15, 2011)

Please contact Office of Technology Transfer Rice University for more information.